



mgr Karol Kozakiewicz

PERYLENE DIIMIDE AND BENZOTHIADIAZOLE DERIVATIVES:

design, synthesis, and evaluation of their photosensitizing and photocatalytic activity in the hydrogen evolution reaction

Pochodne perylenodiimidu oraz benzotiadiazoli: projektowanie, synteza i ocena ich aktywności fotokatalitycznej do reakcji uwalniania wodoru

PhD Dissertation

Supervisor: prof. dr hab. Beata Liberek

Assisting supervisor: dr hab. Illia Serdiuk, prof. UG

Completed on the Department of Organic Chemistry, Faculty of Chemistry, University of Gdańsk

GDAŃSK 2025

The research was financed by NCBiR within the LIDER XI project LIDER/47/0190/L-11/19/NCBR/2020, project manager: dr hab. Illia Serdiuk, prof. UG



Quantum chemical calculations were performed on the computers of the Wroclaw Centre for Networking and Supercomputing (WCSS), Poland.



"You may live to see man-made horrors beyond your comprehension."

- Nikola Tesla, 1898

Table of content

List of abbreviations	6
Abstract	Ο
Streszczenie	
1. Introduction	
1.1 Principles of p	hotocatalysis
1.1.1 Characteri	stics of the good photocatalysts
1.1.2 Uses of pho	otocatalysis in organic synthesis[1]
1.2 Principles of p	hotocatalytic water splitting
1.3 Palladium cata	alysed coupling reactions
1.3.1 Types of Pa	alladium-catalysed couplings
1.3.2 Insight into	o catalytic cycles of palladium catalysed coupling reactions
1.3.3 Application chemistry [65], [66]	ns of palladium-catalysed couplings in medicinal
	as of palladium-catalysed couplings in the synthesis of 7]
1.3.5 Uses of Pa 37	lladium-catalysed couplings in optoelectronic applications
2. Aim of the work	
2.1 Introduction	
2.2 Aim of the wor	·k
2.3 Target compou	ands
2.3.1 Perylene di	imides with donor-acceptor motif
2.3.2 Pervlene di	imides with anchor and donor-acceptor motif

	2.3.3	Benzothiadiazoles	43
3.	Experi	mental section	44
į	8.1 Pe	erylene diimides	45
	3.1.1	$1,7\text{-}\mathrm{Dibromo-}\textit{N,N'}\text{-}\mathrm{bis}(2\text{-}\mathrm{ethylhexyl}) perylene-3,4:9,10\text{-}\mathrm{tetracarboxylio}$	\mathbf{c}
	acid di	imide (A0)	45
	3.1.2	General procedure for synthesis of bay-substituted perylene diimic	des
	with do	onor-acceptor motif (A1-A8)	46
	3.1.3 perylei	General procedure for synthesis of chlorinated and brominated ne diimides with donor-acceptor motif (A9-A12)	
	3.1.4	1-Bromo-7-[2-(4-carboxyphenyl)ethynyl]-N,N'-bis(2-	
	ethylh	exyl)perylene-3,4:9,10-tetracarboxylic acid diimide (B0)	58
	3.1.5	General procedure for synthesis of bay-substituted perylene diimic	des
	with de	onor-acceptor motif with anchor (B1-B10)	59
	3.1.6	General procedure for synthesis of chlorinated and brominat	ted
	perylei	ne diimides with donor-acceptor motif with anchor	67
į	8.2 Pe	erylenemonoimide with anchor moiety	72
į	3.3 Be	enzothiadiazoles	78
	3.3.1	Benzothiadiazoles modified at C4 and C7 carbon atoms (C1-C3)	78
	3.3.2 (C4-C6	5,6-Dichlorobenzothiadiazoles modified at C4 and C7 carbon atoms)	
4.	Result	s and discussion	87
4	l.1 In	troduction and basic terms	87
4	l.2 Do	onor-acceptor type perylene diimides (A1-A12) as precursors	for
		r catalyst	
	4.2.1	Why perylene diimides?	89
	4.2.2	Density functional theory calculations for A1, A3, A5-A8	90
	4.2.3	Synthesis of perylene diimides with donor-acceptor motif (A1-A8)	94
	4.2.4	Photoactivation of PDI – formation of the molecular catalyst	99

	4.3	Chlorinated and brominated PDIs (A9-A12) – further research about		
	molecular catalyst			
	4.4 I	Oonor-acceptor perylene diimides for co-catalysis with TiO ₂ /Platinum		
nanoparticles				
	4.4.1	Why using TiO ₂ nanoparticles		
	4.4.2	Synthesis and analysis		
	4.4.3	Verification of photocatalytic properties in HER 119		
4.5 Chlorinated and brominated perylene diimides with donor-acceptor mot				
with anchor (B11-B15)				
	4.5.1	Screening of compounds - DFT calculations		
	4.5.2	Synthesis and HPLC analysis of selected PDIs with anchors 123		
	4.5.3	Verification of photocatalytic properties in HER		
4.6 Benzothiadiazoles co-catalysis with carbon-based quantum dots 1				
	4.6.1	Screening of compounds - DFT calculations		
	4.6.2	Synthesis and analysis		
	Verif	ication of photocatalytic properties in HER 140		
5	. Sumr	Summary and Conclusions		
6	. Refer	References		
7	. Acad	Academic achievements		

LIST OF ABBREVIATIONS

AA Ascorbic acid

Ac Acetyl

Acac Acetylacetone

ACN Acetonitrile

AnchDA Anchor and Donor-Acceptor

BTDZ Benzothiadiazole

COF Covalent Organic Frameworks

DA Donor-Acceptor

DAD Diode-Array Detector

DBT Dibenzothiophene

DCM Dichloromethane

DFT Density Functional Theory

DMAC 9,9-Dimethyl-9,10-dihydroacridine

DMF Dimethylformamide

DPA Dipicolinic acid

Et Ethyl

GQD Graphene Quantum Dots

HER Hydrogen Evolution Reaction

HOMO Highest Occupied Molecular Orbital

HPLC High-Performance Liquid Chromatography

iPrOH Isopropanol

ISC Inter-System Crossing

LUMO Lowest Unoccupied Molecular Orbital

MALDI-TOF Matrix-Assisted Laser Desorption/Ionization - Time of Flight

Me Methyl

NMP N-Methyl-2-pyrrolidone

NMR Nuclear Magnetic Resonance

NS N,N-dimethylbenzenesulphonamide

NBS N-bromosuccinimide

NCS N-chlorosuccinimide

NIS N-iodosuccinimide

NXS N-halosuccinimide

OER Oxygen Evolution Reaction

OLED Organic Light Emitting Diode

PDI Perylene diimide

Ph Phenyl

PMI Perylene monoimide

PTFE Polytetrafluoroethylene

ppy 2-Phenylpyridine

RT Retention Time

SDS Sodium Dodecyl Sulphate

SED Sacrificial Electron Donor

SNAr Nucleophilic Aromatic Substitution

TADF Thermally Activated Delayed Fluorescence

TEA Triethylamine

THF Tetrahydrofuran

TLC Thin-Layer Chromatography

TMS Trimethylsilyl

TON Turnover Number

UV-Vis Ultraviolet-Visible

ABSTRACT

Photocatalysis, the process of converting light energy into chemical energy, might be a key way of addressing challenges with global energy and fuel availability. One of the most promising direction of research might be using photocatalysis for water splitting to produce hydrogen. Developing efficient, stable, and cost-effective organic photocatalysts is vital for achieving true environment-friendly way of producing this important fuel.

The aim of this work was screening of novel, perylene diimide (PDI) and benzothiadiazole (BTDZ) based organic compounds for use as photocatalysts and photosensitizers in the hydrogen evolution reaction (HER). My work involved designing PDI and BTDZ derivatives together with density functional theory (DFT) calculations, synthesis and confirmation of the identity of obtained compounds. Obtained compounds were tested for photocatalytic activity.

Main strategies employed in the design of target compounds were: obtaining structures containing donor-acceptor (D-A) motif to facilitate charge separation, incorporating anchoring groups for effective attachment to TiO2|Pt nanoparticles, and utilizing the heavy-atom effect to enhance intersystem crossing (ISC) and prolong the lifetime of catalytically active excited states.

In my research, I first synthesized a series of bay-substituted PDI derivatives with a D-A motif (A-series) via palladium-catalyzed Suzuki coupling. Subsequently, I developed a selective, two-step procedure to synthesize PDI derivatives containing a single carboxylic acid anchoring group (B-series), which involved a Sonogashira coupling followed by a Suzuki coupling. For comparison purposes, I also synthesized a model compound (M5), which is a perylenomonoimide (PMI) derivative. To investigate the heavy-atom effect, I synthesized halogenated derivatives of the most promising compounds via halogenation reaction with N-halosuccinimides. To monitor progression of the halogenation, I optimized conditions for analysis of these compounds on HPLC. The BTDZ derivatives (C-series) were synthesized via Suzuki coupling, where I optimized reaction conditions by changing ligand and employing crown ether to

prepare BTDZ derivatives with amino or carboxylic anchoring groups. I confirmed the structures of all obtained compounds using MALDI-TOF MS and ¹H NMR before evaluating their photocatalytic activity.

A key achievement was isolation and confirmation of the structure of the species derived from carbazole-substituted PDI (A4) formed during photoirradiation in the presence of platinum salts. This ring-opened PDI-platinum complex, formed *in situ* during photoirradiation, was proven to be a part of highly active molecular catalyst with a core-shell structure.

The PDI derivatives with an anchoring group (\mathbf{B} -series) successfully photosensitized a $\mathrm{TiO_2}|\mathrm{Pt}$ system, where the brominated carbazole derivative ($\mathbf{B12}$) showed the highest activity, proving the positive impact of the heavy-atom effect. What is very important, these halogenated derivatives functioned without a sacrificial electron donor, confirming enhanced charge separation in the PDI derivatives with heavy atom modified donors.

Finally, the BTDZ derivatives were tested in a completely metal-free system, where they successfully photosensitized graphene quantum dots (GQDs) for HER. In these tests C3 showed outstanding performance. This confirmed the fact that the synthesized compounds are able to act as photosensitizers for HER in fully organic photocatalytic systems.

STRESZCZENIE

Fotokataliza, czyli proces przekształcania energii świetlnej w energię chemiczną, może być kluczowym sposobem na sprostanie wyzwaniom związanym z globalną dostępnością energii i paliw. Jednym z najbardziej obiecujących kierunków badań może być wykorzystanie fotokatalizy do rozszczepienia wody w celu produkcji wodoru. Opracowanie wydajnych, stabilnych i opłacalnych organicznych fotokatalizatorów jest kluczowe dla osiągnięcia prawdziwie przyjaznego dla środowiska sposobu produkcji tego ważnego paliwa.

Celem tej pracy były badania przesiewowe (screening) nowych związków organicznych opartych na perylenodiimidzie (PDI) i benzotiadiazolu (BTDZ), pod kątem ich zastosowania jako fotokatalizatorów i fotouczulaczy w reakcji wydzielania wodoru (HER). Moja praca obejmowała zaprojektowanie odpowiednich pochodnych PDI i BTDZ połączone z obliczeniami z wykorzystaniem teorii funkcjonału gęstości (DFT), syntezę i potwierdzenie tożsamości uzyskanych związków. Otrzymane związki zostały zweryfikowane pod względem właściwości fotokatalitycznych.

Głównymi strategiami zastosowanymi przy projektowaniu docelowych związków były: uzyskanie struktur zawierających motyw donorowo-akceptorowy (D-A) w celu ułatwienia separacji ładunku, wbudowanie grup kotwiczących dla efektywnego przyłączania do nanocząstek TiO2|Pt oraz wykorzystanie efektu ciężkiego atomu do wzmocnienia przejścia międzysystemowego (ISC) i wydłużenia czasu życia katalitycznie aktywnych stanów wzbudzonych.

Początkowo w moich badaniach zsyntetyzowałem serię pochodnych PDI podstawionych w pozycji bay z motywem D-A (seria A) za pomocą sprzęgania Suzuki katalizowanego palladem. Następnie opracowałem selektywną, dwuetapową procedurę syntezy pochodnych PDI zawierających pojedynczą grupę kotwiczącą w postaci grupy karboksylowej (seria B), która obejmowała sprzęganie Sonogashiry, a następnie sprzęganie Suzuki. Do celów porównawczych zsyntezowałem też związek modelowy (M), będący pochodną perylenomonoimidu (PMI). W celu zbadania efektu cieżkiego atomu zsyntetyzowałem halogenowane

pochodne najbardziej obiecujących związków poprzez reakcję halogenowania z użyciem N-halogenosukcynoimidów. W celu śledzenia postępu halogenowania, opracowałem warunki analizy tych związków na HPLC. Pochodne BTDZ (seria C) zostały przeze mnie zsyntetyzowane za pomocą sprzęgania Suzuki. Zoptymalizowałem warunki reakcji poprzez zmianę liganda i zastosowałem eter koronowy, dzięki czemu uzyskałem BTDZ z grupami kotwiczącymi w postaci grupy aminowej lub karboksylowej. Tożsamość otrzymanych związków potwierdziłem za pomocą spektrometrii mas MALDI-TOF oraz ¹H NMR.

Kluczowym osiągnięciem było wyizolowanie i potwierdzenie struktury katalizatora molekularnego pochodzącego od podstawionej karbazolem pochodnej PDI (A4). Tworzący się *in situ* kompleks platyny z otwarto-pierścieniową formą A4, jest częścią wysoce aktywnego katalizatora molekularnego o strukturze nanocząstek typu rdzeń-otoczka.

Pochodne PDI z grupą kotwiczącą (seria **B**) z powodzeniem fotouczulały układ TiO2|Pt, przy czym bromowana pochodna karbazolowa (**B12**) wykazała najwyższą aktywność, co dowodzi pozytywnego wpływu efektu ciężkiego atomu. Co bardzo istotne, halogenowane pochodne działały bez zużywalnego donora elektronów, co potwierdza poprawioną separację ładunku w pochodnych PDI zawierających donory zmodyfikowane ciężkim atomem.

Na koniec, pochodne BTDZ przetestowano w całkowicie wolnym od metali układzie, w którym z powodzeniem fotouczulały grafenowe kropki kwantowe (GQD) w reakcji HER. W tych testach związek C3 wykazał wyjątkową wydajność pomimo braku metalu jako ko-katalizatora. Potwierdziło to tym samym fakt, że zsyntetyzowane związki są w stanie działać jako fotouczulacze do HER w pełni organicznych układach fotokatalitycznych.

1. Introduction

1.1 Principles of Photocatalysis

Photocatalysis is a process of catalysing chemical reaction with use of light, as an energy source, therefore it's a process of converting of light energy into chemical energy, with use of photocatalyst. Photocatalytic reactions are commonly used for polymerization, photocatalytic and purification of air. Most recently, photocatalytic reactions became a popular research topic, as they might be useful for obtaining environment-friendly fuels by carbon dioxide photocatalytic reduction and hydrogen from photocatalytic water splitting.[1]

Mechanism of photocatalysis is straightforward, as it only involves photoexcitation-induced charge separation in photocatalyst and subsequent energy transfer to substrates (Figure 1). Light assisted charge separation leads to formation of hole-electron pair, which are migrating to the surface of the photocatalyst where reaction with substrates occurs. Separated charges are only short-lived species and they are susceptible for recombination and deactivation by various mechanisms. It means that lifetime of separated charges has significant impact on effectiveness of the photocatalysts.

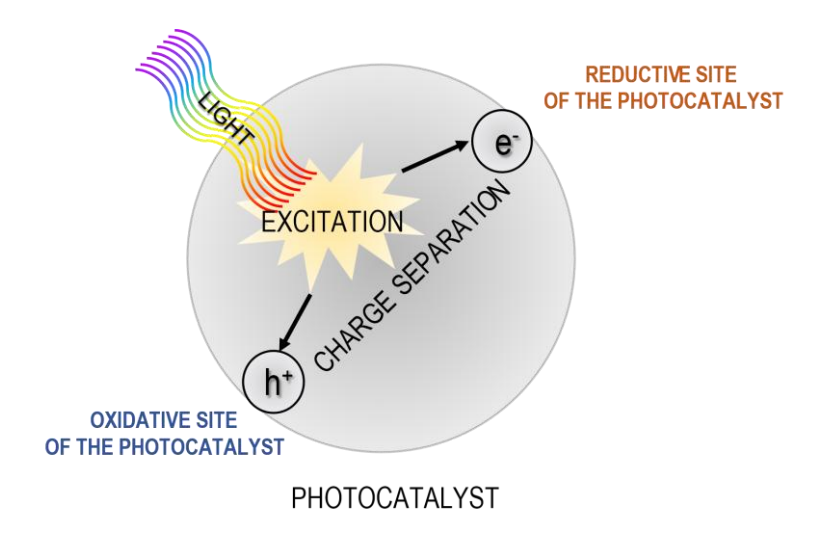


Figure 1 Simplified mechanism of light assisted charge separation in a photocatalyst.

Photosensitization is a conceptually similar process. The key difference is that a photosensitizer is only used as a light harvesting part of photocatalytic systems. Photosensitizer transfer absorbed light energy to the actual catalyst via electron transfer rather than catalysing reactions by itself.

1.1.1 Characteristics of the good photocatalysts

Good photocatalysts must fulfil several criteria:

- 1. Good absorption of light
- 2. Appropriate energy levels of HOMO and LUMO (organic photocatalysts) or valence and conduction bands (inorganic semiconductors) for catalysed reaction
- 3. High charge separation
- 4. High lifetime of charge separation
- 5. High photostability

Vast majority of photocatalysts are based on inorganic semiconductors. Although inorganic semiconducting photocatalysts are, so far, much more efficient than fully organic catalysts, they are based on harmful to the environment heavy metals such as nickel, chromium and cadmium, or expensive noble metals such as palladium, platinum, rhodium, or iridium. Environmental concerns increase need for greener alternative for inorganic photocatalysts.

Organic compounds can only easily meet criteria of good light absorption and appropriate energy levels of HOMO/LUMO. Remaining of mentioned criteria can be problematic to meet. Organic compounds, because of their relatively small size compared to conventional inorganic semiconductors, are prone to recombination of separated charges, therefore reducing chance of successful energy transfer to substrates. Other problem is susceptibility for light bleaching and overall photodegradation. Charge separation on organic compounds leads to formation of highly reactive radical species, which are prone to participating side reactions leading to problems with the photostability. All these problems can be partially bypassed by thoughtful molecular design or by co-catalysis with inorganic semiconductors.

1.1.2 Uses of photocatalysis in organic synthesis[1]

Because of the easiness of procedures, photocatalytic reactions found their use in organic synthesis of various compounds. Separated charges on photocatalyst allow for redox reactions to occur. Most commonly, photocatalysts are used for photooxidation, light driven cross-coupling reactions or formation of *in situ* formation of the singlet oxygen for subsequent reactions with organic molecules. In some cases photocatalytic reactions have superior yields compared to classic approaches.

One of examples of uses of photocatalytic reactions can be synthesis of a potent antimalaria drug artemisinin via photocatalytic of dihydroartemisinic acid (Scheme 1). In this reaction, methylene blue is used as photocatalyst and it allows of formation of hydroperoxide intermediate from dihydroartemisinic acid, which, under acidic conditions, eventually transforms into artemisinin.[2]

Scheme 1 Photooxidation of dihydroartemisinic acid to artemisinin.

Photocatalytic reactions can be also used to insert new organic groups into substrate. One of the works report light-driven trifluoromethylation of alkenes (Scheme 2). This reaction is catalysed by iridium complex and can be performed with use of the sunlight.[3]

Scheme 2 Light-driven trifluoromethylation of styrene.

Synthesis of a important fragrance compound, rose oxide can be achieved from citronellol by light driven hydroperoxide formation via *in situ* formed singlet oxygen (Scheme 3). Synthesis of rose oxide often leads to lower yields via classical routes and photocatalytic synthesis is one of main routes on an industrial scale.[4]

Scheme 3 Synthesis of rose oxide via photooxidation with in situ formed singlet oxygen.

1.2 Principles of photocatalytic water splitting

When it comes to organic photocatalysts for water splitting three types of reactions can be distinguished based on energy levels of HOMO and LUMO orbitals in photocatalysts (Figure 2). In all these reactions **overpotential** is needed to achieve good efficiency.

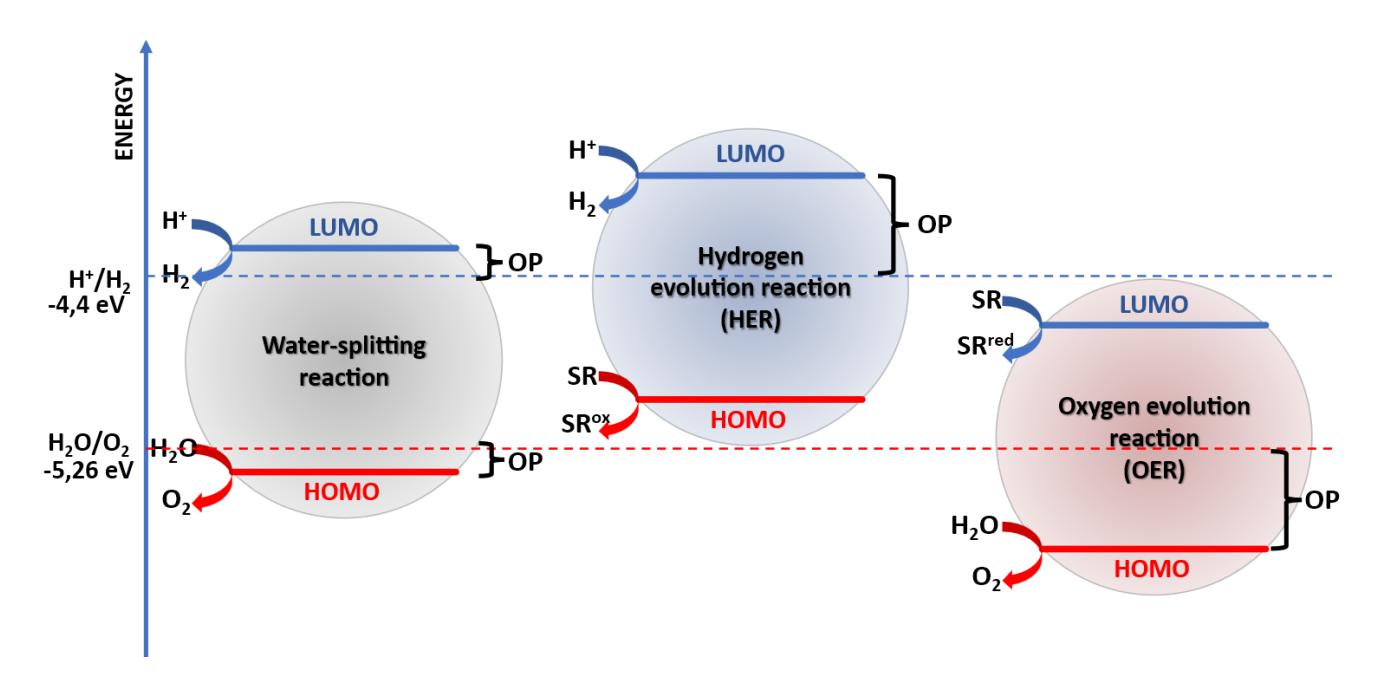


Figure 2 Diagram of basic water-splitting type of reactions. OP - overpotential, SR – a sacrificial reagent, SR^{ox} - oxidized form of the sacrificial reagent, SR^{red} - reduced form of the sacrificial reagent.

While true water-splitting reaction does not rely on any additional reagents to work, Hydrogen Evolution Reaction (HER) and Oxygen Evolution Reaction (OER) need sacrificial reagents (SA) to operate. Sacrificial reagents are cheap and easy available reagents which act like electron donors in the hydrogen evolution reaction, and electron acceptors in the oxygen evolution reaction. It means that

photocatalytic HER and OER are in fact reactions of producing hydrogen and oxygen from water, respectively, from additional substrates. Water-splitting occurs only in conjunction of HER with OER. [5][6]

- 1) **Overall water-splitting reaction** can occur when the energy level of HOMO orbital in the photocatalyst lies below the potential of oxidation of water to oxygen and the LUMO orbital energy level is above the potential of reduction of water to hydrogen. This type of photocatalysis leads to formation of both hydrogen and oxygen without of use of any sacrificial reagents therefore it is the most desirable type of photocatalytic water-splitting reaction.
- 2) **Hydrogen evolution reaction (HER)** can occur when the energy level of HOMO orbital in the photocatalyst lies above the potential of oxidation of water to oxygen and the LUMO orbital energy level is above the potential of reduction of water to hydrogen. This type of photocatalysis leads to evolution of only hydrogen and relies on use of sacrificial reagents which act like hole scavengers. Commonly used sacrificial reagents include triethylamine, triethanolamine, methanol or formic acid. There is some research about using industrial organic waste products like cellulose biomass, proteins, and plastics as sacrificial reagents for this type of reaction. This approach is sometimes called photoreforming.[7]
- 3) **Oxygen evolution reaction (OER)** can occur when the energy level of HOMO orbital in the photocatalyst lies below the potential of oxidation of water to oxygen and the LUMO orbital energy level is below the potential of oxidation of water to oxygen. This type of photocatalysis leads to evolution of only oxygen and relies on use of sacrificial reagents which act like electron scavengers. Commonly used sacrificial reagents are salts containing Fe³⁺, Ag⁺, IO³⁻ ions.

From the practical point of view, overall water splitting and hydrogen evolution reactions are the most desirable types of the reactions. Hydrogen formed during these reactions can be used as a fuel. Nonetheless, the most important issue is comprehending rules behind of all three processes. Understanding of the processes behind WS, HER and OER gives insight and theoretical basis for further design and improvement of photocatalysts. It is also true for other similar reactions like photoreforming or generating fuels from carbon dioxide.

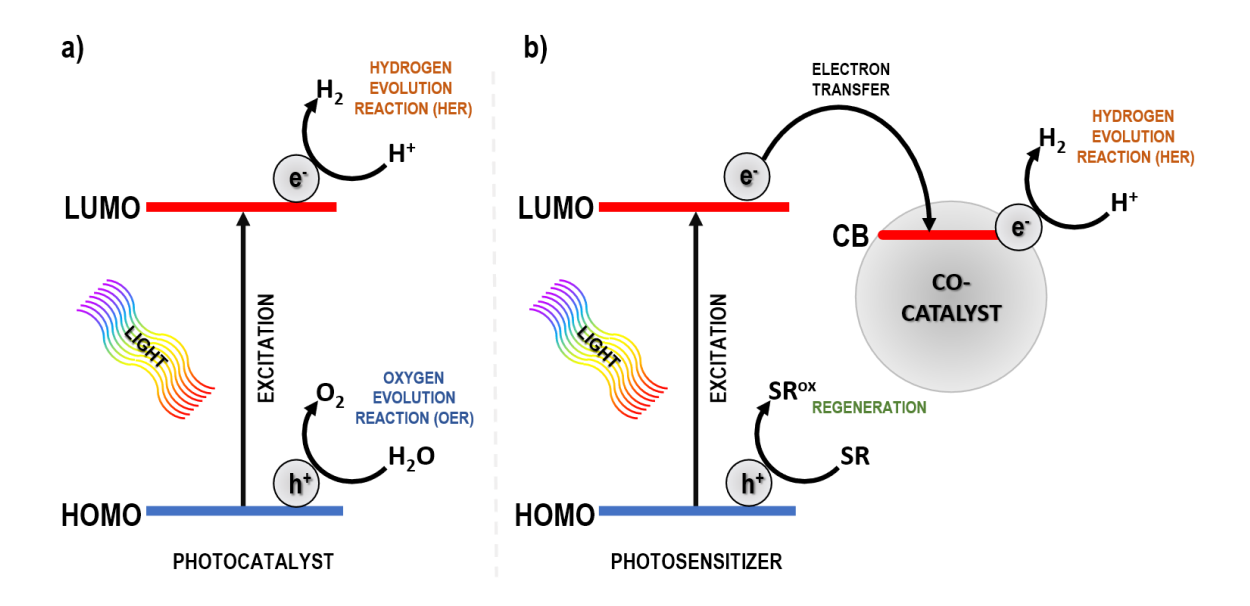


Figure 3 Mechanism of photocatalysis and photosensitizing with organic compounds a) Overall photocatalytic water-splitting reaction b) photosensitizer based photocatalytic hydrogen evolution reaction CB - conductive band of the co-catalyst, SR - sacrificial reagent, SR^{ox} - oxidized form of the sacrificial reagent.

Mechanistically, organic photocatalysts for water splitting work by photoinduced single electron transition from the HOMO to the LUMO forming reactive radical species which then can react with water oxidizing it to oxygen and reducing it to hydrogen (Figure 3). This process is challenging to achieve and often leads to side products and causes major problems with photostability. More often organic molecules are used as photosensitizers in conjunction with inorganic semiconductor co-catalysts for hydrogen evolution reaction. Co-catalysts are often based on titanium dioxide nanoparticles doped with platinum. Photosensitizer acts as a light harvesting part of the whole catalytic system, and it undergoes photoinduced charge separation leading to the formation of holes and reactive electrons (Figure 4). These electrons are then passed to the conductive band of the co-catalyst where they reduce water to hydrogen. Additionally sacrificial reagent is needed to regenerate photosensitizer.

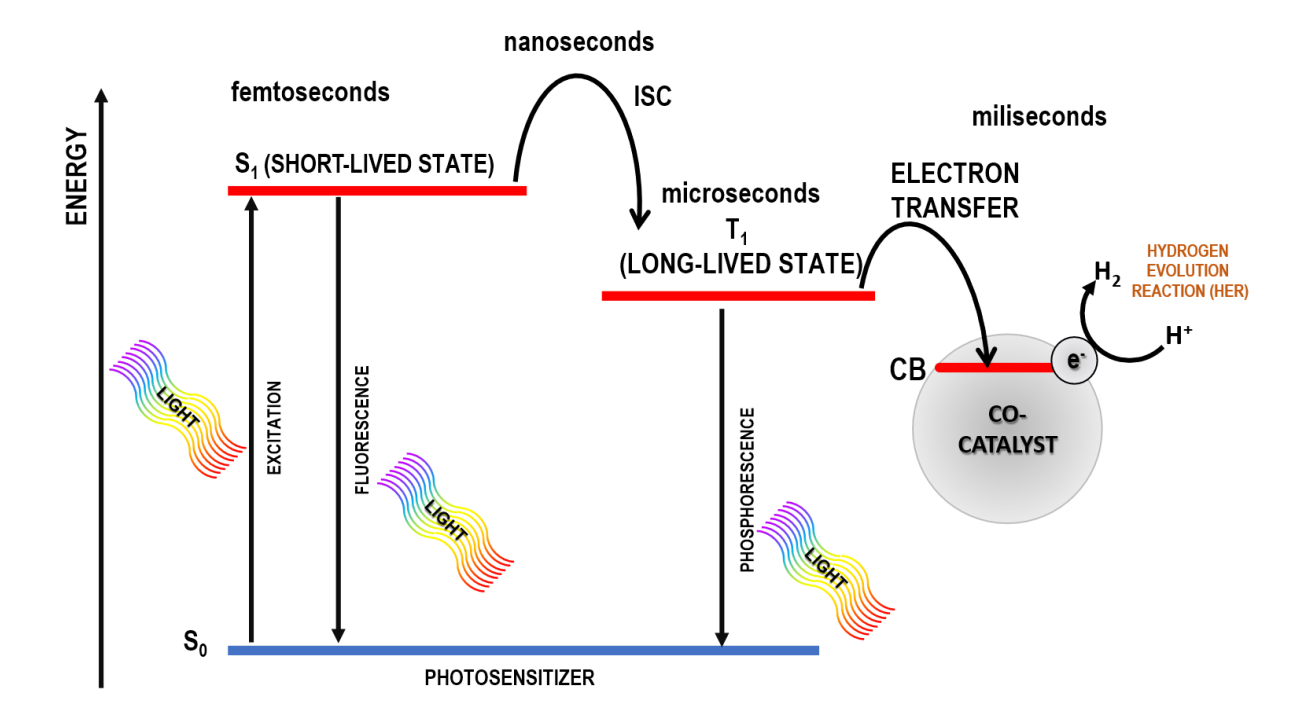


Figure 4 Mechanism of photosensitizer assisted HER, S_0 - ground state, S_1 - 1st singlet state, T_1 - 1st triplet state, ISC - inter-system crossing, CB - conductive band of the catalyst.

A closer look at the timescale of processes occurring during photosensitizer assisted photocatalytic hydrogen evolution reaction reveals several competing processes in which energy can be lost, affecting overall efficiency of the HER.

Photoexcitation of the photosensitizer leads to the formation of the photosensitizer in singlet state S_1 . Its average lifetime in this state lies in the femtoseconds (10^{-15} s) interval on the timescale, therefore it is a very short-lived state compared to other subsequent processes. The photosensitizer in the S_1 state can lose absorbed energy by radiating light in the process of fluorescence. S_1 state can undergo inter-system crossing (ISC) to the triplet state T_1 . ISC is a few orders of magnitude slower, compared to the lifetime of the S_1 state, as its rate lies in nanoseconds (10^{-9} s) interval. The average lifetime of T_1 state lies in the microseconds (10^{-6} s) interval. This long-lived character of the T_1 state makes it the main way of energy storage in the photosensitizer. From the T_1 state, energy can be lost by radiating light in the process of phosphorescence, or it can be passed, via electron transfer, to the conductive band of the co-catalyst, where HER occurs. The process of the electron transfer is even slower, as it lies in the milliseconds (10^{-3} s) interval on the timescale.

1.3 PALLADIUM CATALYSED COUPLING REACTIONS

Reactions of C-C bond formation are one of the most important challenges of organic chemistry. The importance of the C-C bonds formation is best proven by the fact that many Nobel Prizes in chemistry were awarded for this type of reactions: The Grignard reaction (1912), the Diels-Alder reaction (1950), the Wittig reaction (1979) or olefin metathesis reactions (2005) are among them.

Palladium catalysed carbon-carbon bond formation, known as a cross-coupling, is among one of the most versatile and useful tools used in contemporary synthetic chemistry. Before Pd-catalysis era, to create the C-C bond chemists were compelled for using classical reactions, like Friedel-Crafts alkylation and acylation, Sandmeyer and Wurtz reactions, and others. Although those reactions are very useful, their use is limited to certain types of substrates and often cannot be used to synthesize more complex molecules.

Palladium-catalysed couplings were discovered independently by three chemists, Richard F. Heck, Eiichi Negishi, and Akira Suzuki. Their work was awarded with Nobel Prize in chemistry in 2010.[8] These reactions are used to create new carbon-carbon bond between aryl halides and coupling partners. Most common coupling partners are boronic acid derivatives in Suzuki coupling, alkene in Heck coupling and organozinc compounds in Negishi coupling. Vast range of available substrates, high tolerance of many functional groups, easiness, and high yields, make these reactions one of the most used types of reactions used in modern synthesis. The use of palladium catalysed reactions is not only limited to research work, these are also commonly used in industrial synthesis of various pharmaceuticals[9], [10], [11], [12], agrochemicals [13], dyes and pigments for solar cells[14], [15]. It is worth mentioning that palladium-catalysed couplings are also commonly used for carbon-nitrogen bond formation. Buchwald's group are the most important contributors to the studies on C-N catalysed couplings.[16]

1.3.1 Types of Palladium-catalysed couplings

Versatility of uses for palladium catalysed couplings caused rapid rise in interest of the palladium chemistry research. Numerous variants, with various

coupling partners and with use of many different ligands, were later developed. Many of these reactions can be catalysed by other metal complexes, like nickel or cobalt, although most of modern approaches are mostly based on palladium complexes as a metal catalyst.[17] Extensivity of exploration of palladium catalysed cross-coupling reactions can be provided by summary of data from last 40 years shown on the graph below (Figure 5). On the beginning of the recent millennium, rapid growth of number of publications exploring palladium cross-coupling reactions can be noticed, with the leading of the Suzuki and Heck reactions.[18]

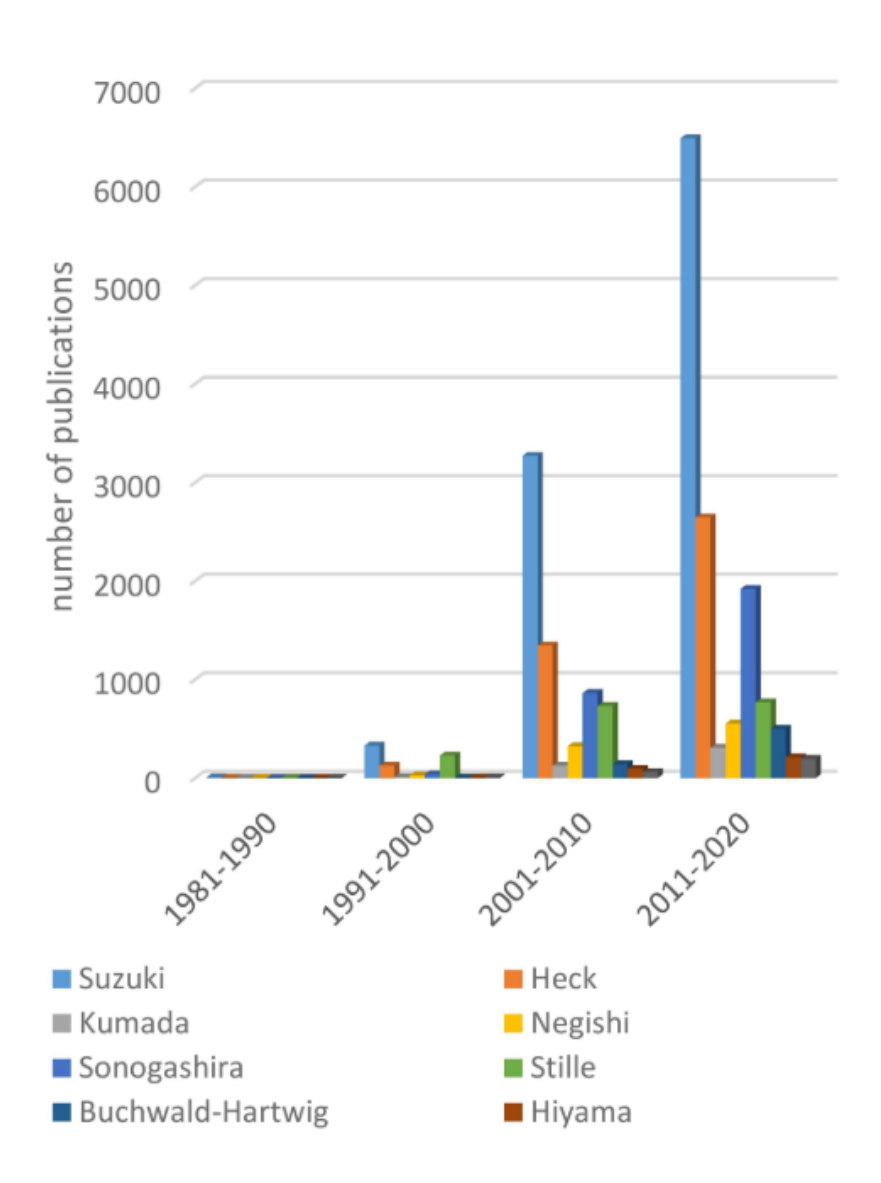


Figure 5 Statistics of cross-coupling reactions reports in literature.[18]

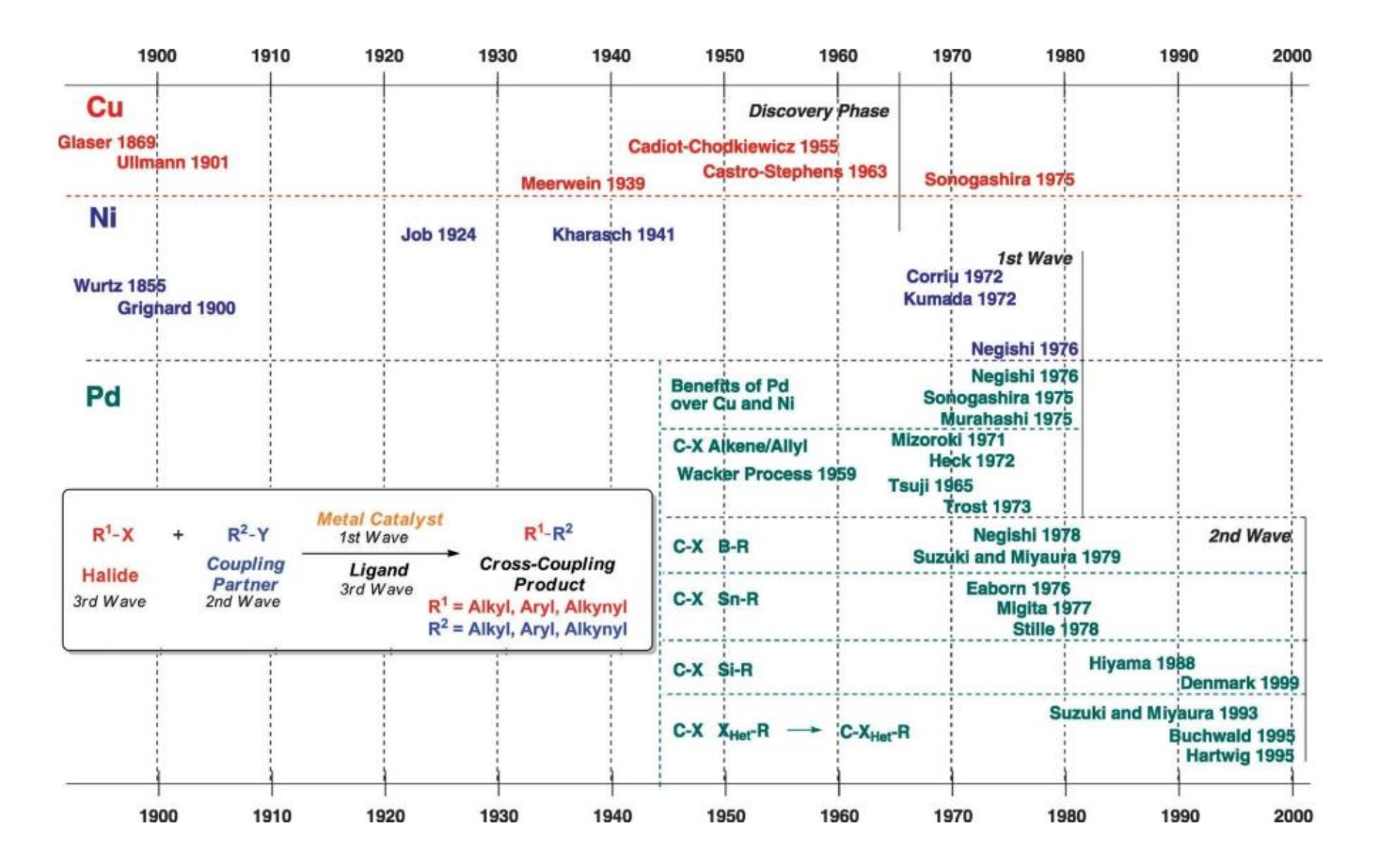


Figure 6 Timeline of development of cross-couplings.[18]

Below is the list of most known palladium catalysed couplings with examples of reactions from original works.

1.3.1.1 Kumada coupling[19], [20], [21]

Scheme 4 Example of Kumada coupling.

The Kumada coupling is a reaction between vinyl or aryl halides, or pseudohalides, and organomagnesium compounds (Grignard reagents). It is useful for introducing alkyl and alkenyl groups into aromatic ring systems (Scheme 4). First reactions of this type, reported by Kumada and co-workers, were based on nickel catalysts, but later, variants with palladium catalysts were developed.

1.3.1.2 Heck reaction[22], [23], [24], [25], [26], [27], [28]

Coupling partner I	Coupling partner II	Product
R1-X (sp ²)	R2-CH=CH2 (sp ²)	R1-CH=CH-R2

Scheme 5 Example of Heck reaction.

The Heck coupling reaction is a particularly useful tool for coupling of aryl or vinyl halides, or pseudohalides, with alkenes (Scheme 5). Alkenes used in this reaction require presence of the at least one vinylic proton. Heck reaction has wide range of possibilities, as it is not limited only to aromatic substrates, but it also allows coupling of two, non-aromatic, vinylic substrates.

1.3.1.3 Sonogashira reaction[29], [30], [31]

Scheme 6 Example of Sonogashira reaction.

The Sonogashira reaction is a reaction between terminal acetylenes and aryl or vinyl halides, or pseudohalides (Scheme 6). It is a less harsh alternative for the Castro–Stephens coupling and opposed to it, copper I halides are used in non-stoichiometric, catalytic amounts in the Sonogashira coupling.

1.3.1.4 Negishi coupling[32], [33], [34]

Scheme 7 Example of Negishi coupling.

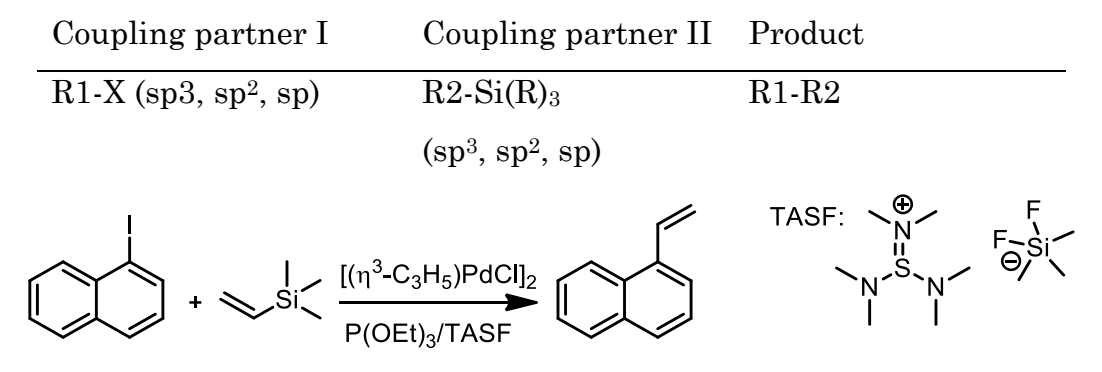
The Negishi coupling allows for coupling of vinyl or aryl halides, or pseudohalides with organozinc compounds (Scheme 7). It is akin to the Kumada coupling but in the Negishi coupling, organozinc compounds are used instead of Grignard reagents.

1.3.1.5 Stille reaction[35], [36], [37]

Scheme 8 Example of Stille reaction.

The Stille reaction is a reaction of organotin compounds with alkyl, alkenyl and acyl halides or pseudohalides (Scheme 8). It is to a great extent close to the Suzuki coupling in terms of a scope and limitations. It can be used when the Suzuki coupling failed to produce expected products. Despite the similar scope, it requires handling of highly neurotoxic organotin compounds, therefore it less preferred than Suzuki reaction.

1.3.1.6 Hiyama coupling[38], [39], [40]



Scheme 9 Example of Hiyama coupling.

The Hiyama coupling is a reaction of organic halides, or pseudohalides with organosilicon compounds (Scheme 9). It requires activation of organosilicon compounds with fluorides or bases. Because of the similar scope and limitations, the Hiyama coupling, in most cases, can be used interchangeably with the Suzuki

coupling. However limited commercial availability of organosilicon substrates, makes this reaction less frequently used compared to the Suzuki coupling.

1.3.1.7 Suzuki reaction[41], [42], [43], [44], [45]

Scheme 10 Example of Suzuki reaction.

The Suzuki reaction allows coupling of boronic acids, their esters, or organotrifluoroborate salts with alkyl, aryl, or vinyl halides or pseudohalides (Scheme 10). It is a very versatile reaction with a broad scope. It is performed under very mild conditions and has high tolerance for diverse functional groups. Building blocks for the Suzuki reaction are fairly non-toxic and widely commercially available, making this reaction one of the most useful tools among palladium catalysed couplings.

1.3.1.8 Buchwald—Hartwig reaction[46], [47], [48], [49]

Coupling partner I	Coupling partner II	Product
R1-X (sp ²)	$R2-NH_2 (sp^3, sp^2)$	R1-NH-R2

$$+ HN \qquad \frac{Pd[(o-tol)_3P]_2}{NaOtBu}$$

Scheme 11 Example of Buchwald-Hartwig reaction.

The Buchwald-Hartwig reaction is a palladium catalysed reaction used to introduce substituted amine groups into sp² hybridised carbon atoms (Scheme 11). Prior to the Buchwald-Hartwig reaction discovery, introduction of amines to aromatic ring systems was significantly more difficult, and required sequence of

multiple reactions, for example nitration, reduction, and subsequent alkylation with alkyl halides. Buchwald-Hartwig reaction can also be used to indirectly introduce primary amine groups via ammonia equivalents, i.e. silylamides[50] or benzophenonimines[51], and subsequent cleavage of formed derivatives by hydrolysis or hydrogenolysis. Some variants of this reaction allow coupling of other atoms, like oxygen in phenols and alcohols[52] or sulphur in thiols and thiophenols[53]. To some extent, in terms of scope, the Buchwald-Hartwig reaction can be seen as a vinyl or aryl (pseudohalide)halide counterpart of the nucleophilic substitution reaction.

1.3.1.9 Fukuyama coupling[54], [55]

Scheme 12 Example of Fukuyama coupling reaction.

The Fukuyama coupling is a reaction used to transform thioesters and organozinc compounds into ketones (Scheme 12). Because of mild conditions and high selectivity, this reaction is compatible with many functional groups such as esters, aldehydes, and ketones, among others.

1.3.2 Insight into catalytic cycles of palladium catalysed coupling reactions

Palladium compounds can exist in a range of oxidation states, 0, +1, +2, +3, +4, +5, most of them are predominantly on +2 state. To take place, cross-coupling reactions require palladium on 0 oxidation state. While metallic palladium nanoparticles, in 0 oxidations state, are capable of catalysing cross-coupling reactions, the most desirable form of palladium catalysis is homogeneous catalysis. [56] Unlike metallic palladium, many palladium(0) compounds are highly

air and water sensitive and ligands have crucial role in stabilization of palladium(0) compounds (Scheme 13).

Scheme 13 Palladium complexes an their reactivity.

Most stable palladium(0) complexes have four ligands with palladium atom having 18 valence electrons. Gradual dissociation of ligands leads to the formation of a palladium complex with 14 valence electrons. It is thought that this 14-electron palladium complex is responsible for the catalytic activity of palladium(0) complexes. Most frequently used ligands are based on phosphine derivatives, notably triphenylphosphine. [57], [58]

Multiple studies of mechanisms and scopes of palladium catalysed coupling reactions were conducted. All suggested mechanisms are akin to each other, only details of for example, ligands association and dissociation, differ. For the sake of clarity, simplified versions of catalytic cycles of the Heck, the Suzuki and the Buchwald-Hartwig reactions are described. The convoluted process of ligands dissociation and association was reduced to absolute minimum. aforementioned simplification also applies to the stereochemistry and the role and types of bases in mentioned reactions. In reality, those aspects are much more complex, and in some cases, solvation, or hydrolysis of the substrates, also affect the way those coupling reactions take place. All these simplifications will allow for easier description of the mechanistic aspect of palladium catalysed couplings, without delving into too many details.

1.3.2.1 Heck coupling catalytic cycle[25], [59], [60]

Heck coupling reaction consists of the following steps (Scheme 14):

R - any organic substituent

L_n - ligands

R

L_nPd⁰

1. oxidative addition

R

2. syn-migratory insertion

R

H

Pd^{||}L_nX

R

Scheme 14 Heck coupling reaction cycle.

1. Oxidative addition

Scheme 15 Oxidative addition step in Heck coupling reaction.

This step is crucial for all of palladium catalysed couplings. During this step, the palladium(0) atom, complexed by the ligands, inserts between carbon-halogen or carbon-(pseudo)halogen bond of organic halide or pseudohalide (Scheme 15). Simultaneously with insertion, palladium changes its oxidation state from 0 to +2. Most commonly used ligands are derivatives of phosphine, for example triphenylphosphine, but N-heterocyclic carbene ligands are also reported to be effective.[61]

The reactivity order of halides and pseudohalides is following:

R-I > R-OTf >> R-Br >> R-Cl

As shown above, the reactivity order of halides in palladium catalysed coupling reactions is comparable to the reactivity order of alkyl halides in nucleophilic substitution reactions. Fluorides are generally inert in commonly used conditions of palladium catalysed coupling reactions. This is the exact opposite to the reactivity order of aryl halides in a nucleophilic aromatic substitution reaction S_NAr, where aryl fluorides are usually the most reactive among aryl halides. Utilization of different reactivity of organic halogens, grants access to diverse synthetic routes of complex organic molecules. Palladium catalysed coupling reactions of mixed halogens, in conjunction with other synthetic methods, for example organolithium chemistry, combine into a very powerful and versatile synthetic tool for modern chemists.

2. Syn-migratory insertion

Scheme 16 Syn-migratory insertion step in Heck coupling reaction.

This step is the deciding step of the Heck reaction. Syn-addition of the palladium(II)-organic (pseudo)halide complex to the alkene leads to the saturated intermediate product of coupling (Scheme 16). The sp³ hybridisation of this intermediate product allows rotation of the newly formed C-C bond. This determines the stereochemistry of the coupling product, as the rotation of C-C will lead to the least hindered conformer. The steric interaction between ligands of the palladium complex and substituents of substrates, attributes to the high preference for *trans*-alkene formation in the Heck coupling reaction.

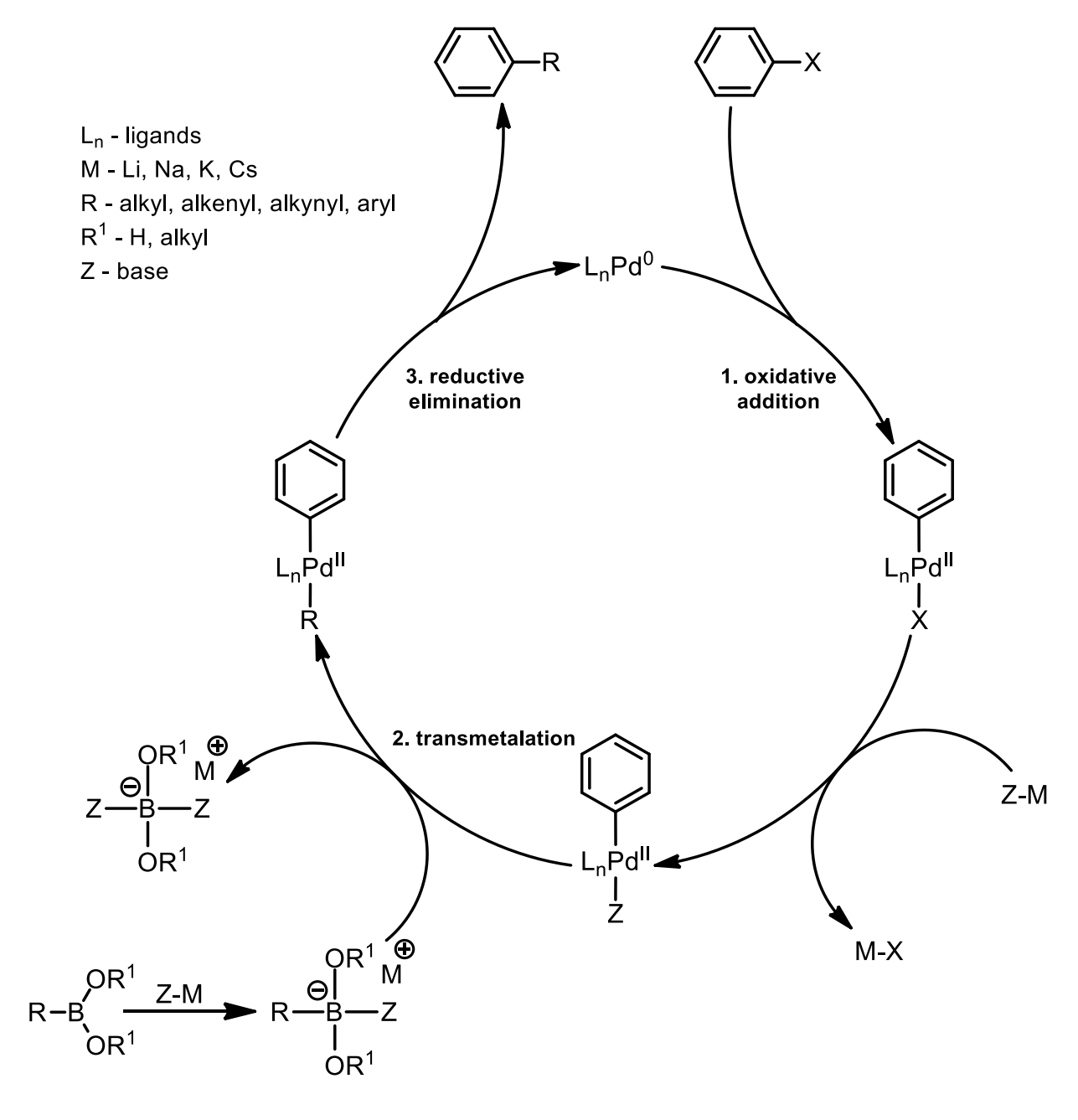
3. Syn- β -hydride elimination

Scheme 17 Syn-β-hydride elimination in Heck coupling reaction.

The last step of the Heck coupling proceeds via the elimination of the hydride anion from the coupling product (Scheme 17). Syn geometry of the palladium(II) complex and one of hydrogen atoms is essential for this step. It leads to the recreation of the double bond in the coupling product, and the eliminated hydride anion bounds to the metal complex centre. Due to the steric hinderance of substituents and bulky ligands, formation of *trans* alkenes is highly favoured. The palladium(II) complex is no longer covalently bounded to a carbon atom, but only weakly coordinated by π electrons from the newly formed double bond. The HPd(II)XL_n complex is a short-lived species, which easily eliminates HX when the base is added. In this way, palladium is being reduced from the +II to the 0 oxidation state and is liberated from the coupling product as the palladium(0) complex. This leads to the regeneration of the catalyst.

1.3.2.2 Suzuki coupling catalytic cycle[44], [57], [62]

Suzuki catalytic cycle consists of following steps (Scheme 18):



Scheme~18~Suzuki~coupling~reaction~catalytic~cycle.

1. Oxidative addition

$$\begin{array}{c} X \\ L_n Pd^0 \end{array}$$

Scheme 19 Oxidative addition step in Heck coupling reaction.

This step was also described in Heck coupling reaction, as it proceeds in the same manner and is crucial for all palladium catalysed coupling reactions (Scheme 19).

2. Transmetalation

$$R-B \xrightarrow{OR^{1}} Z-M \longrightarrow R^{1} \xrightarrow{\Theta} B \longrightarrow Z$$

$$\downarrow OR^{1}$$

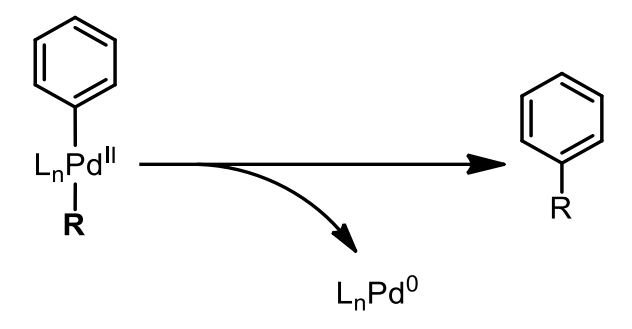
$$\uparrow OR^{1}$$

$$\downarrow O$$

Scheme 20 Transmetalation step of the Suzuki coupling reaction.

Transmetalation is the key step in Suzuki coupling. In this step, a coupling partner – a boronic acid, or its derivative, is activated by a base (Scheme 20). Basic environment is necessary for the activation of the coupling partner. Without a base, this reaction cannot occur. After activation, the boronic derivative is reacting with the palladium(II) complex formed in the first step of the reaction. Organic part of boronic derivative connects to the palladium(II) atom and boric acid salt is formed as a side product. Palladium(II) complex, containing organic parts coming from both of coupling partners, is being formed.

3. Reductive elimination



Scheme 21 Reductive amination step of the Suzuki coupling reaction.W

Reductive elimination is the last step of Suzuki coupling reaction. In this step, oxidation state of the palladium decreases from +II to 0, while coupling of fragments, coming from both of the (pseudo)halide and the boronic acid derivative, simultaneously occurs (Scheme 21). The final product of coupling is being formed and the catalyst is being regenerated. This step can be seen as reverse reaction to oxidative addition, and often is in equilibrium with it, as in case with oxidative addition of organic halides to palladium(0). However, newly formed C-C covalent bond is thermodynamically stable, thus this step of the Suzuki coupling is irreversible. This stability of formed products is the driving force of the Suzuki reaction.

1.3.2.3 Buchwald-Hartwig catalytic cycle[49], [63], [64]

Buchwald-Hartwig coupling reaction, in some steps, resembles some of other Palladium catalysed reactions. The first step is oxidative addition (Scheme 22).

$$\begin{array}{c} \text{NHR} \\ \text{NHR} \\ \text{NHR} \\ \text{S. reductive elimination} \\ \text{Ph}_2 \\ \text{Ph}_2 \\ \text{Ph}_2 \\ \text{Ph}_2 \\ \text{NHR} \\ \text{NaOtBu} \\ \text{NaOtBu} \\ \text{NaN} \\ \text{NaX} \\ \end{array}$$

Scheme 22 Buchwald-Hartwig catalytic cycle.

1. Oxidative addition

Scheme 23 Oxidative addition step of the Buchwald-Hartwig reaction.

This step was also described in Heck coupling reaction, as it proceeds in the same manner and is crucial for all palladium catalysed coupling reactions (Scheme 23). In the Buchwald-Hartwig reaction, bidentate ligands are most commonly used, as it reduces the chance of occurring of undesired β -hydride elimination reaction.

2. Activation and coordination of the amine

Scheme 24 Activation and coordination of the amine in the Buchwald-Hartwig reaction.

During this step, sodium tert-butoxide replaces halogen ligand and such a formed complex is more susceptible for coordination of the amine. Amine replaces tert-butoxide ligand and tert-butanol is formed as a side product (Scheme 24).

3. Reductive elimination

$$\begin{array}{c|c} & & & & \\ & \text{Ph}_2\text{P}, & & & \\ & \text{Ph}_2\text{P}, & \text{NHR} & -[\text{Pd}(\text{dppf})]^0 \end{array}$$

Scheme 25 Reductive elimination step in the Buchwald-Hartwig reaction.

This is the last step of the Buchwald-Hartwig coupling reaction. Amine complex collapses, oxidation state of the palladium decreases from +II to 0, original catalyst is restored and coupling product is formed (Scheme 25).

1.3.3 Applications of palladium-catalysed couplings in medicinal chemistry [65], [66]

Many pharmacologically active compounds contain aromatic ring systems or substituted arylamine motifs. Because of the ability to form new C-C or C-N bonds, palladium-catalysed coupling reactions allowed for the development and synthesis of numerous pharmaceutical drugs. Those kinds of reactions significantly accelerated development of medicinal chemistry.

Brexpiprazole can be an example of a pharmaceutical drug obtained with the use of palladium catalysed coupling (Scheme 26). Brexpiprazole is an atypical antipsychotic drug used in treatment of schizophrenia and major depressive disorder. One of the substrates is obtained via Buchwald-Hartwig reaction which is used to introduce piperazine into benzotiophene moiety.

Scheme 26 Synthesis of brexipiprazole with the use of Palladiu-catalysed coupling.

Another example of pharmaceutical drug obtained via palladium-catalysed coupling reactions is antihistamine drug olopatadine used in treatment of allergic conjunctivitis and allergic rhinitis (Scheme 27). One route to olopatadine is via the Sonogashira coupling with 3-butyn-1-ol and subsequent palladium catalysed intramolecular cyclization of the coupling product to olopatadine.

Scheme 27 Synthesis of olopatadine.

1.3.4 Applications of palladium-catalysed couplings in the synthesis of natural products[67]

Many natural products exhibit pharmacological activity. Some of them exist only in minute amounts and are particularly difficult to extract from organisms producing them. Assessment of pharmacological properties requires relatively large amounts of pure compounds. Those amounts are very often inaccessible by extraction, as many biological sources are rare and difficult to obtain. This makes chemical synthesis very often better option, as it gives access to high amounts of pure compounds, without need of handling of large volumes of rare raw biological materials.

Lynamycin D is a compound isolated from marine actinomycete bacteria. It has capability of fighting with drug-resistant pathogenic bacteria. It was successfully synthesized from simple substrates via the Suzuki coupling (Scheme 28).

Scheme 28 Synthesis of Lynamycin D.

Mycophenolic acid is a potent immunosuppressant drug isolated from *Penicillium sp.* Fungus. It is used in organ transplant and to treat various autoimmune diseases like Crohn's disease or lupus. The Stille coupling was successfully used to synthesize this compound (Scheme 29).

Scheme 29 Synthesis of mycophenolic acid via Stille coupling.

Lycorane is an alkaloid from the lycorine-type group. It does not possess any particular pharmaceutical activity, though it is used as a substrate for synthesis of alkaloid derivatives with various pharmaceutical activity. The intramolecular Heck reaction found its application in the synthesis of the (\pm) - γ -lycorane (Scheme 30).

Scheme 30 Synthesis of lycorane.

(+)-Anatoxin-a is a potent neuromuscular blocking agent isolated from cyanobacteria. It works as very potent agonist of nicotinic acetylcholine receptors. Although highly toxic, it is extensively used in studies of functions of nicotinic acetylcholine receptors. It is useful tool which gives insight into diseases characterised by low acetylcholine levels, for example myasthenia gravis or Alzheimer disease. One of the synthetic routes utilize the Sonogashira coupling (Scheme 31).

Scheme 31 Synthesis of (+)-anatoxin-a trifuloroacetate.

1.3.5 Uses of Palladium-catalysed couplings in optoelectronic applications

Palladium coupling reactions allow for creating and expanding aromatic ring systems forming extended conjugated π electron systems. Because of easiness and versatileness it is unsurprising that these reactions found their use in synthesis of various organic optoelectronic materials, including photosensitizers and photocatalysts, where conjugation of π electrons determine most of properties of these materials.

The Buchwald coupling reaction was used in synthesis of many OLED (Organic Light Emitting Diode) emitters. Example below is from the work reporting novel, highly efficient blue OLED emitter (Scheme 32).[68]

Scheme~32 Application of Buchwald coupling for synthesis of OLED emitter.

Another example shows application of the Suzuki coupling in synthesis of blue OLED emitter (Scheme 33).[69]

Scheme 33 Application of Suzuki coupling for synthesis of OLED emitter.

The Suzuki coupling was also employed in synthesis of an organic solar-cell sensitizer shown below (Scheme 34).[70]

 $Scheme\ 34$ Application of Suzuki coupling for synthesis of solar cell sensithizer.

2. AIM OF THE WORK

2.1 Introduction

Global warming is currently one of the biggest problem the humanity is facing. The rapid rise of Earth's average temperature is associated with increased incidence of wildfires, floods, hurricanes, and other extreme weather phenomena. Relying on fossil fuels speeds up climate change and deterioration of natural environment, therefore alternative energy sources are now the only rational and valid solutions for climate change problem.

There are many alternative energy sources to fossil fuels. Wind, geothermal, solar or water movement energy are among them. Those renewable sources have both advantages and disadvantages. Most of them are unpredictable, and they are bound to strict locations, i.e. sunny, or windy areas, or places with thermal springs. Such requirements make those energy sources less useful in areas where there are no thermal springs, and winds and sun occur in limited timeframe throughout the year. Mentioned problem can be solved by converting energy into storable fuel.

Hydrogen seems to be a perfect candidate for energy storage. It is a non-toxic gas with high energy density and low molecular weight. The only product of the combustion of hydrogen is water, making it fully environment friendly fuel. Hydrogen can be obtained from ubiquitous water; the only difficulty is a way in which it is obtained from water. There are various methods of hydrogen production from water. It can be produced by electrolysis, by thermolysis, or most recently by photocatalysis. In order for hydrogen to be fully environment friendly fuel, it must be obtained with the use of renewable energy sources. Therefore, using solar energy in photocatalytic water splitting is the most promising method for obtaining green hydrogen.[71][72]

2.2 AIM OF THE WORK

The aim of the work was to design, synthesize and verify the action of organic compounds that could be used as photocatalysts or photosensitizers in water splitting for the production of hydrogen. Compounds selected for the research are based on perylenediimide and benzothiadiazole cores, as there are reports of successfully working HER and OER photosensitizers and photocatalysts based on mentioned moieties. DFT calculations were used for screening of the target compounds.

2.3 TARGET COMPOUNDS

I divided the target compounds into the following groups:

2.3.1 Perylene diimides with donor-acceptor motif

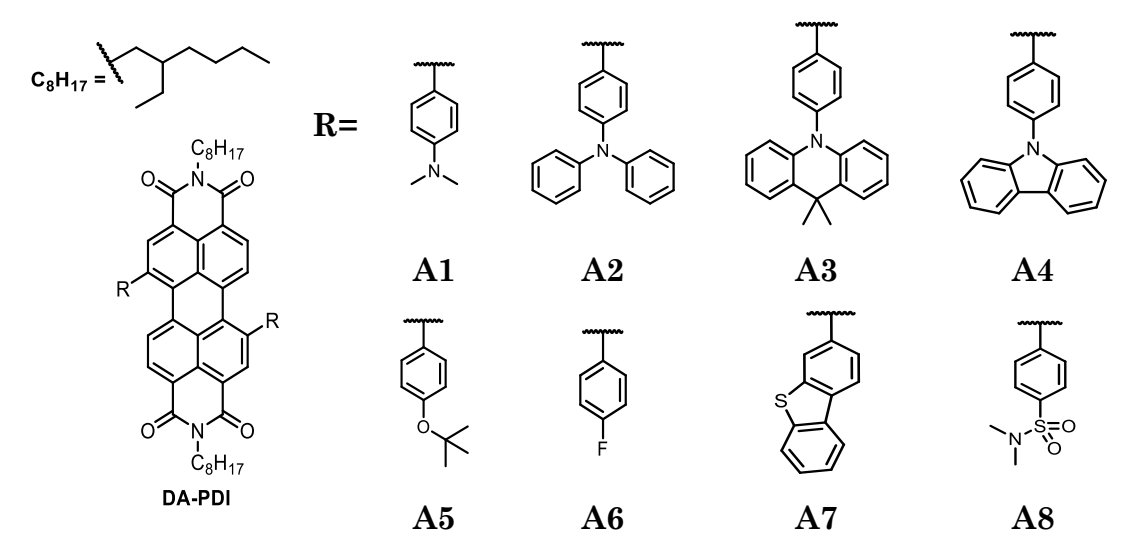


Figure 7 Target perylene diimides (PDI) with donor-acceptor (DA) motif.

2.3.1.1 Halogenated perylene diimides with donor-acceptor motif

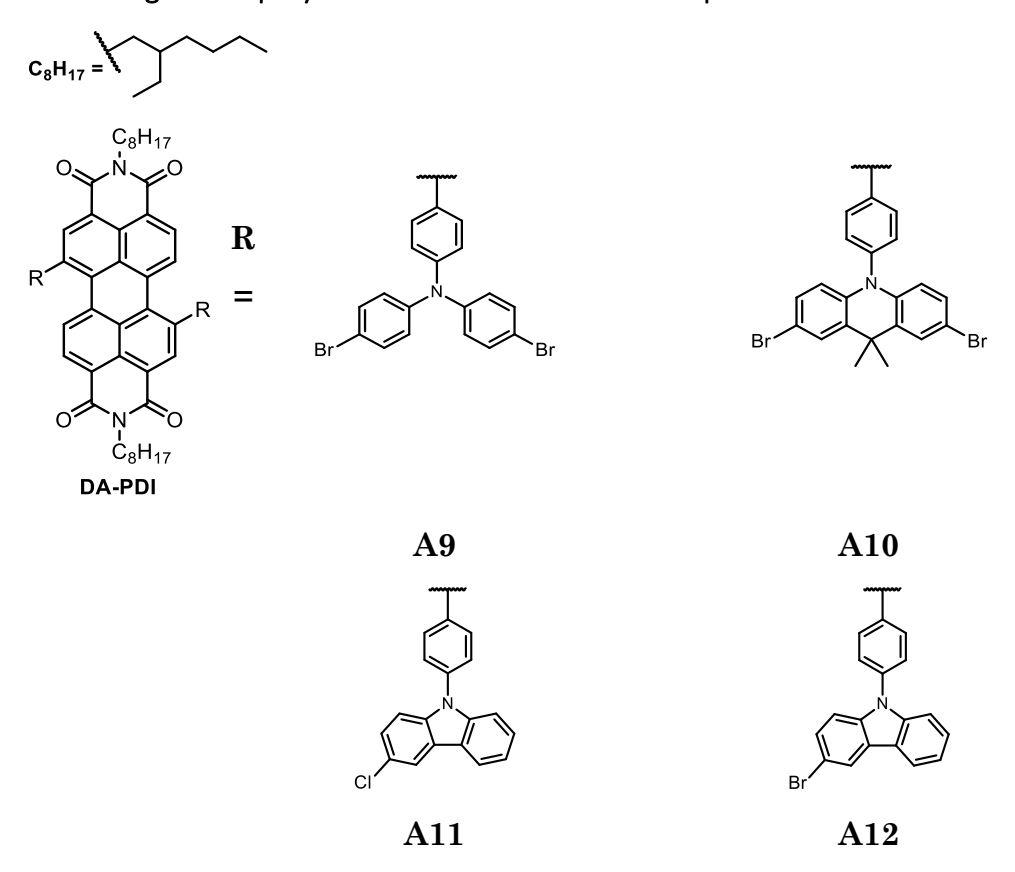


Figure 8 Target halogenated perylene diimides (PDI) with donor-acceptor (DA) motif.

2.3.2 Perylene diimides with anchor and donor-acceptor motif

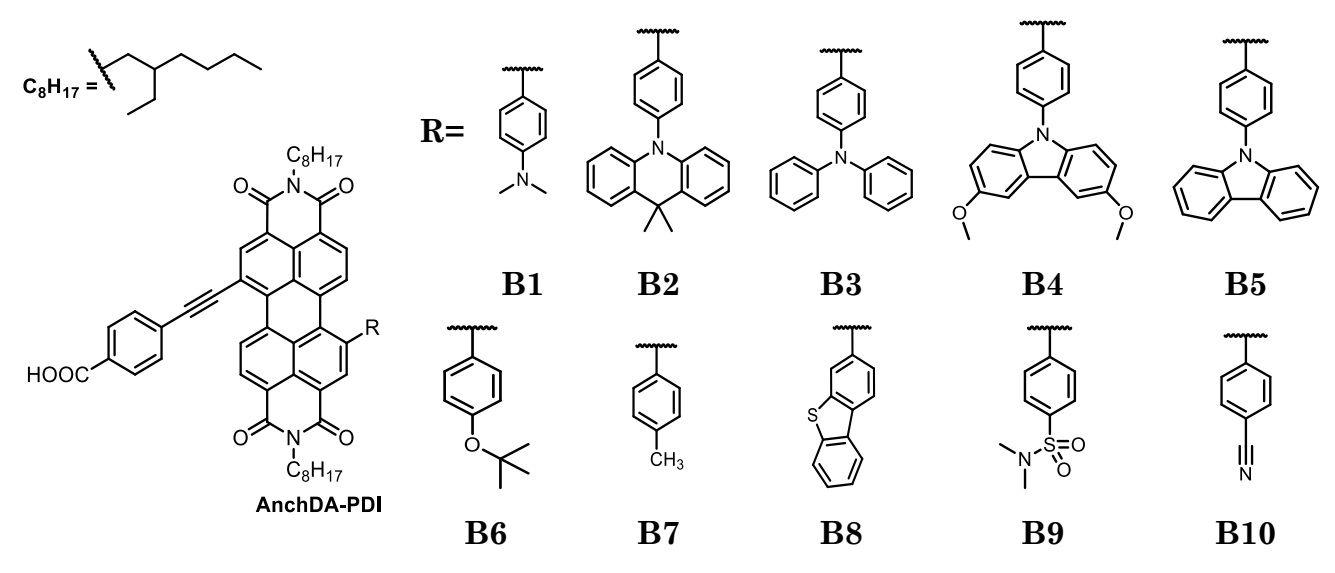


Figure 9 Target perylene diimides (PDI) with anchor and donor-acceptor motif (AnchDA).

2.3.2.1 Perylene monoimide model compound

Compounds from the **B** series were inspired by the already known photosensitizer based on perylene monoimide with anchoring group. Mentioned monoimide **M5** was synthesized as a model compound.

Figure 10 Model perylene monoimide ${\bf M5}$

2.3.2.2 Halogenated derivatives of perylene diimides with anchor and donor-acceptor motif

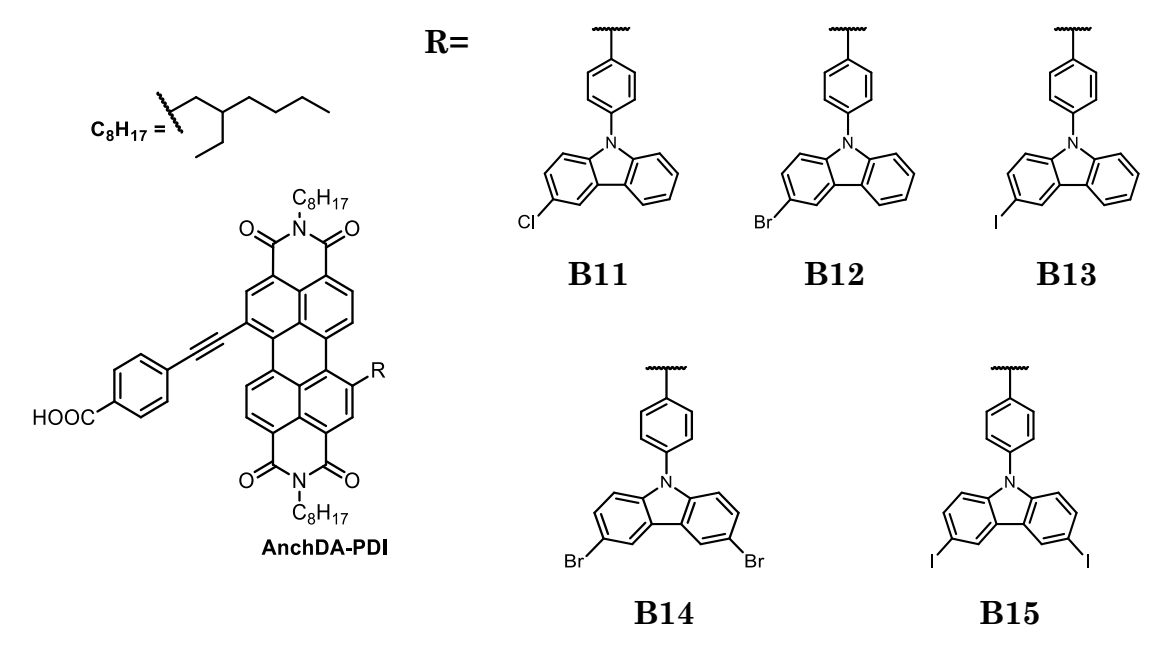


Figure 11 Halogenated derivatives of perylene diimides (PDI) with anchor and donor-acceptor motif (AnchDA-PDI).

2.3.3 Benzothiadiazoles

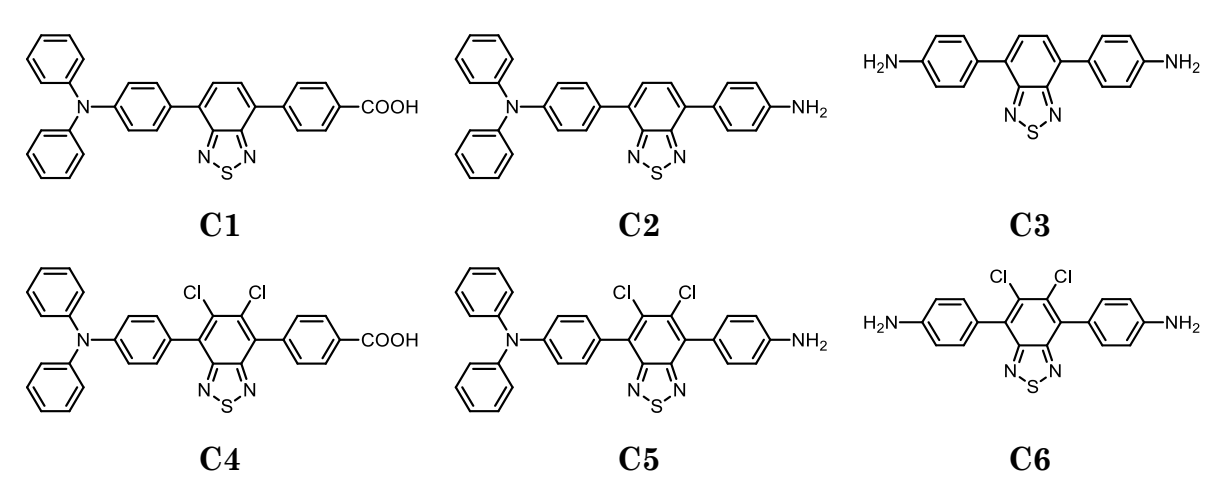


Figure 12 Target benzothiadiazoles

3. EXPERIMENTAL SECTION

General remarks

Solvents and chemical reagents were purchased and used without further purification. Triethylamine for Sonogashira coupling was dried with 4 Å molecular sieves. The Schlenk apparatus was used for selected reactions carried out in the absence of oxygen.

Progress of the reactions was monitored using Thin-Layer Chromatography (TLC) or High-Performance Liquid Chromatography (HPLC). TLC was conducted on aluminium plates coated with E. Merck Kieselgel 60 F254 (0.2 mmol), using the eluent systems indicated in procedures below. HPLC was performed on Dionex Ultimate 3000 with UV-Vis DAD detector on column Luna 5 μ m C18, TMS-endcapped 100 Å 250 x 4.6 mm.

Compounds were purified on chromatographic columns using silica gel SiliaFlash® GE60, 600-200 µm (70-230 mesh).

The 1 H and 13 C NMR spectra were recorded on the Bruker Avance III 500 MHz (500.13/125.76 MHz), using standard experimental conditions in CDCl₃, CDCl₃:Acetone-D₆ = 3:1, or THF-D₈, with internal Me₄Si.

Positive-ion mode MALDI-TOF mass spectra were obtained using the Bruker Biflex III spectrometer with 4-cyano-4-hydroxycinnamic acid or 2,5-dihydroxybenzoic acid matrices.

Density Functional Theory calculations were performed on Gaussian 16. The B3LYP hybrid functional along with Lan-L2DZ basis set were used.

Photocatalytic tests were done with the cooperation with Dr Illia Serdiuk's research group (E. Hoffman, M. Rybczyńska, M. Mońka) from Faculty of Mathematics, Physics and Informatics, University of Gdansk.

3.1 PERYLENE DIIMIDES

3.1.1 1,7-Dibromo-N,N'-bis(2-ethylhexyl)perylene-3,4:9,10-tetracarboxylic acid diimide (A0)

1,7-Dibromoperylene-3,4,9,10-tetracarboxylic dianhydride (1.1 g, 2 mmol) and 2-ethylhexylamine (5 mL, 3.95 g, 30.6 mmol) in glacial acetic acid (50 mL) were heated under the reflux for 24 h. Then, it was evaporated and the oily residue was added to the mixture of methanol and water (2:1 v:v). Crude product was filtered off under the reduced pressure, dried, and purified on column chromatography (eluent: chloroform : hexane : methanol, 100:100:1), Fraction containing purified product was evaporated to dryness yielding **A0** (1.1 g, 71%, orange-red powder); 1 H NMR (CDCl₃): δ 9.47 (d, J = 8.24 Hz, 2 H, H_{Ar}), 8.91 (s, 2 H, H_{Ar}), 8.68 (d, J = 7.94 Hz, 2 H, H_{Ar}), 4.18 (dd, J = 12.81 Hz, 7.94 Hz, 2 H, NCH), 4.12 (dd, J = 12.81 Hz, 7.02 Hz, 2 H, NCH'), 1.95 (hep, J = 6.41 Hz, 2 H, CH), 1.44-1.30 (m, 16 H, 8 x CH₂), 0.95 (t, J = 7.32 Hz, 6 H, 2 x CH₃), 0.90 (t, J = 7.02 Hz, 6 H, 2 x CH₃); MALDITOF-MS m/z: Calcd for C₄₀H₄₀Br₂N₂O₄ 770.1355; Found 771.174 (M+H)+.

3.1.2 General procedure for synthesis of bay-substituted perylene diimides with donor-acceptor motif (A1-A8)

Substrate A0 (77.2 mg, 0.1 mmol), boronic acid or its ester (2-8 eq), K₂CO₃ (276 mg, 2 mmol) and Pd(PPh₃)₄ (25 mg, 0.0216 mmol) were added to a round bottom flask equipped with a magnetic stir-bar and with silicone septum. The mixture of dioxane and water (5 mL, 4:1 v:v) was added thru the septum. Flask was connected to the Schlenk apparatus thru the injection needle and degassed 3 times by alternately opening vacuum and argon valve. After replacing the air in the flask with argon, everything was stirred on magnetic stirrer and heated in 50 °C for 12 h. After the reaction was completed, crude mixture was evaporated to dryness on rotary evaporator. Water (30 mL) was added to the dry residue and it was extracted with DCM. DCM extracts were evaporated to dryness and subsequently purified on column chromatography yielding A1-A8.

3.1.2.1 1,7-Bis(4-*N*,*N*-dimethylaminophenyl)-*N*,*N*-bis(2-ethylhexyl)perylene-3,4:9,10-tetracarboxylic acid diimide (A1)

Reaction of **A0** (25.7 mg, 0.0332 mmol) with 4-(*N*,*N*-dimethylamino)-phenylboronic acid (22 mg, 0.133 mmol, 4 eq) in the presence of K_2CO_3 (70 mg, 0.5 mmol) and Pd(PPh₃)₄ (5 mg, 0.004 mmol), followed by purification with column chromatography (eluent: chloroform : hexane, 1:1) led to **A1** (14.3 mg, 50%, dark green crystalline powder); ¹H NMR (CDCl₃): δ 8.43 (s, 2 H, H_{Ar}), 8.02 (d, *J* = 7.93 Hz, 2 H, H_{Ar}), 7.80 (d, *J* = 8.24 Hz, 2 H, H_{Ar}), 7.30 (d, *J* = 8.54 Hz, 4 H, H_{Ar}), 6.68 (d, *J* = 8.55 Hz, 4 H, H_{Ar}), 4.10 (dd, *J* = 13.12 Hz, *J* = 7.93 Hz, 2 H, NCH), 4.05 (dd, *J* = 13.12 Hz, *J* = 6.72 Hz, 2 H, NCH'), 2.99 (s, 12 H, 4 x CH₃), 1.87 (hep, *J* = 6.41 Hz, 2 H, CH), 1.31 (m, 8 H, 4 x CH₂), 1.24 (m, 8 H, 4 x CH₂), 0.86 (t, *J* = 7.32 Hz, 6 H, 2 x CH₃), 0.82 (t, *J* = 7.02 Hz, 6 H, 2 x CH₃); ¹³C NMR (CDCl₃): δ 163.0, 162.9 (C=O), 149.5, 140.1, 134.3, 130.7, 129.1, 128.4, 128.3, 127.9, 127.8, 128.1, 120.7, 120.1, 112.3 (C_{Ar}), 39.3 (CH₃), 43.2, 36.9, 29.8, 27.7, 23.0, 22.1, 13.1, 9.7 (C_{Alk}); MALDITOF-MS m/z: Calcd for C₅₆H₆₀N₄O₄ 852.461; Found 853.471 (M+H)⁺.

3.1.2.2 1,7-Bis(4-*N*,*N*-diphenylaminophenyl)-*N*,*N*-bis(2-ethylhexyl)perylene-3,4:9,10-tetracarboxylic acid diimide (A2)

Reaction of **A0** (53.27 mg, 0.069 mmol) with 4-(N,N-diphenylaminophenyl)-boronic acid (83 mg, 0.287 mmol, 4.16 eq) in the presence of K₂CO₃ (250 mg, 1.78 mmol) and Pd(PPh₃)₄ (15 mg, 0.012 mmol), followed by purification with column chromatography (eluent: toluene : ethyl acetate, 10:1) yielded **A2** (67,2 mg 89%, dark pink powder); ¹H NMR (CDCl₃): δ 8.61 (s, 2 H, H_{Ar}), 8.24 (d, J = 7.97 Hz, 2 H, H_{Ar}), 8.06 (d, J = 8.23 Hz, 2 H, H_{Ar}), 7.39 (d, J = 8.51 Hz, 4 H, H_{Ar}), 7.35 (t, J = 8.23/7.42 Hz, 8 H, H_{Ar}), 7.22 (d, J = 7.69 Hz, 8 H, H_{Ar}), 7.15 (d, J = 8.78 Hz, 4 H, H_{Ar}), 7.12 (t, J = 7.41 Hz, 4 H, H_{Ar}), 4.18 (dd, J = 12.91 Hz, 7.96 Hz, 2 H, NCH), 4.12 (dd, J = 12.91 Hz, 6.86 Hz, 2 H, NCH'), 1.97 (hep, J = 6.31 Hz, 2 H, CH), 1.46-1.38 (m, 8 H, 4 x CH₂), 1.37-1.29 (m, 8 H, 4 x CH₂), 0.95 (t, J = 7.41 Hz, 6 H, 2 x CH₃), 0.91 (t, J = 7.14/6.86 Hz, 6 H, 2 x CH₃); MALDITOF-MS m/z: Calcd for C₇₆H₆₈N₄O₄ 1100.524; Found 1101.430 (M+H)⁺

3.1.2.3 1,7-Bis[4-(9,9-Dimethyl-9,10-dihydroacridin-10-yl)phenyl]-*N*,*N*-bis(2-ethylhexyl)perylene-3,4:9,10-tetracarboxylic acid diimide (A3)

Reaction of **A0** (50.9 mg, 0.066 mmol) with 9,9-dimethyl-10-(4-(4,4,5,5-tetramethyl-1,3,2-dioxaborolan-2-yl)phenyl)-9,10-dihydroacridine (110 mg, 0.267 mmol, 4.05 eq) in the presence of K₂CO₃ (250 mg, 1.78 mmol) and Pd(PPh₃)₄ (15 mg, 0.012 mmol), followed by purification with column chromatography (eluent: toluene: ethyl acetate, 10:1) yielded **A3** (64.6 mg 83%, dark pink powder); ¹H NMR (CDCl₃): δ 8.82 (s, 2 H, H_{Ar}), 8.32 (d, J = 7.97 Hz, 2 H, H_{Ar}), 8.08 (d, J = 8.23 Hz, 2 H, H_{Ar}), 7.88 (d, J = 8.51 Hz, 4 H, H_{Ar}), 7.55 (t, J = 8.24/7.69 Hz, 8 H, H_{Ar}), 7.19 (td, J = 7.14 Hz, J = 1.37 Hz, 4 H, H_{Ar}), 7.04 (td, J = 7.14 Hz, J = 1.10 Hz, 4 H, H_{Ar}), 6.49 (dd, J = 8.24 Hz, J = 0.82 Hz, 4 H, H_{Ar}), 4.22 (dd, J = 13.18 Hz, J = 7.96 Hz, 2 H, NCH), 4.16 (dd, J = 13.18 Hz, J = 6.86 Hz, 2 H, NCH'), 1.99 (hep, J = 6.31/6.59 Hz, 2 H, CH), 1.76 (s, 12 H, 4 x CH₃), 1.43 (m, 8 H, 4 x CH₂), 1.35 (m, 8 H, 4 x CH₂), 0.98 (t, J = 7.41 Hz, 6 H, 2 x CH₃); MALDITOF-MS m/z: Calcd for C₈₂H₇₆N₄O₄ 1180.587; Found 1165.619 (M-CH₃)⁺, 1181.725 (M+H)⁺.

3.1.2.4 1,7-Bis-[4-(Carbazol-9-yl)phenyl]-*N*,*N*-bis(2-ethylhexyl)perylene-3,4:9,10-tetracarboxylic acid diimide (A4)

Reaction of **A0** (77.2 mg, 0.1 mmol) with 4-[(carbazol-9-yl)phenyl]boronic acid (229 mg, 0.8 mmol, 8 eq) in the presence of K_2CO_3 (276 mg, 2 mmol) and $Pd(PPh_3)_4$ (25 mg, 0.0216 mmol), followed by purification with column chromatography (eluent: toluene: ethyl acetate, 10:1) yielded **A4** (101 mg 92%, dark violet powder); (CDCl₃): δ 8.76 (s, 2 H, H_{Ar}), 8.33 (d, J = 8.24 Hz, 2 H, H_{Ar}), 8.19 (d, J = 7.69 Hz, 4 H, H_{Ar}), 8.09 (d, J = 7.96 Hz, 2 H, H_{Ar}), 7.84 (t, J = 8.24 Hz, 4 H, H_{Ar}), 7.75 (d, J = 8.51 Hz, 4 H, H_{Ar}), 7.52 (m, 8 H, H_{Ar}), 7.35 (m, J = 7.96 Hz, J = 7.68 Hz, 4 H, H_{Ar}), 4.19 (dd, J = 13.18 Hz, 7.69 Hz, 2 H, NCH), 4.14 (dd, J = 13.18 Hz, 6.59 Hz, 2 H, NCH'), 1.96 (hep, J = 6.31 Hz, 2 H, CH), 1.44-1.37 (m, 8 H, 4 x CH₂), 1.36-1.29 (m, 8 H, 4 x CH₂), 0.95 (t, J = 7.41 Hz, 6 H, 2 x CH₃), 0.89 (t, J = 7.14/6.87 Hz, 6 H, 2 x CH₃); MALDITOF-MS m/z: Calcd for $C_{76}H_{64}N_4O_4$ 1096.493; Found 1098.551 (M+2H)+.

3.1.2.5 1,7-Bis[4-(t-Butyloxy)phenyl]-*N*,*N*-bis(2-ethylhexyl)perylene-3,4:9,10-tetracarboxylic acid diimide (A5)

Reaction of **A0** (38.6 mg, 0.05 mmol) with 4-tert-butyloxyphenylboronic acid (21.4 mg, 0.11 mmol, 2,2 eq) in the presence of K₂CO₃ (40 mg, 0.289 mmol) and Pd(PPh₃)₄ (5 mg, 0.004 mmol), followed by purification with column chromatography (eluent: chloroform : hexane, 1:3) yielded **A5** (41.9 mg 92%, dark pink powder); ¹H NMR (CDCl₃): δ 8.57 (s, 2 H, H_{Ar}), 8.09 (d, J = 8.24 Hz, 2 H, H_{Ar}), 7.80 (d, J = 8.24 Hz, 2 H, H_{Ar}), 7.43 (d, J = 8.55 Hz, 4 H, H_{Ar}), 7.11 (d, J = 8.24 Hz, 4 H, H_{Ar}), 4.16 (dd, J = 13.12 Hz, J = 7.63 Hz, 2 H, NCH), 4.10 (dd, J = 13.13 Hz, J = 6.72 Hz, 2 H, NCH'), 1.93 (hep, J = 6.41/6.10 Hz, 2 H, CH), 1.45 (s, 18 H, 6 x CH₃), 1.38 (m, 8 H, 4 x CH₂), 1.32 (m, 8 H, 4 x CH₂), 0.94 (t, J = 7.63/7.32 Hz, 6 H, 2 x CH₃), 0.89 (t, J = 7.02/6.71 Hz, 6 H, 2 x CH₃); ¹³C NMR (CDCl₃): δ 163.8, 163.7 (C=O), 156.2, 140.7, 136.8, 135.3, 134.9, 132.4, 129.9, 129.8, 129.3, 129.2, 127.5, 125.4, 122.1, 121.8 (C_{Ar}), 29.0 (CH₃), 44.3, 38.0, 30.8, 28.7, 24.0, 23.1, 14.1, 10.7 (C_{Alk}); MALDITOF-MS m/z: Calcd for C₆₀H₆₆N₂O₆ 910.492; Found 911.532 (M+H)⁺.

3.1.2.6 1,7-Bis(4-fluorophenyl)-*N*,*N*-bis(2-ethylhexyl)perylene-3,4:9,10-tetracarboxylic acid

Reaction of **A0** (38.6 mg, 0.05 mmol) with 4-fluorophenylboronic acid (15.3 mg, 0.11 mmol, 2,2 eq) in the presence of K₂CO₃ (40 mg, 0.289 mmol) and Pd(PPh₃)₄ (5 mg, 0.004 mmol), followed by purification with column chromatography (eluent: chloroform : hexane, 1:2) yielded **A6** (33.0 mg 82%, dark pink powder); ¹H NMR (CDCl₃): δ 8.55 (s, 2 H, H_{Ar}), 8.16 (d, J = 8.24 Hz, 2 H, H_{Ar}), 7.76 (d, J = 8.24 Hz, 2 H, H_{Ar}), 7.52 (dd, J = 8.24 Hz, J = 5.18 Hz, 4 H, H_{Ar}), 7.21 (t, J = 8.54 Hz, J = 8.24 Hz, 4 H, H_{Ar}), 4.16 (dd, J = 13.12 Hz, J = 7.63 Hz, 2 H, NCH), 4.10 (dd, J = 13.13 Hz, J = 6.72 Hz, 2 H, 1.38 (m, 8 H, 4 x CH₂), 1.31 (m, 8 H, 4 x CH₂), 0.93 (t, J = 7.32 Hz, 6 H, 2 x CH₃), 0.89 (t, J = 7.02/6.41 Hz, 6 H, 2 x CH₃); ¹³C NMR (CDCl₃): δ 163.7, 163.6 (C=O), 162.1, 139.9, 138.0, 135.2, 134.6, 132.4, 131.0, 130.9, 130.1, 129.5, 129.2, 127.6, 122.3, 122.0, 117.5 (C_{Ar}), 44.3, 38.0, 30.7, 28.7, 24.0, 23.1, 14.1, 10.7 (C_{Alk}); MALDITOF-MS m/z: Calcd for C₅₂H₄₈F₂N₂O₄ 802.358; Found 801.043 (M-H)⁺.

3.1.2.7 1,7-Bis(4-Dibenzothiophen-3-yl)-*N,N*-bis(2-ethylhexyl)perylene-3,4:9,10-tetracarboxylic acid diimide (A7)

Reaction of A0 (31.2 mg, 0.041 mmol) with dibenzothiophene-3-boronic acid (30 mg, 0,13 mmol, 3,2 eq) in the presence of K_2CO_3 (70 mg, 0.51 mmol) and $Pd(PPh_3)_4$ (15 mg, 0.12 mmol), followed by purification with column chromatography (eluent: DCM: hexane, 1:4), yielded A7 (32.6 mg 81%, dark purple powder); MALDITOF-MS m/z: Calcd for $C_{64}H_{54}N_2O_4S_2$ 978.352; Found 980.400 (M+2H)+.

3.1.2.8 1,7-Bis[4-(*N*,*N*-Dimethylsulfamoyl)phenyl)]-*N*,*N*-bis(2-ethylhexyl)perylene-3,4:9,10-tetracarboxylic acid diimide (A8)

Reaction of **A0** (38.6 mg, 0.05 mmol) with 4-(dimethylaminosulfonamido)-phenylboronic acid (25.2 mg, 0.11 mmol, 2.2 eq) in the presence of K_2CO_3 (40 mg, 0.29 mmol) and $Pd(PPh_3)_4$ (5 mg, 0.04 mmol), followed by purification with column chromatography (eluent: chloroform : hexane, 1:2), yielded **A8** (32.3 mg 66%, dark pink powder); ¹H NMR (CDCl₃): δ 8.55 (s, 2 H, H_{Ar}), 8.16 (d, J = 8.24 Hz, 2 H, H_{Ar}),

7.76 (d, J = 8.24 Hz, 2 H, H_{Ar}), 7.52 (dd, J = 8.24 Hz, J = 5.18 Hz, 4 H, H_{Ar}), 7.21 (t, J = 8.54 Hz, J = 8.24 Hz, 4 H, H_{Ar}), 4.16 (dd, J = 13.12 Hz, J = 7.63 Hz, 2 H, NCH), 4.10 (dd, J = 13.13 Hz, J = 6.72 Hz, 2 H, 1.38 (m, 8 H, 4 x CH₂), 1.31 (m, 8 H, 4 x CH₂), 0.93 (t, J = 7.32 Hz, 6 H, 2 x CH₃), 0.89 (t, J = 7.02/6.41 Hz, 6 H, 2 x CH₃); 13C NMR (CDCl₃): δ 163.7, 163.6 (C=O), 162.1, 139.9, 138.0, 135.2, 134.6, 132.4, 131.0, 130.9, 130.1, 129.5, 129.2, 127.6, 122.3, 122.0, 117.5 (C_{Ar}), 44.3, 38.0, 30.7, 28.7, 24.0, 23.1, 14.1, 10.7 (C_{Alk}); MALDITOF-MS m/z: Calcd for C₅₆H₆₀N₄O₈S₂ 980.385; Found 981.473 (M+H)⁺.

3.1.3 General procedure for synthesis of chlorinated and brominated perylene diimides with donor-acceptor motif (A9-A12)

X=Cl or Br
$$X \longrightarrow X/H$$
 $X/H \longrightarrow X/H$ $C_8H_{17} \longrightarrow C_8H_{17} \longrightarrow X/H$ $X/H \longrightarrow X/H$ X

A2, A3 or A4 (1 eq.), N-chlorosuccinimide or N-bromosuccinimide (2-4.4 eq.) were dissolved in chloroform (5 mL) and stirred at 30 °C under argon for 12 h. The reaction mixture was protected from light. The reaction progress was monitored by the TLC analysis. After the completion of reaction solvent was evaporated and the residue was washed with a mixture of methanol and water (1:2 v:v). The obtained product was purified on column chromatography using DCM: Hexane, 1:1 (v:v) as the eluent.

3.1.3.1 1,7-Bis(4-*N*,*N*-di(4-bromophenyl)aminophenyl)-*N*,*N*-bis(2-ethylhexyl)perylene-3,4:9,10-tetracarboxylic acid diimide (A9)

Reaction of **A2** (10.6 mg, 0.0096 mmol) with N-bromosuccinimide (7.5 mg, 0.0421 mmol, 4.4 eq) yielded **A9** (13.3 mg 98%, dark pink powder); ¹H NMR (CDCl₃): δ 8.64 (s, 2 H, H_{Ar}), 8.25 (d, J = 7.96 Hz, 2 H, H_{Ar}), 8.04 (d, J = 7.96 Hz, 2 H, H_{Ar}), 7.47 (d, J = 8.79 Hz, 8 H, H_{Ar}), 7.44 (d, J = 8.51 Hz, 4 H, H_{Ar}), 7.15 (d, J = 8.51 Hz, 4 H, H_{Ar}), 7.08 (d, J = 8.79 Hz, 8 H, H_{Ar}), 4.19 (dd, J = 12.90 Hz, J = 7.96 Hz, 2 H, NCH), 4.13 (dd, J = 12.91 Hz, J = 6.86 Hz, 2 H, NCH'), 1.97 (hep, J = 6.32 Hz, 2 H, CH), 1.42 (m, 8 H, 4 x CH₂), 1.34 (m, 8 H, 4 x CH₂), 0.97 (t, J = 7.42/7.14 Hz, 6 H, 2 x CH₃), 0.92 (t, J = 7.14/6.86 Hz, 6 H, 2 x CH₃); MALDITOF-MS m/z: Calcd for C₇₆H₆₄Br₄N₄O₄ 1412.166; Found 1412.206, 1414.214, 1416.222, 1418.236, 1420.244 (M⁺)

3.1.3.2 1,7-Bis[4-(2,7-dibromo-9,9-dimethyl-9,10-dihydroacridin-10-yl)phenyl]-*N*,*N*-bis(2-ethylhexyl)perylene-3,4:9,10-tetracarboxylic acid diimide (A10)

$$\begin{array}{c|c} C_8H_{17} & Br \\ \hline O & N & O \\ \hline Br & C_8H_{17} \\ \hline A10 \\ \end{array}$$

Reaction of A3 (11.5 mg, 0.0097 mmol) with N-bromosuccinimide (7.6 mg, 0.043 mmol, 4.4 eq) yielded A10 (13.5 mg 93%, dark pink powder); ¹H NMR (CDCl₃): 8.79 (s, 2 H, H_{Ar}), 8.28 (d, J = 7.97 Hz, 2 H, H_{Ar}), 8.07 (d, J = 7.97 Hz, 2 H, H_{Ar}), 7.89 (d, J = 8.24 Hz, 4 H, H_{Ar}), 7.59 (d, J = 2.20 Hz, 4 H, H_{Ar}), 7.50 (d, J = 8.24 Hz, 4 H, H_{Ar}), 7.26 (dd, J = 8.79 Hz, J = 2.20 Hz, 4 H, H_{Ar}), 6.35 (d, J = 8.79 Hz, 4 H, H_{Ar}), 4.22 (dd, J = 13.18 Hz, J = 7.97 Hz, 2 H, NCH), 4.15 (dd, J = 13.18 Hz, J = 6.59 Hz, 2 H, NCH'), 1.99 (hep, J = 6.31/6.59 Hz, 2 H, CH), 1.71 (s, 12 H, 4 x CH₃), 1.43 (m, 8 H, 4 x CH₂), 1.35 (m, 8 H, 4 x CH₂), 0.98 (t, J = 7.69/7.13 Hz, 6 H, 2 x CH₃), 0.92 (t, J = 7.14 Hz, 6 H, 2 x CH₃); MALDITOF-MS m/z: Calcd for $C_{82}H_{72}Br_4N_4O_4$ 1492.229; Found 1491.165 (M-H)+, 1494.195, 1496.193, 1498.208, 1500.194 (M+).

3.1.3.3 1,7-Bis-[4-(3-chlorocarbazol-9-yl)phenyl]-*N*,*N*-bis(2-ethylhexyl)perylene-3,4:9,10-tetracarboxylic acid diimide (A11)

Reaction of **A4** (26.9 mg, 0.0245 mmol) with N-chlorosuccinimide (11.0 mg, 0.082 mmol, 3.3 eq) yielded difficult to separate mixture of **A11** and its impurity **impA11** (22,5 mg, dark pink powder); MALDITOF-MS m/z for **A11**: Calcd for $C_{76}H_{62}Cl_2N_4O_4$ 1164.415; Found 1165.411, 1166.383 (M⁺); MALDITOF-MS m/z for imp**A11**: Calcd for $C_{76}H_{60}Cl_4N_4O_4$ 1232.337; Found 1232.276, 1233.295, 1234.321, 1235.315, 1237.333, 1239.336 (M⁺).

3.1.3.4 1,7-Bis-[4-(3-bromocarbazol-9-yl)phenyl]-*N*,*N*-bis(2-ethylhexyl)perylene-3,4:9,10-etracarboxylic acid diimide (A12)

Reaction of **A4** (15.0 mg, 0.014 mmol) with N-bromosuccinimide (11.0 mg, 0.029 mmol, 2 eq) yielded difficult to separate mixture of **A12** and its impurities **impA12** and imp'**A12** (14.9 mg, dark violet powder); MALDITOF-MS m/z for **A12**: C₇₆H₆₂Br₂N₄O₄ 1252.314; Found 1252.155, 1254.167, 1256.178 (M+); MALDITOF-MS m/z for imp**A12**: Calcd for C₇₆H₆₁Br₃N₄O₄ 1330.244; Found 1330.063, 1332.071, 1336.097 (M+); MALDITOF-MS m/z for imp'**A12**: Calcd for C₇₆H₆₀Br₄N₄O₄ 1408.135; Found 1409.982, 1411.984, 1413.988, 1415.989 (M+).

3.1.4 1-Bromo-7-[2-(4-carboxyphenyl)ethynyl]-*N,N'*-bis(2-ethylhexyl)perylene-3,4:9,10-tetracarboxylic acid diimide (B0)

A0 (563 mg, 0.729 mmol), 4-ethynylbenzoic acid (106.8 mg, 0.73 mmol), CuI (12 mg, 0.063 mmol), Pd(PPh₃)4 (25 mg, 0.0216 mmol) were added to a round bottom flask equipped with a magnetic stir-bar and with silicone septum. Then, toluene (42 mL) and triethylamine (16 mL) were added thru the septum and flask was connected to the Schlenk apparatus thru the injection needle and degassed 3 times by alternately opening vacuum and argon valve. After replacing the air in the flask with argon, all was stirred on magnetic stirrer and heated in 50 °C for 12 h. After the reaction was completed, reaction mixture was evaporated to dryness and the crude product was purified on column chromatography. At first pure chloroform was used to remove unreacted A0, then 1% acetic acid in chloroform was used to wash down **B0**. Fraction containing purified product was evaporated to dryness yielding **B0** (249.8 mg, 41%, red-purple powder); ¹H NMR (CDCl3): δ $9.87 (d, J = 8.24 Hz, 1 H, H_{Ar}), 9.56 (dd, J = 8.23 Hz, J = 3.02 Hz, 1 H, H_{Ar}), 8.95 (s, J = 8.24 Hz, 1 H, H_{Ar}), 8.95 (s, J = 8$ 1 H, H_{Ar}), 8.87 (s, 1 H, H_{Ar}), 8.76 (dd, J = 7.96 Hz, J = 2.20 Hz, 1 H, H_{Ar}), 8.69 (d, J $= 7.92 \text{ Hz}, 1 \text{ H}, \text{H}_{Ar}$, 8.18 (d, J = 8.24 Hz, 2 H, H_{Ar}), 7.72 (d, J = 7.68 Hz, 2 H, H_{Ar}), 4.23 (dd, J = 12.63 Hz, J = 7.96 Hz, 2 H, NCH), 4.18 (dd, J = 12.90 Hz, J = 7.69 Hz,2 H, NCH'), 1.99 (hep, J = 6.45 Hz, 2 H, CH), $1.44 \text{ (m, 8 H, 4 x CH}_2)$, $1.36 \text{ (m, 8 H, 4 x CH}_2)$ $4 \times CH_2$), 0.99 (t, J = 7.41 Hz, 6 H, 2 x CH₃), 0.93 (t, J = 7.41 Hz, 6 H, 2 x CH₃); MALDITOF-MS m/z: Calcd for C₄₉H₄₅BrN₂O₆ 836.246; Found 836.216 (M)⁺.

3.1.5 General procedure for synthesis of bay-substituted perylene diimides with donor-acceptor motif with anchor (B1-B10)

Compound **B0** (20 mg, 0.0239 mmol), boronic acid or its ester (1.1-6.27 eq), K₂CO₃ (70 mg, 0.5 mmol) and Pd(PPh₃)₄ (7 mg, 0.006 mmol) were added to a round bottom flask equipped with a magnetic stir-bar and with silicone septum. Then, the mixture of dioxane and water (4 mL, 4:1 v:v) was added thru the septum. Flask was connected to the Schlenk apparatus thru the injection needle and degassed 3 times by alternately opening vacuum and argon valve. After replacing the air in the flask with argon, everything was stirred on magnetic stirrer and heated in 50 °C for 12 h. After the reaction was completed, reaction mixture was evaporated to dryness. Water (30 mL) was added to the dry residue and it was extracted with DCM. Organic extract was evaporated to dryness, and the residue was purified on column chromatography. At first pure chloroform was used to remove less polar impurities, then 1% acetic acid in chloroform was used to wash down **B1-B10**.

3.1.5.1 1-[4-(Dimethylamino)phenyl]-7-[3-(4-carboxyphenyl)prop-2-ynyl]-*N*,*N*′-bis(2-ethylhexyl) -3,4:9,10-tetracarboxylic acid diimide (B1)

Reaction of **B0** (23.5 mg, 0.028 mmol) with 4-(*N*,*N*-dimethylamino)phenylboronic acid (20.5 mg, 0.125 mmol, 4.46 eq) in the presence of K₂CO₃ (70 mg, 0.5 mmol) and Pd(PPh₃)₄ (7 mg, 0.006 mmol) gave **B1** (14.3 mg, 58%, dark crystalline powder with green reflexes); 1 H NMR (CDCl₃): δ 9.83 (d, J = 6.41 Hz, 1 H, H_{Ar}), 8.73 (s, 1 H, H_{Ar}), 8.70 (d, J = 8.24 Hz, 1 H, H_{Ar}), 8.59 (d, J = 10.99 Hz, 1 H, H_{Ar}), 8.15 (s, 1 H, H_{Ar}), 8.15 (bd, 1 H, H_{Ar}), 8.10 (d, J = 7.02 Hz, 1 H, HAr), 8.00 (d, J = 10.68 Hz, 1 H, H_{Ar}), 7.71 (d, J = 6.11 Hz, 2 H, H_{Ar}), 7.67 (d, J = 7.02 Hz, 1 H, H_{Ar}), 6.76 (d, J = 6.10 Hz, 1 H, H_{Ar}), 6.74 (d, J = 7.02 Hz, 1 H, H_{Ar}), 4.14 (m, 4 H, NCH, NCH'), 3.06 (s, 6 H, 2 x CH₃) 1.96 (m, 2 H, CH), 1.40 (m, 8 H, 4 x CH₂), 1.31 (m, 8 H, 4 x CH₂), 0.96 (bt, 6 H, 2 x CH₃), 0.90 (bt, 6 H, 2 x CH₃); MALDITOF-MS m/z: Calcd for C₅₇H₅₅N₃O₆ 877.409; Found 878.489 (M+H)⁺.

3.1.5.2 1-[4-(9,9-Dimethyl-9,10-dihydroacridin-10-yl)phenyl]-7-[2-(4-carboxyphenyl)ethynyl]-*N*,*N*'-bis(2-ethylhexyl)perylene-3,4:9,10-tetracarboxylic acid diimide (B2)

Reaction of **B0** (20.8 mg, 0.0249 mmol) with 9,9-dimethyl-10-(4-(4,4,5,5-tetramethyl-1,3,2-dioxaborolan-2-yl)phenyl)-9,10-dihydroacridine (20 mg, 0.0486 mmol, 1.95 eq) in the presence of K_2CO_3 (70 mg, 0.5 mmol) and $Pd(PPh_3)_4$ (7 mg 0.006 mmol) yielded **B2** (22.8 mg, 88%, dark pink powder); 1H NMR (CDCl3): δ 9.94 (d, J = 9.16 Hz, 1 H, H_{Ar}), 8.76 (d, J = 7.94 Hz, 1 H, H_{Ar}), 8.75 (s, 1 H, H_{Ar}), 8.19 (s, 1 H, H_{Ar}), 8.17 (d, J = 7.02 Hz, 2 H, H_{Ar}), 7.70 (m, 4 H, H_{Ar}), 7.56 (t, J = 7.63/7.33 Hz, 2 H, H_{Ar}), 7.49 (m, 4 H, H_{Ar}), 7.16 (d, J = 6.41 Hz, 1 H, H_{Ar}), 7.14 (d, J = 7.32 Hz, 1 H, H_{Ar}) 7.01 (2 x t, J = 7.63/7.33 Hz, 2 H, H_{Ar}), 6.44 (d, J = 8.24 Hz, 2 H, H_{Ar}) 4.23 (m, 2 H, NCH), 4.10 (m, 2 H, NCH), 1.96 (m, 2 H, CH), 1.72 (s, 6 H, 2 x CH₃), 1.43 (m, 8 H, 4 x CH₂), 1.35 (m, 8 H, 4 x CH₂), 0.99 (t, J = 7.62 Hz, 3 H, 1 x CH₃), 0.95 (t, J = 7.63 Hz, 3 H, 1 x CH₃), 0.90 (m, 6 H, 2 x CH₃); MALDITOF-MS m/z: Calcd for $C_{70}H_{63}N_3O_6$ 1041.472; Found 1043.842 (M+2H)+, 1026.916 (M-CH₃)+

3.1.5.3 1-[4-(Diphenylamino)phenyl]-7-[2-(4-carboxyphenyl)ethynyl]-*N,N'*-bis(2-ethylhexyl)perylene-3,4:9,10-tetracarboxylic acid diimide (B3)

Reaction of **B0** (20 mg, 0.0239 mmol) with 4-(*N*,*N*-diphenylamino)phenylboronic acid (20.1 mg, 0.0695 mmol, 2.91 eq) in the presence of K₂CO₃ (70 mg, 0.5 mmol) and Pd(PPh₃)₄ (7 mg 0.006 mmol), led to **B3** (23.1 mg, 96%, dark pink powder); ¹H NMR (TDF): δ 9.73 (d, J = 8.24 Hz, 1 H, HAr), 8.56 (d, J = 8.24 Hz, 1 H, HAr), 8.53 (d, J = 7.33 Hz, 1 H, HAr), 8.49 (s, 1 H, HAr), 8.46 (s, 1 H, HAr), 8.42 (d, J = 7.63 Hz, 1 H, HAr), 8.18 (m, 3 H, HAr), 7.96 (t, J = 8.54/8.24 Hz, 1 H, HAr), 7.72 (m, 2 H, HAr), 7.51 (m, 4 H, HAr), 7.18 (m, 4 H, HAr), 7.10 (m, 2 H, HAr), 7.06 (2 x t, J = 6.71 Hz, 2 H, HAr), 4.07 (m, 4 H, NCH, NCH'), 1.94 (m, 2 H, CH), 1.38 (m, 16 H, 8 x CH₂), 0.93 (m, 12 H, 4 x CH₃); MALDITOF-MS m/z: Calcd for C₆₇H₅₉N₃O₆ 1001.440; Found 1002.557 (M+H)⁺.

3.1.5.4 1-[4-(3,6-Dimethoxycarbazol-9-yl)phenyl]-7-[2-(4-carboxyphenyl)ethynyl]-*N,N'*-bis(2-ethylhexyl)perylene-3,4:9,10-tetracarboxylic acid diimide (B4)

Reaction of **B0** (21 mg, 0.025 mmol) with 3,6-dimethoxy-9-[4-(4,4,5,5-tetramethyl-1,3,2-dioxaborolan-2-yl)phenyl]carbazole (12.5 mg, 0.029 mmol, 1.16 eq) in the presence of K_2CO_3 (70 mg, 0.5 mmol) and $Pd(PPh_3)_4$ (7 mg 0.006 mmol) gave **B4** (23.1 mg, 87%, dark violet powder); ¹H NMR (TDF): δ 9.90 (d, J = 7.94 Hz, 1 H, HAr), 8.66 (d, J = 7.94 Hz, 1 H, HAr), 8.63 (s, 1 H, HAr), 8.55 (s, 1 H, HAr), 8.17 (d, J = 7.63 Hz, 1 H, HAr), 8.12 (d, J = 7.93 Hz, 2 H, HAr), 8.02 (d, J = 9.16 Hz, 2 H, HAr), 7.80 (d, J = 8.54 Hz, 2 H, HAr), 7.77-7.41 (m, 6 H, HAr), 7.02 (d, J = 7.02 Hz, 2 H, HAr), 4.09 (m, 4 H, NCH, NCH'), 3.90 (s, 6 H, 2 x OCH3), 1.98 (m, 2 H, CH), 1.37 (m, 16 H, 8 x CH₂), 0.96 (t, J = 7.63/7.02 Hz, 3 H, 1 x CH₃), 0.91 (m, 9 H, 3 x CH₃); MALDITOF-MS m/z: Calcd for $C_{69}H_{61}N_3O_8$ 1059.446; Found 1059.444 (M)+.

3.1.5.5 1-[4-(Carbazol-9-yl)phenyl]-7-[2-(4-carboxyphenyl)ethynyl]-*N,N'*-bis(2-ethylhexyl)perylene-3,4:9,10-tetracarboxylic acid diimide (B5)

Reaction of **B0** (109.5 mg, 0.13 mmol) with 4-[(carbazol-9-yl)phenyl]boronic acid (97.58 mg, 0.34 mmol, 2.61 eq) in the presence of K_2CO_3 (276 mg, 2 mmol) and $Pd(PPh_3)_4$ (25 mg, 0.022 mmol) yielded **B5** (111.2 mg, 85%, dark violet powder); ¹H NMR (CDCl3:Acetone-D₆ = 3:1): δ 9.77 (d, J = 8.24 Hz, 1 H, HAr), 8.64 (s, 1 H, HAr), 8.58 (d, J = 7.96 Hz, 1 H, HAr), 8.55 (s, 1 H, HAr), 8.08 (d, J = 8.24 Hz, 1 H, HAr), 7.98 (d, J = 6.87 Hz, 4 H, HAr), 7.92 (d, J = 7.96 Hz, 1 H, HAr), 7.61 (d, J = 8.24 Hz, 2 H, HAr), 7.55 (d, J = 7.68 Hz, 4 H, HAr), 7.32 (t, J = 8.24 Hz, 2 H, HAr), 7.31 (d, J = 8.24 Hz, 1 H, HAr), 7.13 (t, J = 7.41 Hz, 2 H, HAr), 7.12 (d, J = 6.86 Hz, 1 H, HAr), 4.00 (m, 2 H, NCH), 3.91 (m, 2 H, NCH'), 1.75 (m, 2 H, CH), 1.21 (m, 8 H, 4 x CH₂), 1.13 (m, 8 H, 4 x CH₂), 0.77 (t, J = 7.41 Hz, 3 H, 1 x CH₃), 0.74 (t, J = 7.69 Hz, 3 H, 1 x CH₃), 0.69 (m, 6 H, 2 x CH₃); MALDITOF-MS m/z: Calcd for $C_{67}H_{57}N_3O_6$ 999.425; Found 1000.662 (M+H)+.

3.1.5.6 1-[4-(*t*-Butyloxy)phenyl]-7-[2-(4-carboxyphenyl)ethynyl]-*N*,*N*′-bis(2-ethylhexyl)perylene-3,4:9,10-tetracarboxylic acid diimide (B6)

Reaction of **B0** (16 mg, 0.019 mmol) with 4-(t-butoxy)phenylboronic acid (16 mg, 0.082 mmol, 4.31 eq) in the presence of K₂CO₃ (70 mg, 0.5 mmol) and Pd(PPh₃)₄ (7 mg 0.006 mmol) led to **B6** (16.6 mg, 96%, dark pink powder); MALDITOF-MS m/z: Calcd for C₅₉H₅₈N₂O₇ 907.117; Found 908.934 (M+H)⁺.

3.1.5.7 1-(4-Methylphenyl)-7-[2-(4-carboxyphenyl)ethynyl]-*N,N'*-bis(2-ethylhexyl)perylene-3,4:9,10-tetracarboxylic acid diimide (B7)

Reaction of **B0** (13.9 mg, 0.0166 mmol) with p-tolylboronic acid (14 mg, 0.104 mmol, 6.27 eq) in the presence of $K_2CO_3(70 \text{ mg}, 0.5 \text{ mmol})$ and $Pd(PPh_3)_4$ (7 mg 0.006 mmol) gave **B7** (13.9 mg, 98%, dark purple powder); ¹H NMR (TDF): δ 9.69 (d, J = 8.24 Hz, 1 H, H_{Ar}), 8.53 (d, J = 8.24 Hz, 1 H, H_{Ar}), 8.43 (s, 1 H, H_{Ar}), 8.36 (s, 1 H, H_{Ar}), 8.10 (d, J = 7.32 Hz, 2 H, H_{Ar}), 7.90 (d, J = 6.71 Hz, 1 H, H_{Ar}), 7.74 (d, J = 7.63 Hz, 2 H, H_{Ar}), 7.71 (d, J = 8.85 Hz, 1 H, H_{Ar}), 7.68 (d, J = 8.24 Hz, 1 H, H_{Ar}), 7.66 (d, J = 8.24 Hz, 1 H, H_{Ar}), 7.50 (d, J = 7.02 Hz, 1 H, H_{Ar}), 7.66 (d, J = 8.24 Hz, 1 H, H_{Ar}),

4.09 (m, 2 H, NCH), 4.00 (m, 2 H, NCH'), 2.41 (s, 3 H, 1 x CH3), 1.96 (m, 1 H, CH), 1.88 (m, 1 H, CH'), 1.38 (m, 16 H, 8 x CH₂), 0.95 (t, J = 7.33 Hz, 3 H, 1 x CH₃), 0.91 (t, J = 7.02 Hz, 9 H, 3 x CH₃); MALDITOF-MS m/z: Calcd for $C_{56}H_{52}N_2O_6$ 848.383; Found 849.486 (M+H)+.

3.1.5.8 1-(4-Dibenzothiophen-3-yl)-7-[2-(4-carboxyphenyl)ethynyl]-*N,N'*-bis(2-ethylhexyl)perylene-3,4:9,10-tetracarboxylic acid diimide (B8)

In the reaction of **B0** (40.6 mg, 0.0485 mmol) with dibenzothiophen-3-ylboronic acid (40 mg, 0.175 mmol, 3.6 eq) in the presence of K₂CO₃ (140 mg, 1 mmol) and Pd(PPh₃)₄ (15 mg, 0.013 mmol) yielded **B8** (45.0 mg, 99%, dark purple powder); ¹H NMR (TDF): δ 9.87 (d, J = 7.63 Hz, 1 H, HAr), 8.75 (s, 1 H, HAr), 8.67 (d, J = 9.16 Hz, 1 H, HAr), 8.62 (bs, 1 H, HAr), 8.58 (s, 1 H, HAr), 8.13 (d, J = 8.24 Hz, 2 H, HAr), 8.02 (d, J = 8.54 Hz, 1 H, HAr), 7.98 (d, J = 9.16 Hz, 1 H, HAr), 7.93 (bt, 2 H, HAr), 8.79 (d, J = 6.41 Hz, 4 H, HAr), 7.76 (d, J = 7.02 Hz, 2 H, HAr), 4.12 (m, 2 H, NCH), 4.00 (m, 2 H, NCH'), 1.99 (m, 2 H, CH), 1.39 (m, 16 H, 8 x CH₂), 0.92 (m, 12 H, 4 x CH₃); MALDITOF-MS m/z: Calcd for C₆₁H₅₂N₂O₆S 940.355; Found 941.334 (M+H)⁺.

3.1.5.9 1-[4-(N,N-Dimethylsulfamoyl)phenyl)]-7-[2-(4-carboxyphenyl)ethynyl]-N,N'-bis(2-ethylhexyl)perylene-3,4:9,10-tetracarboxylic acid diimide (B9)

Reaction of **B0** (14.3 mg, 0.0171 mmol) with 4-(*N*,*N*-dimethylsulfamoyl)phenylboronic acid (14 mg, 0.061 mmol, 3.57 eq) in the presence of K₂CO₃ (70 mg, 0.5 mmol) and Pd(PPh₃)₄ (7 mg 0.006 mmol) led to **B9** (15.5 mg, 97%, dark pink powder); ¹H NMR (TDF): 8 9.80 (d, J = 7.94 Hz, 1 H, H_{Ar}), 8.65 (d, J = 8.24 Hz, 1 H, H_{Ar}), 8.48 (s, 1 H, H_{Ar}), 8.44 (s, 1 H, H_{Ar}), 8.10 (d, J = 7.63 Hz, 2 H, H_{Ar}), 8.06 (d, J = 8.24 Hz, 1 H, H_{Ar}), 7.90 (d, J = 7.63 Hz, 2 H, H_{Ar}), 7.74 (d, J = 7.32 Hz, 2 H, H_{Ar}), 7.69 (d, J = 7.63 Hz, 2 H, H_{Ar}), 7.66 (d, J = 7.94 Hz, 1 H, H_{Ar}), 4.12 (m, 2 H, NCH), 4.01 (m, 2 H, NCH'), 2.72 (s, 3 H, NCH3), 2.57 (s, 3 H, NCH3'), 1.97 (m, 1 H, CH), 1.89 (m, 1 H, CH'), 1.36 (m, 16 H, 8 x CH₂), 0.95 (t, J = 7.32 Hz, 3 H, 1 x CH₃), 0.91 (t, J = 7.32 Hz, 9 H, 3 x CH₃); MALDITOF-MS m/z: Calcd for C₅₇H₅₅N₃O₈S 941.371; Found 942.624 (M+H)⁺.

3.1.5.10 1-(4-Cyanophenyl)-7-[2-(4-carboxyphenyl)ethynyl]-*N,N'*-bis(2-ethylhexyl)perylene-3,4:9,10-tetracarboxylic acid diimide (B10)

Reaction of **B0** (15 mg, 0.0179 mmol) with 4-cyanophenylboronic acid (4 mg, 0.0272 mmol, 1.5 eq) in the presence of K_2CO_3 (70 mg, 0.5 mmol) and $Pd(PPh_3)_4$ (7 mg 0.006 mmol) gave **B10** (15.0 mg, 97%, dark violet powder); ¹H NMR (TDF): δ 9.80 (d, J = 7.94 Hz, 1 H, H_{Ar}), 8.64 (d, J = 7.63 Hz, 1 H, H_{Ar}), 8.50 (s, 1 H, H_{Ar}), 8.43 (s, 1 H, H_{Ar}), 8.10 (d, J = 7.33 Hz, 2 H, H_{Ar}), 8.05 (d, J = 7.93 Hz, 1 H, H_{Ar}), 7.87 (d, J = 7.33 Hz, 2 H, H_{Ar}), 7.74 (d, J = 7.32 Hz, 2 H, H_{Ar}), 7.70 (d, J = 7.32 Hz, 2 H, H_{Ar}), 7.66 (d, J = 7.94 Hz, 1 H, H_{Ar}), 4.12 (m, 2 H, NCH), 4.01 (m, 2 H, NCH'), 1.97 (m, 1 H, CH), 1.89 (m, 1 H, CH'), 1.38 (m, 16 H, 8 x CH₂), 0.93 (m, 12 H, 4 x CH₃); MALDITOF-MS m/z: Calcd for $C_{56}H_{49}N_3O_6$ 860.020; Found 861.430 (M+H)⁺.

3.1.6 General procedure for synthesis of chlorinated and brominated perylene diimides with donor-acceptor motif with anchor

B5 (1 eq.), N-chlorosuccinimide, N-bromosuccinimide, or a solution of N-iodosuccinimide in 1% acetic acid in chloroform (1.1-2.1 eq.) were added to chloroform (5 mL) and stirred at 30 °C under argon for 12 h. The reaction mixture was protected from light. The reaction progress was monitored by the HPLC analysis. After the completion of reaction solvent was evaporated and the residue was washed with the mixture of methanol and water (1:2, v:v). The obtained product was purified on column chromatography using chloroform first and then 1% acetic acid in chloroform as the eluent.

3.1.6.1 1-[4-(3-chlorocarbazol-9-yl)phenyl]-7-[2-(4-carboxyphenyl)-ethynyl]-*N*,*N*'-bis(2-ethyl-hexyl)perylene-3,4:9,10-tetracarboxylic acid diimide (B11)

Reaction of **B5** (12.8 mg, 0.0128 mmol) with N-chlorosuccinimide (3.2 mg, 0.024 mmol, 1.875 eq) yielded **B11** (10.9 mg 83%, violet powder); 1 H NMR (500 MHz, TDF): δ 10.03 (d, J = 7.81 Hz, 1 H, HAr), 8.82 (d, J = 10.25 Hz, 1 H, H_{Ar}), 8.80 (s, 1 H, H_{Ar}), 8.72 (s, 1 H, H_{Ar}), 8.29 (d, J = 8.30 Hz, 1 H, H_{Ar}), 8.28 (d, J = 7.32 Hz, 1 H, H_{Ar}), 8.23 (s, 1 H, H_{Ar}), 8.21 (d, J = 7.81 Hz, 1 H, H_{Ar}), 8.16 (d, J = 7.81 Hz, 2 H, H_{Ar}), 7.90 (d, J = 7.80 Hz, 1 H, H_{Ar}), 7.86 (d, J = 7.81 Hz, 2 H, H_{Ar}), 7.80 (d, J = 8.30 Hz, 2 H, H_{Ar}), 7.57 (d, J = 8.78 Hz, 1 H, H_{Ar}), 7.55 (d, J = 8.79 Hz, 1 H, H_{Ar}), 7.50 (t, J = 6.83/8.30 Hz, 1 H, H_{Ar}), 7.49 (d, J = 8.30 Hz, 1 H, H_{Ar}), 7.45 (d, J = 8.78 Hz, 1 H, H_{Ar}), 7.31 (t, J = 6.83/8.30 Hz, 1 H, H_{Ar}), 4.18 (m, 2 H, NCH), 4.11 (m, 2 H, NCH), 2.02 (m, 1 H, CH), 1.95 (m, 1 H, CH), 1.42 (m, 8 H, 4 x CH₂), 1.36 (m, 8 H, 4 x CH₂), 0.98 (t, J = 7.33/9.27 Hz, 3 H, 1 x CH₃), 0.92 (m, 9 H, 3 x CH₃); MALDITOF-MS m/z: Calcd for $C_{67}H_{56}ClN_3O_6$ 1034.650; Found 1035.4 (M+H)+.

3.1.6.2 1-[4-(3-bromocarbazol-9-yl)phenyl]-7-[2-(4-carboxyphenyl)ethynyl]-*N,N'*-bis(2-ethyl-hexyl)perylene-3,4:9,10-tetracarboxylic acid diimide (B12)

Reaction of **B5** (12.2 mg, 0.0122 mmol) with N-bromosuccinimide (4.2 mg, 0.0236 mmol, 1.9 eq) yielded **B12** (12.1 mg 92%, dark violet powder); ¹H NMR (500 MHz, TDF): δ 9.93 (d, J = 7.93 Hz, 1 H, H_{Ar}), 8.73 (d, J = 7.94 Hz, 1 H, H_{Ar}), 8.66 (s, 1 H, H_{Ar}), 8.65 (s, 1 H, H_{Ar}), 8.36 (s, 1 H, H_{Ar}), 8.24 (d, J = 7.93 Hz, 1 H, H_{Ar}), 8.19 (d, J = 7.94 Hz, 1 H, H_{Ar}), 8.13 (d, J = 7.63 Hz, 2 H, H_{Ar}), 8.09 (d, J = 7.93 Hz, 1 H, H_{Ar}), 7.86 (d, J = 7.93 Hz, 2 H, H_{Ar}), 7.80 (d, J = 7.93 Hz, 2 H, H_{Ar}), 7.78 (d, J = 7.33 Hz, 2 H, H_{Ar}), 7.55 (d, J = 7.32 Hz, 2 H, H_{Ar}), 7.48 (t, J = 7.32 Hz, 1 H, H_{Ar}), 7.47 (d, J = 7.32 Hz, 1 H, H_{Ar}), 7.31 (t, J = 7.32 Hz, 1 H, H_{Ar}), 4.16 (m, 2 H, NCH), 4.06 (m, 2 H, NCH'), 2.00 (m, 1 H, CH), 1.93 (m, 1 H, CH'), 1.45-1.31 (m, 16 H, 8 x CH₂), 0.97 (t, J = 7.32/9.16 Hz, 3 H, 1 x CH₃), 0.92 (m, 9 H, 3 x CH₃); MALDITOF-MS m/z: Calcd for C₆₇H₅₆BrN₃O₆ 1077.335; Found 1077.4, 1079.5 (M)⁺.

3.1.6.3 1-[4-(3-iodocarbazol-9-yl)phenyl]-7-[2-(4-carboxyphenyl)ethynyl]-*N,N'*-bis(2-ethyl-hexyl)perylene-3,4:9,10-tetracarboxylic acid diimide (B13)

Reaction of **B5** (11.0 mg, 0.011 mmol) with N-iodosuccinimide (2.7 mg, 0.012 mmol, 1.1 eq) dissolved in 1 mL of 1% acetic acid in chloroform, yielded **B13** (10.1 82%, dark violet powder); 1 H NMR (500 MHz, TDF): δ 9.94 (d, J = 8.24 Hz, 1 H, H_{Ar}), 8.74 (d, J = 8.24 Hz, 1 H, H_{Ar}), 8.68 (s, 1 H, H_{Ar}), 8.66 (s, 1 H, H_{Ar}), 8.55 (s, 1 H, H_{Ar}), 8.24 (d, J = 7.94 Hz, 1 H, H_{Ar}), 8.18 (d, J = 7.01 Hz, 1 H, H_{Ar}), 8.13 (d, J = 7.94 Hz, 2 H, H_{Ar}), 8.09 (d, J = 8.24 Hz, 1 H, H_{Ar}), 7.86 (d, J = 7.94 Hz, 2 H, H_{Ar}), 7.81 (d, J = 7.01 Hz, 2 H, H_{Ar}), 7.77 (d, J = 7.93 Hz, 2 H, H_{Ar}), 7.72 (d, J = 9.16 Hz, 1 H, H_{Ar}), 7.50 (d, J = 7.32 Hz, 1 H, H_{Ar}), 7.48 (t, J = 7.94 Hz, 1 H, H_{Ar}), 7.37 (d, J = 8.54 Hz, 1 H, H_{Ar}), 7.30 (t, J = 7.94 Hz, 1 H, H_{Ar}), 4.16 (m, 2 H, NCH), 4.07 (m, 2 H, NCH), 2.01 (m, 1 H, CH), 1.93 (m, 1 H, CH), 1.45-1.31 (m, 16 H, 8 x CH₂), 0.97 (t, J = 7.02/8.54 Hz, 3 H, 1 x CH₃), 0.91 (m, 9 H, 3 x CH₃); MALDITOF-MS m/z: Calcd for C₆₇H₅₆IN₃O₆ 1125.321; Found 1125.5 (M)+, 1126.5 (M+H)+.

3.1.6.4 1-[4-(3,6-dibromocarbazol-9-yl)phenyl]-7-[2-(4-carboxyphenyl)ethynyl]-*N,N'*-bis(2-ethylhexyl)perylene-3,4:9,10-tetracarboxylic acid diimide (B14)

Reaction of **B5** (10.0 mg, 0.01 mmol) with N-bromosuccinimide (3.7 mg, 0.021 mmol, 2.1 eq) yielded **B14** (10.1 mg 87%, dark violet powder); MALDITOF-MS m/z: Calcd for $C_{67}H_{55}Br_2N_3O_61155.246$; Found 1154.3, 1156.3, 1158.3, 1160.3 (M)⁺.

3.1.6.5 1-[4-(3,6-diiodocarbazol-9-yl)phenyl]-7-[2-(4-carboxyphenyl)ethynyl]-*N,N'*-bis(2-ethylhexyl)perylene-3,4:9,10-tetracarboxylic acid diimide (B15)

Reaction of **B5** (9.8 mg, 0.0098 mmol) with N-iodosuccinimide (4.7 mg, 0.021 mmol, 2.1 eq) yielded **B15** (11.4 mg 92%, dark violet powder); ¹H NMR (500 MHz, TDF): δ 10.01 (d, J = 8.55 Hz, 1 H, H_{Ar}), 8.78 (d, J = 8.24 Hz, 1 H, H_{Ar}), 8.77 (s, 1 H, H_{Ar}), 8.69 (s, 1 H, H_{Ar}), 8.59 (s, 2 H, H_{Ar}), 8.26 (d, J = 7.63 Hz, 1 H, H_{Ar}), 8.14 (d, J = 8.24 Hz, 2 H, H_{Ar}), 8.12 (d, J = 7.94 Hz, 1 H, H_{Ar}), 7.88 (d, J = 7.93 Hz, 2 H, H_{Ar}), 7.84 (d, J = 8.24 Hz, 2 H, H_{Ar}), 7.76 (d, J = 7.94 Hz, 4 H, H_{Ar}), 7.37 (d, J = 8.54 Hz, 2 H, H_{Ar}), 4.16 (m, 2 H, NCH), 4.09 (m, 2 H, NCH'), 2.01 (m, 1 H, CH), 1.94 (m, 1 H, CH'), 1.38 (m, 16 H, 8 x CH₂), 0.97 (t, J = 7.33 Hz, 3 H, 1 x CH₃), 0.91 (m, 9 H, 3

x CH₃); MALDITOF-MS m/z: Calcd for C₆₇H₅₅I₂N₃O₆ 1251.218; Found 1252.4

 $(M+H)^{+}$.

3.2 PERYLENEMONOIMIDE WITH ANCHOR MOIETY

 $Scheme~35~{\rm Synthetic~route~to~model~perylene~monoimide~\bf M5}.$

3.2.1.1 N-(2,5-di-tert-butylphenyl)perylene-3,4-dicarboxylic imide (M1)

Perylene-3,4,9,10-tetracarboxylic dianhydride (5.5 g, 14 mmol) and 2,5-ditert-butylaniline (1.575 g, 7.65 mmol), Zn(OAc)₂·2H₂O (0.65 g, 3 mmol), imidazole (28 g) were placed in Teflon autoclave reactor and heated in 190 °C furnace for 24 h. The reactor was cooled down to the room temperature and 150 ml of 1:1 mixture of 2 M HCl and MeOH was added to the reaction mixture. The precipitate was filtered off on a glass fritted funnel and air dried. The crude product was dissolved in 100 ml of DCM and filtered thru the column filled with silica gel. First less polar, yellow side products were eluted and discarded and then 400 mL of DCM was used to elute red M1. Fraction containing title compound was concentrated to 75 mL and 100 mL of hot methanol was added. The solution was left in the fridge at 4 °C for 24 hours after which precipitated solid was filtered-off on the glass fritted funnel. The solid was air dried yielding M1 (1.53 g, 21%, brick-red powder); MALDITOF-MS m/z: Calcd for C₃₆H₃₁NO₂ 509.235; Found 510.286 (M+H)⁺.

3.2.1.2 1,6,9-tribromo-N-(2,5-di-tert-butylphenyl)perylene-3,4-dicarboxylic imide (M2)

M2

Bromine (0.71 mL, 13.7 mmol) dissolved in chloroform (5 mL) was added dropwise to the solution of M1 (122.2 mg, 0.24 mmol) in chloroform (10 mL). The mixture was heated in 60 °C for 4 h. After the reaction was completed, it was washed with aqueous saturated solution of Na₂S₂O₃ and then evaporated to dryness. The dry residue was purified on column chromatography (eluent: chloroform: hexane 2:1). Fraction containing purified product was evaporated to dryness, which yields M2 (77.6 mg, 43%, brick-red powder); ¹H NMR (CDCl₃): δ $9.32 \text{ (dd, } J = 7.63 \text{ Hz, } J = 0.92 \text{ Hz, } 1 \text{ H, } H_{Ar}), 9.11 \text{ (d, } J = 8.24 \text{ Hz, } 1 \text{ H, } H_{Ar}), 8.92 \text{ (s, } 1 \text{ Hz, } 1 \text{ Hz, } 1 \text{ Hz})$ 1 H, H_{Ar}), 8.90 (s, 1 H, H_{Ar}), 8.44 (dd, J = 8.24 Hz, J = 0.91 Hz, 1 H, H_{Ar}), 7.98 (d, J $= 8.24 \text{ Hz}, 1 \text{ H}, \text{ H}_{Ar}$, 7.80 (t, J = 8.24/7.93 Hz, 1 H, H_{Ar}), 7.60 (d, J = 8.55 Hz, 1 H, H_{Ar}), 7.47 (dd, J = 8.54 Hz, J = 2.44 Hz, 1 H, H_{Ar}), 6.98 (d, J = 2.12 Hz, 1 H, H_{Ar}), 1.33 (s, 9 H, 3 x CH₃), 1.30 (s, 9 H, 3 x CH₃); MALDITOF-MS m/z: Calcd for C₃₆H₂₈Br₃NO₂ 742.967; Found 743.474, 745.486, 747.492 (M)+.

3.2.1.3 9-bromo-1,6-di(4-tert-butylphenoxy)-N-(2,5-di-tert-butylphenyl)perylene-3,4-dicarboxylic imide (M3)

A solution of **M2** (51 mg, 0.0684 mmol), 4-tert-butylphenol (21.6 mg, 0.144 mmol, 2.11 eq) and anhydrous K_2CO_3 (70 mg, 0.51 mmol) in anhydrous DMF (1.7 mL) was heated and stirred at 100 °C for 18 h. After that time, the solution was allowed to cool to room temperature and 3.5 mL of water was added. The formed precipitate was filtered off on a glass fritted funnel and washed with 5 mL of cold $H_2O/MeOH$ (1:1) mixture. The crude product was purified on column chromatography (eluent: DCM: hexane 1:1). Fraction containing purified product was evaporated to dryness yielding **M3** (30 mg, 49%, red-purple powder); MALDITOF-MS m/z: Calcd for $C_{56}H_{54}BrNO_4$ 883.324; Found 883.619, 884.629, 885.651 (M)+.

3.2.1.4 9-[2-(4-methoxycarbonylphenyl)ethynyl]-1,6-di(4-tert-butylphenoxy)-N-(2,5-di-tert-butylphenyl)perylene-3,4-dicarboxylic imide (M4)

M3 (16 mg, 0.0181 mmol), methyl 4-ethynylbenzoate (8.4 mg, 0.052 mmol, 2.9 eq.), dry toluene (3 mL), dry triethylamine (1 mL) and a stir-bar were added to a screw-cap vial. Argon gas was bubbled through the solution for 30 minutes. After that time Pd(PPh₃)₄ (4 mg) and CuI (4 mg) were added to the solution and bubbling of argon gas was continued for another 30 minutes. Next, the vial was screwcapped and wrapped in aluminium foil to protect from light. It was then stirred and heated in 60 °C for 24 hours. After the reaction was completed, solvents were evaporated to dryness. Crude product was purified on a column chromatography (eluent: DCM: hexane 2:1). Fraction containing purified product was evaporated to dryness yielding M4 (16 mg, 91%, red-purple powder); ¹H NMR (CDCl₃): δ 9.43 $(d, J = 7.58 \text{ Hz}, 1 \text{ H}, H_{Ar}), 9.34 (d, J = 8.24 \text{ Hz}, 1 \text{ H}, H_{Ar}), 8.54 (d, J = 8.24 \text{ Hz}, 1 \text{ H}, H_{Ar})$ H_{Ar}), 8.31 (s, 1 H, H_{Ar}), 8.29 (s, 1 H, H_{Ar}), 8.08 (d, J = 8.24 Hz, 2 H, H_{Ar}), 8.02 (d, J = 8.24 Hz, 2 H, H_{Ar}), 8.02 (d, J = 8.24 Hz, 2 H, H_{Ar}), 8.02 (d, J = 8.24 Hz, 2 H, H_{Ar}), 8.02 (d, J = 8.24 Hz, 2 H, H_{Ar}), 8.02 (d, J = 8.24 Hz, 2 H, H_{Ar}), 8.02 (d, J = 8.24 Hz, 2 H, H_{Ar}), 8.02 (d, J = 8.24 Hz, 2 H, H_{Ar}), 8.02 (d, J = 8.24 Hz, 2 H, H_{Ar}), 8.02 (d, J = 8.24 Hz, 2 H, H_{Ar}), 8.02 (d, J = 8.24 Hz, 2 H, H_{Ar}), 8.02 (d, J = 8.24 Hz, 2 H, H_{Ar}), 8.02 (d, J = 8.24 Hz, 2 H, H_{Ar}), 8.02 (d, J = 8.24 Hz, 2 H, H_{Ar}), 8.02 (d, J = 8.24 Hz, 2 H, H_{Ar}), 8.02 (d, J = 8.24 Hz, H_{Ar}), 8.03 (d, J = 8.24 Hz, H_{Ar}), 8.04 (d, J = 8.24 $= 8.24 \text{ Hz}, 4 \text{ H}, \text{H}_{Ar}), 7.85 \text{ (d, } J = 8.24 \text{ Hz}, 1 \text{ H}, \text{H}_{Ar}), 7.72 \text{ (m, } 3 \text{ H}, \text{H}_{Ar}), 7.59 \text{ (d, } J = 8.24 \text{ Hz}, 1 \text{ H}, \text{H}_{Ar}), 7.85 \text{ (d, } J = 8.24 \text{ Hz}, 1 \text{ H}, \text{H}_{Ar}), 7.85 \text{ (d, } J = 8.24 \text{ Hz}, 1 \text{ H}, \text{H}_{Ar}), 7.85 \text{ (d, } J = 8.24 \text{ Hz}, 1 \text{ H}, \text{H}_{Ar}), 7.85 \text{ (d, } J = 8.24 \text{ Hz}, 1 \text{ H}, \text{H}_{Ar}), 7.85 \text{ (d, } J = 8.24 \text{ Hz}, 1 \text{ H}, \text{H}_{Ar}), 7.85 \text{ (d, } J = 8.24 \text{ Hz}, 1 \text{ H}, \text{H}_{Ar}), 7.85 \text{ (d, } J = 8.24 \text{ Hz}, 1 \text{ H}, \text{H}_{Ar}), 7.85 \text{ (d, } J = 8.24 \text{ Hz}, 1 \text{ H}, \text{H}_{Ar}), 7.85 \text{ (d, } J = 8.24 \text{ Hz}, 1 \text{ H}, \text{H}_{Ar}), 7.85 \text{ (d, } J = 8.24 \text{ Hz}, 1 \text{ H}, \text{H}_{Ar}), 7.85 \text{ (d, } J = 8.24 \text{ Hz}, 1 \text{ H}, \text{H}_{Ar}), 7.85 \text{ (d, } J = 8.24 \text{ Hz}, 1 \text{ H}, \text{H}_{Ar}), 7.85 \text{ (d, } J = 8.24 \text{ Hz}, 1 \text{ H}, \text{H}_{Ar}), 7.85 \text{ (d, } J = 8.24 \text{ Hz}, 1 \text{ H}, \text{H}_{Ar}), 7.85 \text{ (d, } J = 8.24 \text{ Hz}, 1 \text{ H}, \text{H}_{Ar}), 7.85 \text{ (d, } J = 8.24 \text{ Hz}, 1 \text{ H}, \text{H}_{Ar}), 7.85 \text{ (d, } J = 8.24 \text{ Hz}, 1 \text{ H}, \text{H}_{Ar}), 7.85 \text{ (d, } J = 8.24 \text{ Hz}, 1 \text{ H}, \text{H}_{Ar}), 7.85 \text{ (d, } J = 8.24 \text{ Hz}, 1 \text{ H}, \text{H}_{Ar}), 7.85 \text{ (d, } J = 8.24 \text{ Hz}, 1 \text{ H}, \text{H}_{Ar}), 7.85 \text{ (d, } J = 8.24 \text{ Hz}, 1 \text{ H}, \text{H}_{Ar}), 7.85 \text{ (d, } J = 8.24 \text{ Hz}, 1 \text{ H}, \text{H}_{Ar}), 7.85 \text{ (d, } J = 8.24 \text{ Hz}, 1 \text{ H}, \text{H}_{Ar}), 7.85 \text{ (d, } J = 8.24 \text{ Hz}, 1 \text{ H}, \text{H}_{Ar}), 7.85 \text{ (d, } J = 8.24 \text{ Hz}, 1 \text{ H}, \text{H}_{Ar}), 7.85 \text{ (d, } J = 8.24 \text{ Hz}, 1 \text{ H}, \text{H}_{Ar}), 7.85 \text{ (d, } J = 8.24 \text{ Hz}, 1 \text{ H}, \text{H}_{Ar}), 7.85 \text{ (d, } J = 8.24 \text{ Hz}, 1 \text{ H}, \text{H}_{Ar}), 7.85 \text{ (d, } J = 8.24 \text{ Hz}, 1 \text{ H}, \text{H}_{Ar}), 7.85 \text{ (d, } J = 8.24 \text{ Hz}, 1 \text{ H}, \text{H}_{Ar}), 7.85 \text{ (d, } J = 8.24 \text{ Hz}, 1 \text{ H}, \text{H}_{Ar}), 7.85 \text{ (d, } J = 8.24 \text{ Hz}, 1 \text{ H}, \text{H}_{Ar}), 7.85 \text{ (d, } J = 8.24 \text{ Hz}, 1 \text{ H}, \text{H}_{Ar}), 7.85 \text{ (d, } J = 8.24 \text{ Hz}, 1 \text{ Hz}, 1 \text{ Hz}), 7.85 \text{ (d, } J = 8.24 \text{ Hz}, 1 \text{ Hz}), 7.85 \text{ (d, } J = 8.24 \text{ Hz}, 1 \text{ Hz}), 7.85 \text{ (d, } J =$ 8.23 Hz, 4 H, H_{Ar}), 7.54 (d, J = 8.54 Hz, 1 H, H_{Ar}), 7.09 (dd, J = 8.85 Hz, J = 2.75Hz, 1 H, H_{Ar}), 6.93 (d, J = 2.75 Hz, 1 H, H_{Ar}), 3.95 (s, 3 H, OCH₃), 1.34 (s, 18 H, 6 x CH₃), 1.29 (s, 9 H, 3 x CH₃), 1.25 (s, 9 H, 3 x CH₃); MALDITOF-MS m/z: Calcd for C₆₆H₆₁NO₆ 963.449; Found 964.474, 965.475 (M+H)+.

3.2.1.5 9-[2-(4-carboxyphenyl)ethynyl]-1,6-di(4-tert-butylphenoxy)-N-(2,5-di-tert-butylphenyl)perylene-3,4-dicarboxylic imide (M5)

M4 (12 mg, 0.0124 mmol), KOH (14 mg, 0.25 mmol), methanol (3 mL), THF (2 mL), water (0.7 mL) and a stir-bar were added to a screw-cap vial. The mixture was heated at 60 °C for 3 hours and then evaporated to dryness. Crude product was dissolved in DCM with 0.1% AcOH and filtered thru 4 cm layer of silica gel. The solution containing purified product was evaporated to dryness yielding M5 (11 mg, 93%, red-purple powder); MALDITOF-MS m/z: Calcd for C₆₅H₅₉NO₆ 949.434; Found 950.501 (M+H)+, 988.449 (M+K)+.

3.3 Benzothiadiazoles

3.3.1 Benzothiadiazoles modified at C4 and C7 carbon atoms (C1-C3)

Scheme 36 Synthetic route to C1-C3.

3.3.1.1 4-Bromo-7-[4-(Diphenylamino)phenyl]-2,1,3-benzothiadiazole (CO1)

4,7-Dibromo-2,1,3-benzothiadiazole (58.8 mg, 0.2 mmol), 4-(N,N-diphenylamino)phenylboronic acid (65.6 mg, 0.22 mmol), 18-crown-6 ether (2 mg) and K_2CO_3 (210 mg, 1.52 mmol), dioxane (5 mL), water (1 mL) and a stir-bar were

added to a screw-cap vial. Argon gas was bubbled through the solution for 30 minutes. After that time Pd(PPh₃)₄ (22 mg) was added to the solution and bubbling of argon gas was continued for another 30 minutes. Next the vial was screw-capped and wrapped in aluminium foil to protect from light. It was then stirred and heated in 30 °C for 24 hours. After the reaction was completed, dioxane was evaporated in the stream of compressed air. Crude product was extracted with DCM. DCM extract was evaporated and purified on a column chromatography (eluent: 0.1% NEt₃ in a mixture of hexane : toluene : ethyl acetate 7:6:1). Fraction containing purified product was evaporated to dryness yielding **C01** (55.7 mg, 50%, orange crystalline powder); ¹H NMR (CDCl₃): δ 7.89 (d, J = 7.32 Hz, 1 H, H_{Ar}), 7.80 (d, J = 7.32 Hz, 2 H, H_{Ar}), 7.54 (d, J = 7.63 Hz, 1 H, H_{Ar}), 7.29 (t, J = 7.32 Hz, 4 H, H_{Ar}), 7.18 (d, J = 7.32 Hz, 6 H, H_{Ar}), 7.07 (t, J = 7.32 Hz, 2 H, H_{Ar}); MALDITOF-MS m/z: Calcd for **C01** C₂₄H₁₆BrN₃S 458.382; Found 459.025, 460.037 (M)⁺.

3.3.1.2 4-[4-Carboxyphenyl]-7-[4-(N,N-diphenylamino)phenyl]-2,1,3-benzothiadiazole (C1)

A mixture containing C01 (14.5 mg), 4-carboxyphenylboronic acid (14.5 mg, 0.087 mmol), K_2CO_3 (20 mg, 0.145 mmol), dioxane (5 mL), water (1 mL) and a stirbar were added to a screw-cap vial. Argon gas was bubbled through the solution for 30 minutes. After that time $Pd(PPh_3)_4$ (5 mg) was added and argon gas was bubbled through the solution for another 30 minutes. Next the vial was screw-capped and wrapped in aluminium foil to protect the mixture from light. It was then stirred and heated in 50 °C for 24 hours. After the reaction was completed, dioxane was evaporated in the stream of compressed air. Crude product was extracted with DCM. DCM extract was evaporated and purified on a column chromatography (eluent: 0.1% AcOH in a mixture of toluene ethyl: acetate 6:1). Fraction containing purified product was evaporated to dryness yielding C1 (8.7 mg, 55%, orange crystals); ¹H NMR (CDCl₃): δ 8.29 (d, J = 7.94 Hz, 2 H, H_{Ar}), 8.11 (d, J = 7.94 Hz, 2 H, H_{Ar}), 7.90 (d, J = 8.24 Hz, 2 H, H_{Ar}), 7.85 (d, J = 7.32 Hz, 1 H,

 H_{Ar}), 7.79 (d, J = 7.32 Hz, 1 H, H_{Ar}), 7.31 (t, J = 7.63 Hz, 2 H, H_{Ar}), 7.30 (d, J = 7.93 Hz, 2 H, H_{Ar}), 7.21 (t, J = 9.31 Hz, 2 H, H_{Ar}), 7.20 (d, J = 8.24 Hz, 4 H, H_{Ar}), 7.08 (t, J = 7.32 Hz, 2 H, H_{Ar}); MALDITOF-MS m/z: Calcd for $C_{31}H_{21}N_3O_2S$ 499.135; Found 500.200 (M+H)+.

3.3.1.3 4-[4-(Amino)phenyl]-7-[4-(diphenylamino)phenyl]-2,1,3-benzothiadiazole (C2)

A mixture containing C01 (43.2 mg), 4-(amino)phenylboronic acid pinacol ester (30 mg, 0.137 mmol), NaHCO₃ (250 mg, 2.98 mmol), THF (5 mL), water (1 mL) and a stir-bar were added to a screw-cap vial. Argon gas was bubbled through the solution for 30 minutes. After that time [Pd₂(dba)₃] (5 mg) and tris-(otolyl)phosphine (5 mg) were added and argon gas was bubbled through the solution for another 30 minutes. Next the vial was screw-capped and wrapped in aluminium foil to protect a reaction mixture from light. It was then stirred and heated in 50 °C for 24 hours. After the reaction was completed, THF was evaporated in the stream of compressed air. Crude product was extracted with DCM. DCM extract was washed with water and then evaporated on rotary evaporator. Crude product was purified on a column chromatography (eluent: 0.1% NEt3 in a mixture of toluene: ethyl acetate 6:1). Fraction containing purified product was evaporated to dryness. Purified product was recrystallised from the mixture of DCM and nhexane yielding pure C2 (18.9 mg, 43%, orange crystals); ¹H NMR (CDCl₃): δ 7.87 $(d, J = 8.24 \text{ Hz}, 2 \text{ H}, H_{Ar}), 7.83 (d, J = 8.24 \text{ Hz}, 2 \text{ H}, H_{Ar}), 7.72 (d, J = 7.32 \text{ Hz}, 1 \text{ H}, 1 \text{ H})$ H_{Ar}), 7.69 (d, J = 7.32 Hz, 1 H, H_{Ar}), 7.29 (t, J = 7.63 Hz, 2 H, H_{Ar}), 7.28 (d, J = 7.63 Hz) Hz, 2 H, H_{Ar}), 7.20 (t, J = 9.15 Hz, 2 H, H_{Ar}), 7.19 (d, J = 8.24 Hz, 4 H, H_{Ar}), 7.06 (t, $J = 7.02 \text{ Hz}, 2 \text{ H}, \text{ H}_{Ar}$, 6.85 (d, $J = 8.24 \text{ Hz}, 2 \text{ H}, \text{ H}_{Ar}$), 3.90 (b, 2 H, NH₂); MALDITOF-MS m/z: Calcd for C₃₀H₂₂N₄S 470.135; Found 471.144 (M+H)+.

3.3.1.4 4,7-Bis[4-(amino)phenyl]-2,1,3-benzothiadiazole (C3)

$$H_2N$$
 N
 N
 S
 N
 S

4,7-Dibromo-2,1,3-benzothiadiazole (35.2)0.124mg, mmol), (amino)phenylboronic acid pinacol ester (66.5 mg, 0.304 mmol), NaHCO₃ (250 mg, 2.98 mmol), THF (5 mL), water (1 mL) and a stir-bar were added to a screw-cap vial. Argon gas was bubbled through the solution for 30 minutes. After that time [Pd₂(dba)₃] (5 mg) and tris-(o-tolyl)phosphine (5 mg) were added and argon gas was bubbled through the solution for another 30 minutes. Next the vial was screwcapped and wrapped in aluminium foil to protect from light. It was then stirred and heated in 50 °C for 24 hours. After the reaction was completed, THF was evaporated in the stream of compressed air. Crude product was extracted with DCM. DCM extract was evaporated and purified on a column chromatography (eluent: 0.1% NEt₃ in a mixture of hexane : toluene : ethyl acetate 7:6:1). Fraction containing purified product was evaporated to dryness. Purified product was recrystallised from the mixture of DCM and n-hexane yielding pure C3 (30.5 mg, 80%, orange crystals); ¹H NMR (CDCl₃): δ 7.81 (d, J = 7.94 Hz, 4 H, H_{Ar}), 7.66 (s, 2 H, H_{Ar}), 6.83 (d, J = 7.63 Hz, 4 H, H_{Ar}), 3.82 (b, 4 H, 2 x NH_2); MALDITOF-MS m/z: Calcd for C₁₈H₁₄N₄S 318.403; Found 318.102 (M+).

3.3.2 5,6-Dichlorobenzothiadiazoles modified at C4 and C7 carbon atoms (C4-C6)

$$CI \longrightarrow NH_2 \longrightarrow NH$$

Scheme 37 Synthetic route to C4-C6.

3.3.2.1 3,6-dibromo-4,5-dichlorobenzene-1,2-diamine (CO2)

4,5-dichlorobenzene-1,2-diamine (2 g, 11.3 mmol), acetonitrile (50 mL) and 48% hydrobromic acid (10 mL, 88.4 mmol) were added to a two-neck round bottom flask equipped with a magnetic stir-bar, a dropping funnel and a reflux condenser. The mixture was heated under a mild reflux for 1 hour. After this time, bromine (2.5 mL, 48.8 mmol) was added dropwise thru the dropping funnel. After the addition of all bromine the mixture turned into an orange suspension. Heating was turned off and the mixture was mixed for 2 h at room temperature. The precipitate was filtered off on a glass fritted funnel and washed with cold acetonitrile until the filtrate was colourless. The crude product was allowed to air dry on the funnel and then transferred to a beaker. Water (30 mL) was added to the crude product, and under a vigorous stirring sodium carbonate was added to the suspension until pH was around 8. The precipitate was then filtered off on the glass fritted funnel and washed with cold water. After the washing, the product was air dried to yield C02 (3.2 g, 85%, beige powder). ¹³C NMR (CDCl₃): δ 151.3 (CAr), 138.4 (CAr), 114.9 (CAr); MALDITOF-MS m/z: Calcd for C₆H₄Br₂Cl₂N₂ 331.812; Found 331.782, 332.775, 333.782, 334.775. 335.781 (M)+.

3.3.2.2 4,7-dibromo-5,6-dichloro-2,1,3-benzothiadiazole (CO3)

C01 (452.2 mg, 1.35 mmol) and triethylamine (0.81 mL, 5.85 mmol) were added to a round bottom flask, equipped with a stir-bar, and dissolved in DCM (5 mL). A solution of thionyl chloride (0.63 mL, 8.64 mmol) in DCM (2.5 mL) was added dropwise with vigorous stirring to that mixture. All was stirred overnight. When the reaction was finished, the reaction mixture was evaporated to dryness on the

rotatory evaporator. Crude product was washed with cold methanol on a glass fritted funnel and air dried yielding **C03** (475.4 mg, 97%, beige powder). MALDITOF-MS m/z: Calcd for C₆N₂Br₂Cl₂S 359.753; Found 360.791, 361.767, 362.787, 364.786 (M)⁺.

3.3.2.3 4-Bromo-5,6-dichloro-7-[4-(dimethylamino)phenyl]-2,1,3-benzothiadiazole (CO4)

C03 (72.4 mg, 0.2 mmol), 4-(N,N-diphenylamino)phenylboronic acid (65.6 mg, 0.22 mmol), 18-crown-6 ether (2 mg) and K₂CO₃ (210 mg, 1.52 mmol), dioxane (5 mL), water (1 mL) and a stir-bar were added to a screw-cap vial. Argon gas was bubbled through the solution for 30 minutes. After that time Pd(PPh₃)₄ (22 mg) was added to the solution and bubbling of argon gas was continued for another 30 minutes. Next the vial was screw-capped and wrapped in aluminium foil to protect from light. It was then stirred and heated in 30 °C for 24 hours. After the reaction was completed, dioxane was evaporated in the stream of compressed air. Crude product was extracted with DCM. DCM extract was evaporated and purified on a column chromatography (eluent: 0.1% NEt₃ in a mixture of toluene ethyl: acetate 6:1). Fraction containing purified product was evaporated to dryness yielding C04 (55.7 mg, 50%, orange crystals); MALDITOF-MS: Calcd for C₂₄H₁₄BrCl₂N₃S 524.947; Found: m/z 524.949, 527.005, 528.030, 530.028 (M)⁺.

3.3.2.4 4-[4-(Carboxy)phenyl]-5,6-dichloro-7-[4-(diphenylamino)phenyl]-2,1,3-benzothiadiazole (C4)

 ${\bf C04}$ (10 mg, 0.019 mmol), 4-(carboxy)phenylboronic acid (3.5 mg, 0.0208 mmol), ${\bf K}_2{\bf CO}_3$ (10 mg, 0.0723 mmol), dioxane (5 mL), water (1 mL) and a stir-bar

were added to a screw-cap vial. Argon gas was bubbled through the solution for 30 minutes. After that time Pd(PPh₃)₄ (22 mg) was added and argon gas was bubbled through the solution for another 30 minutes. Next the vial was screw-capped and wrapped in aluminium foil to protect from light. It was then stirred and heated in 50 °C for 24 hours. After the reaction was completed, dioxane was evaporated in the stream of compressed air. Crude product was extracted with DCM. DCM extract was evaporated and purified on a column chromatography (eluent: 0.1% AcOH in a mixture of toluene: ethyl acetate 6:1). Fraction containing purified product was evaporated to dryness yielding C4 (10.0 mg, 92%, orange crystals); 1 H NMR (CDCl₃): δ 8.31 (d, J = 8.54 Hz, 2 H, H_{Ar}), 7.69 (d, J = 8.54 Hz, 2 H, H_{Ar}), 7.46 (d, J = 8.85 Hz, 2 H, H_{Ar}), 7.33 (t, J = 7.32 Hz, 2 H, H_{Ar}), 7.32 (t, J = 7.33 Hz, 2 H, H_{Ar}), 7.24 (dd, J = 8.55 Hz, J = 1.22 Hz, 4 H, H_{Ar}), 7.20 (d, J = 8.85 Hz, 2 H, H_{Ar}), 7.10 (tt, J = 7.33 Hz, J = 1.22 Hz, 2 H, H_{Ar}); MALDITOF-MS m/z: Calcd for $C_{31}H_{19}Cl_2N_3O_2S$ 567.058 483; Found 567.069 M+, 568.083 (M+H)+.

3.3.2.5 4-[4-(Amino)phenyl]-5,6-dichloro-7-[4-(diphenylamino)phenyl]-2,1,3-benzothiadiazole (C5)

C04 (38.8 mg, 0.074 mmol), 4-(amino)phenylboronic acid pinacol ester (16.9 mg, 0.078 mmol), NaHCO₃ (50 mg, 0.59 mmol), THF (5 mL), water (1 mL) and a stir-bar were added to a screw-cap vial. Argon gas was bubbled through the solution for 30 minutes. After that time [Pd₂(dba)₃] (5 mg) and tris-(o-tolyl)phosphine (5 mg) were added and argon gas was bubbled through the solution for another 30 minutes. Next the vial was screw-capped and wrapped in aluminium foil to protect from light. It was then stirred and heated in 50 °C for 24 hours. After the reaction was completed, THF was evaporated in the stream of compressed air. Crude product was extracted with DCM. DCM extract was evaporated and purified on a column chromatography (eluent: 0.1% NEt₃ in a mixture of toluene: ethyl

acetate 6:1). Fraction containing purified product was evaporated to dryness. Purified product was recrystallised from the mixture of DCM and *n*-hexane yielding pure **C5** (21.7 mg, 55%, orange crystals); MALDITOF-MS m/z: Calcd for C₃₀H₂₀Cl₂N₄S 538.078; Found 538.100, 540.108 (M)⁺.

3.3.2.6 4,7-Bis[4-(amino)phenyl]-5,6-dichloro-2,1,3-benzothiadiazole (C6)

$$H_2N$$
 N
 N
 S
 N
 $C6$

C03 (109 mg, 0.3 mmol), 4-(amino)phenylboronic acid pinacol ester (166 mg, 0.76 mmol), NaHCO₃ (250 mg, 2.98 mmol), THF (5 mL), water (1 mL) and a stirbar were added to a screw-cap vial. Argon gas was bubbled through the solution for 30 minutes. After that time [Pd₂(dba)₃] (18 mg) and tris-(o-tolyl)phosphine (18 mg) were added and argon gas was bubbled through the solution for another 30 minutes. Next the vial was screw-capped and wrapped in aluminium foil to protect from light. It was then stirred and heated in 50 °C for 24 hours. After the reaction was completed, THF was evaporated in the stream of compressed air. Crude product was extracted with DCM. DCM extract was evaporated and purified on a column chromatography (eluent: 0.1% NEt₃ in a mixture of toluene : ethyl acetate 6:1). Fraction containing purified product was evaporated to dryness. Purified product was recrystallised from the mixture of DCM and n-hexane yielding pure C6 (35.8 mg, 31%, orange crystals); ¹H NMR (CDCl₃): δ 7.40 (d, J = 8.55 Hz, 4 H, H_{Ar}), 6.85 (d, J = 8.54 Hz, 4 H, H_{Ar}), 3.88 (b, 4 H, 2 x NH₂); MALDITOF-MS m/z: Calcd for C₁₈H₁₂Cl₂N₄S 386.016 Found 386.074 (M)+, 387.080 (M+H)+.

4. RESULTS AND DISCUSSION

4.1 Introduction and basic terms

In order to fully grasp concepts discussed in subsequent paragraphs, it is necessary to familiarize with key, basic concepts and terms. Some of the topics contained in current section, were already covered in the literature review. In this paragraph it is presented in more condensed form.

Photocatalytic system is a multi-complementary system capable of catalysing chemical reactions with the use of energy in form of light.

Photosensitizer is a substance which is able to absorb energy in form of light and subsequently pass it on another chemical species. Usually it is a part of photocatalytic system and is unactive and unable to catalyse reactions on its own.

Photocatalyst is a substance which in the presence of light causes acceleration of a chemical reaction. The reaction is taking place directly on/via the photocatalyst, without any additional intermediary species.

Sacrificial reagent is a reagent which accepts or donates electrons during

Turnover number (TON) is a parameter characterizing catalyst photocatalytic system activity. One of the definitions of TON is number of moles of product that can be formed by one mole of catalyst before it loses its activity. TON = $\frac{n_{prod.}}{n_{cat.}}$. This value is dimensionless.

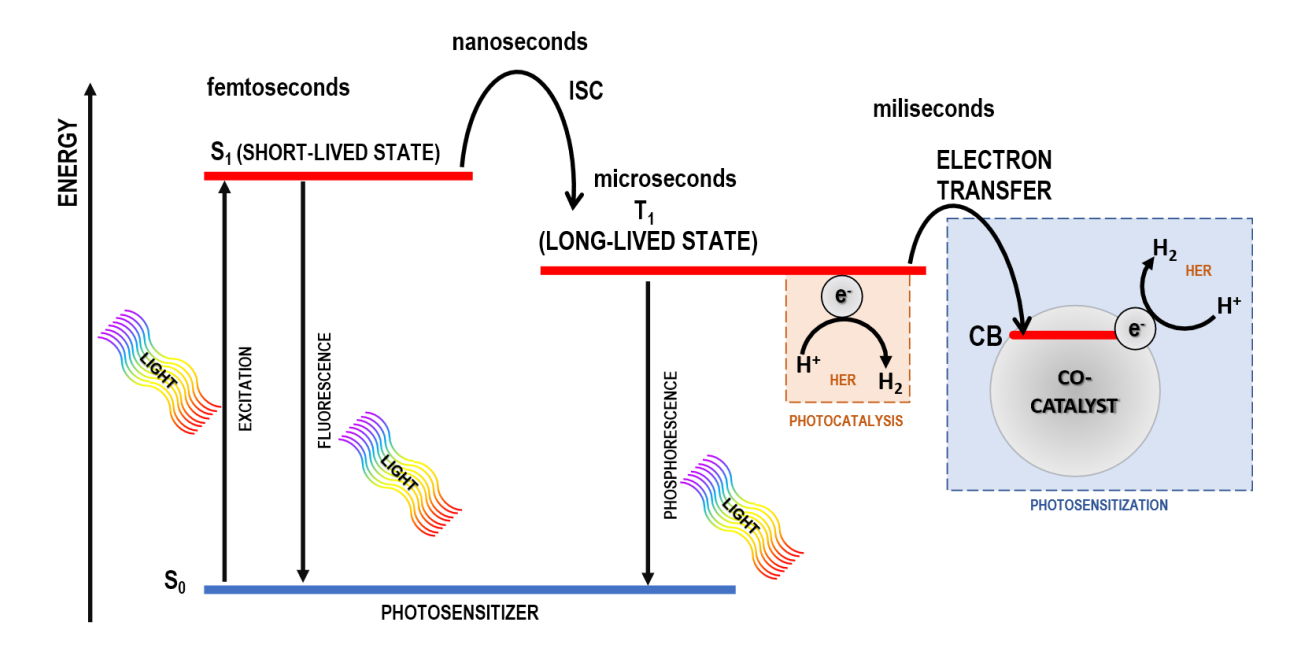


Figure 13 Mechanism of photosensitizer assisted and photocatalytic HER, S_0 - ground state, S_1 - 1st singlet state, T_1 - 1st triplet state, ISC - inter-system crossing, CB - conductive band of the catalyst.

Looking on the scheme of mechanism of photocatalytic and photosensitizer assisted HER shown above (Figure 13) leaves few clues how overall efficiency can be improved:

- 1) Rate of the fluorescence should be reduced. Fluorescence is the main way of losing absorbed energy, therefore reducing the rate of the fluorescence should effectively improve chance of occurrence of subsequent processes.
- 2) Rate of the ISC should be increased as it results with higher number of excited photosensitizer in long-lived T₁ state.
- 3) Lifetime of the T₁ state should be improved, as it works as a way of storing absorbed energy. Increasing lifetime of this state can effectively raise the chance of passing the electron to the co-catalyst which is the slowest process of the all.

All these improvements may be achieved by thoughtful molecular design.

4.2 Donor-acceptor type perylene diimides (A1-A12) as precursors for molecular catalyst

4.2.1 Why perylene diimides?

Perylene diimides seem to be good candidates for water splitting photosensitizers and photocatalysts. Good absorption of light, high stability and facility of synthesis and modification. Experimental and theoretical research shows that perylene diimides substituted in the bay area with N-phenylcarbazole have adequate HOMO and LUMO levels for water splitting reaction (Table 1). Moreover it exhibits strong and broad light absorption between 400-650 nm (Figure 14) making it a good candidate for photocatalyst and photosensitizer for HER and OER reactions.[73]

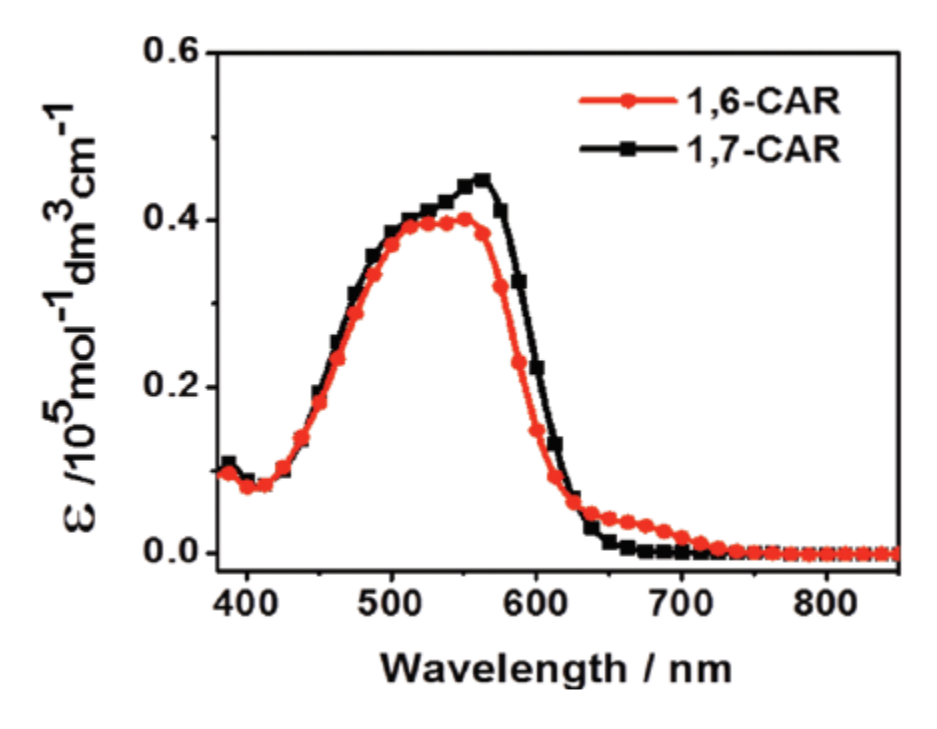


Figure 14 Absorption spectra of regioisomers of bay substituted perylene diimides.[73]

 $Table\ 1$ Energy levels and photophysical properties of regioisomers of bay disubstituted perylene diimide derivatives.

absorpti maxim (nm) in chlorofo	a coefficient (104 mol-1·dm3·m-1)	absorption maxima in solid state (nm)	emission maxima in chloroform (nm)	fluorescence lifetime τ (ns)	optical band gap (eV)	HOMO (eV)	LUMO (eV)	
561	4,494	565	651	3,4	1,87	-5,30	-3,82	_
523	4,100	507						

The aim was to introduce various substituents with different electron effects in the bay position of the perylene diimides core and investigate their influence on HER reaction in the various photocatalytic systems including system with platinum as a co-catalyst. Selected substituents have differing electron donating proportions, starting from the most electron rich to the least electron rich substituents. Donor-acceptor character of the molecule should generally improve charge separation. It should also improve efficiency by reducing the rate of the fluorescence by increasing lifetime of the T_1 state.

4.2.2 Density functional theory calculations for A1, A3, A5-A8

Computational methods were employed to assess the effects of introducing substituents in the bay area, ranging from electron-donating to electron-withdrawing, on the properties of perylene diimide derivatives. Using DFT methods I optimized geometries of the six PDI derivatives which structurally resemble the later synthesised A1, A3, A5-A8 (Figure 15). Calculated electronic transitions of PDI derivatives are listed on the Figure 15. Additionally I visualized HOMO and LUMO and estimated their energy levels.

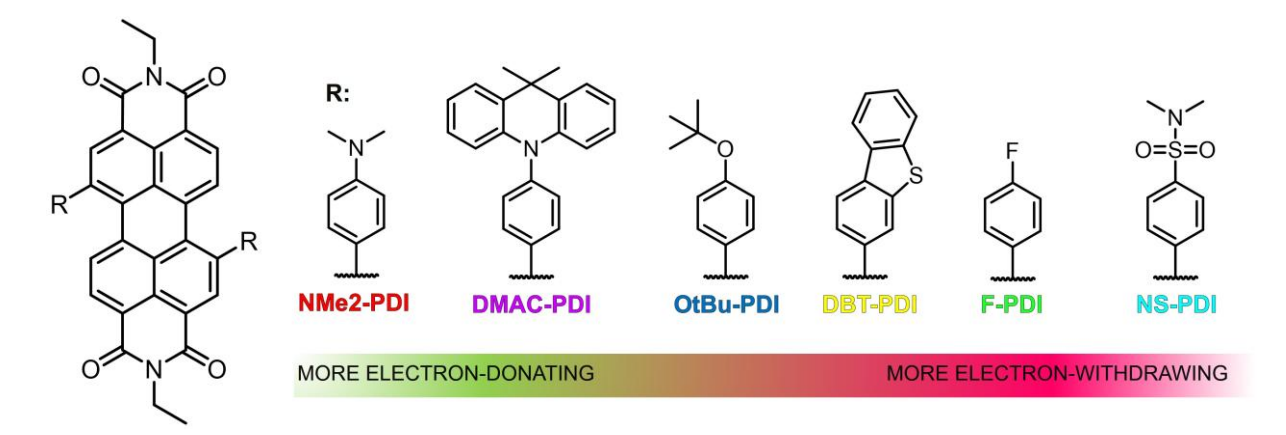


Figure 15 Optimized structures ranging from electron-donating to electron-withdrawing (similar to compounds A1, A3, A5-A8 respectively).

Substituents for calculations were chosen based on the availability of the boronic building-blocks in the laboratory and chemical supply companies. For calculations I selected ethyl group as N-substituent of the imides. Ethyl group retains some of the character of longer alkyl chains, yet having fewer atoms to optimize, it shortens calculations significantly. Obtained results can be extrapolated on other derivatives, such as perylene diimides witch anchoring group for example.

Based on the results, in almost all model PDIs, except DMAC-PDI, HOMO \rightarrow LUMO (S₀ \rightarrow S₁) transitions are responsible for the strong visible absorption (Figure 16). In DMAC-PDI, HOMO \rightarrow LUMO transition is weak and visible spectrum band is coming from lower HOMO-2 \rightarrow LUMO transition (S₀ \rightarrow S₂). This is caused by the spatial separation of HOMO and LUMO in DMAC-PDI (Figure 17), making this transition forbidden in its nature. In contrast, HOMO and LUMO of DMAC-NMe₂ are not spatially separated, therefore, it exhibits bands coming from both HOMO \rightarrow LUMO and lower orbital HOMO-2 \rightarrow LUMO transitions (Figure 18).

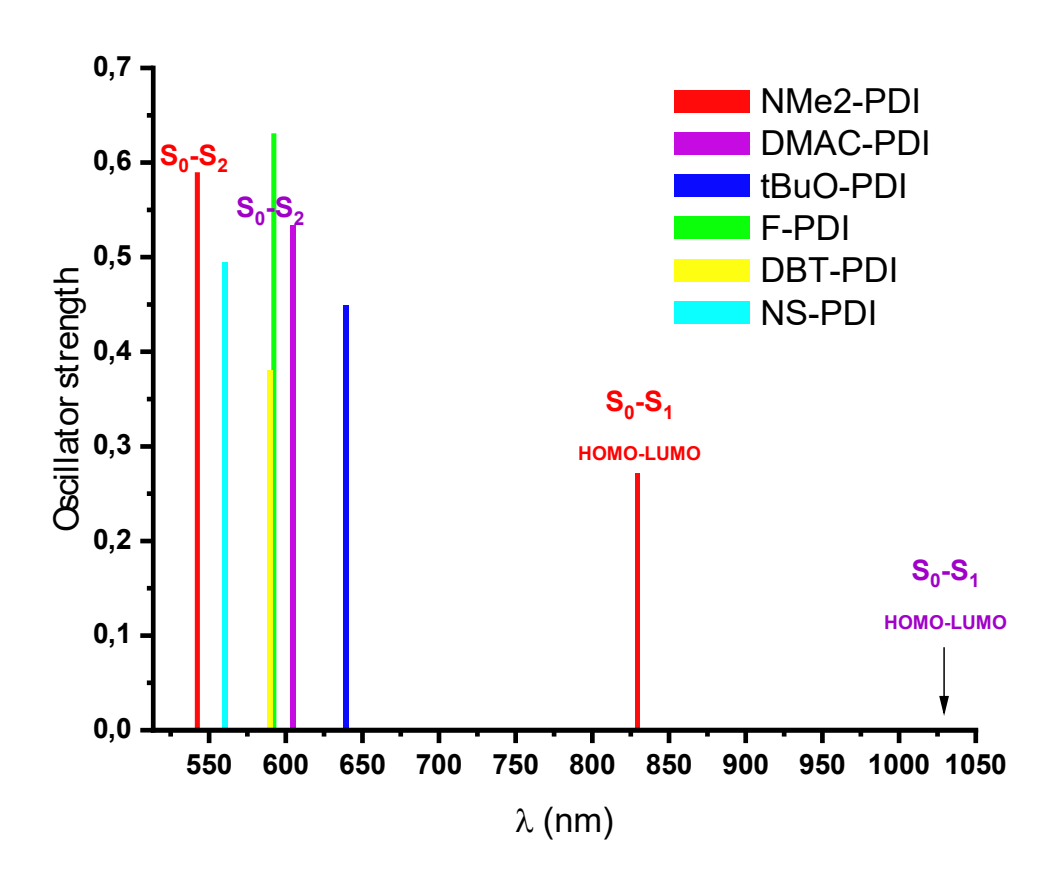


Figure 16 HOMO \rightarrow LUMO transitions in visible spectrum. For NMe2-PDI and DMAC-PDI there are additional transitions in visible spectrum coming from lower orbitals (S₀-S₂ on the scheme).

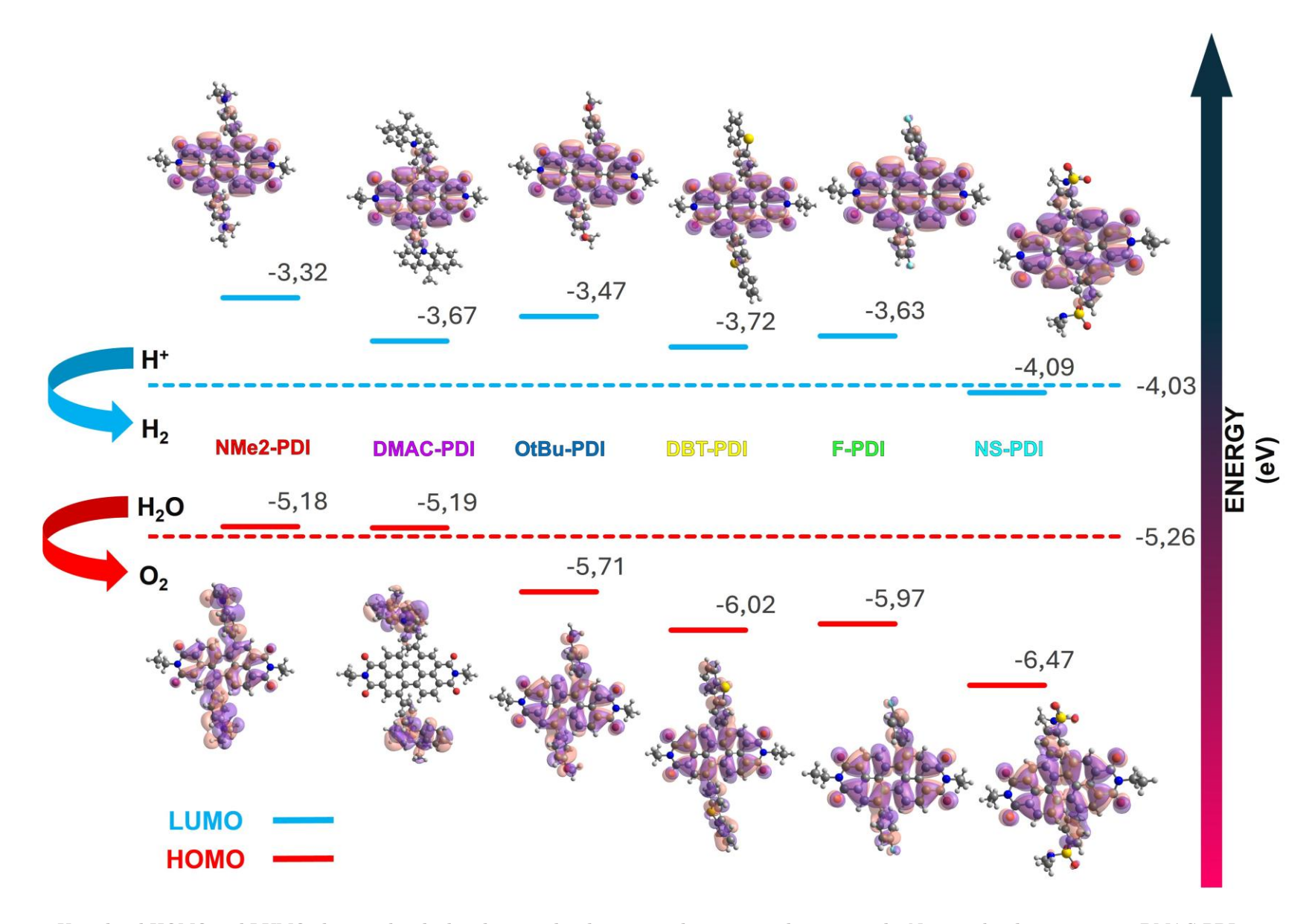


Figure 17 Visualised HOMO and LUMO along with calculated energy levels compared to water redox potentials. Notice orbital separation in DMAC-PDI.

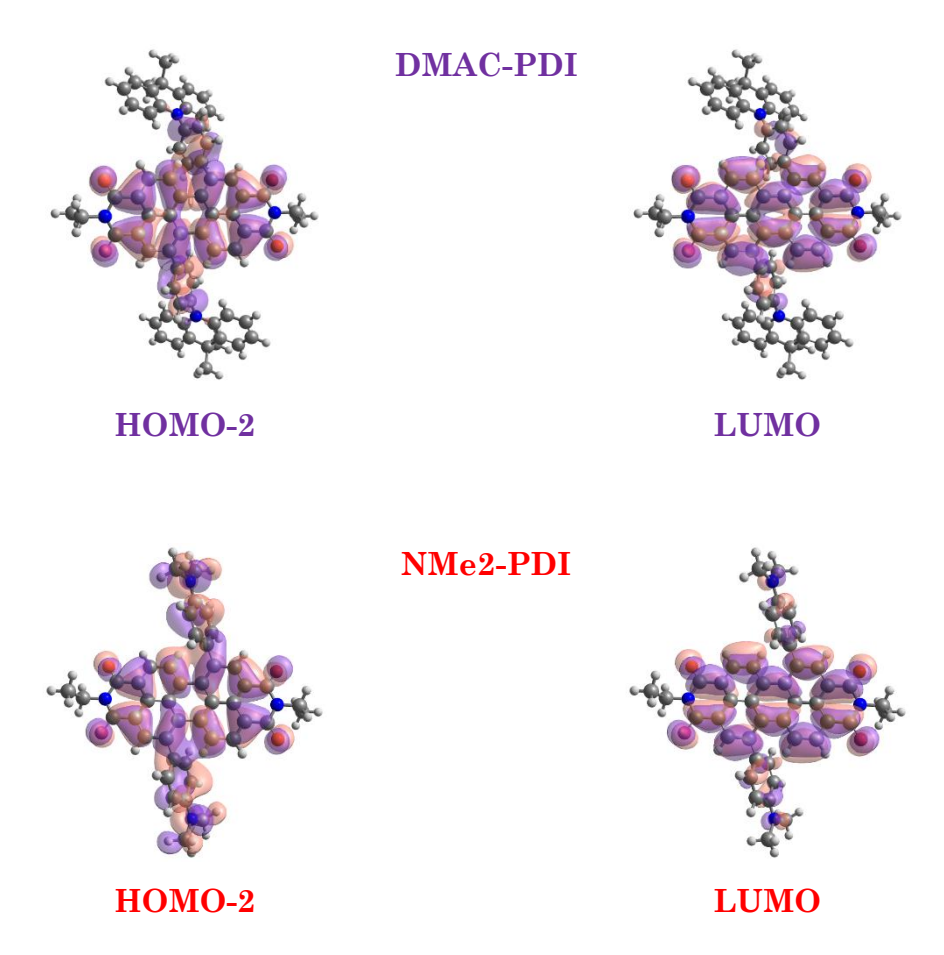


Figure 18 Electronic transitions from lower orbitals, responsible for bands in visible spectrum of DMAC-PDI and NMe2-PDI.

From the visualisations of the HOMO and LUMO (Figure 17) it is concluded that HOMO is localized on the bay substituents which act as an electron density donor. Similarly, LUMO is localized on the perylene diimide core, which acts as an electron density acceptor.

Insertion of highly electron-withdrawing substituents tends to increase energy gap between HOMO and LUMO. It also decreases LUMO energy close or below the level of water reduction to hydrogen, thus making these compounds unsuitable for HER.

Highly electron-donating substituents tend to increase HOMO and LUMO overlapping. Furthermore these substituents have minor effect on LUMO levels. What is crucial, their LUMO levels are above water reduction energy levels,

making these molecules good candidates for photocatalytic water-splitting reaction.

In the case of DMAC-PDI, conformation tied to the rotation of the bond between the PDI core is twisted. Therefore HOMO and LUMO are spatially separated. Creating molecules with twisted donor-acceptor motif is a common approach for designing molecules exhibiting thermally activated delayed fluorescence (TADF). TADF phenomenon effectively increases fluorescence lifetime. [74] This might be beneficial for photocatalytic water-splitting reaction, as it reduces energy loss via fluorescence.

4.2.3 Synthesis of perylene diimides with donor-acceptor motif (A1-A8)

I synthesized perylene diimide derivatives via Suzuki coupling of dibrominated PDI derivative **A0** with various boronic derivatives (Scheme 38). The selection of synthesized compounds was closely related to the DFT calculations described in the subsection **4.2.2**.

$$\begin{array}{c} & & \\$$

Scheme 38 Synthesis of A1-A8

Many reactions with organometallic compounds require strictly inert atmosphere, as organometallic species are often sensitive to oxygen or humidity. This applies to most of palladium catalysed coupling reactions, therefore palladium catalysed couplings are commonly performed with the use of Schlenk apparatus. There are some exceptions, proving that Schlenk apparatus might not always be needed, as traces of oxygen may have crucial role in the progress of some variants of the Suzuki reaction. [75][58][76]

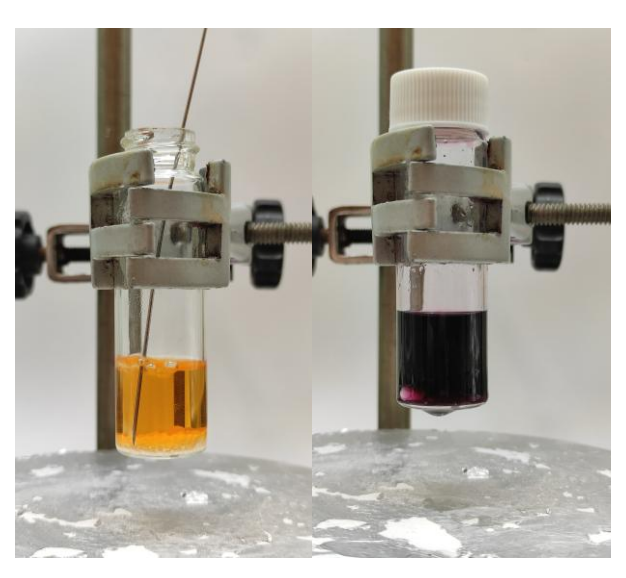


Figure 19 On the left is a vial during the process of flushing with argon. On Tthe right is the vial after closing and heating for 24 hours.

In my experimental work I developed a method of Suzuki coupling which can be performed in a vial without Schlenk apparatus. Thus I dissolved substrates in a screw-cap vial with PTFE seal. Subsequently the solution was flushed with argon gas thru needle for around 30 minutes prior closing the vial (**Figure 19**). Closed vial is then heated and the content was mixed with magnetic stir bar. Use of dioxane, with relatively high boiling point, and mild reaction temperatures, assure that there is no pressure build-up in the vials. This method allows for efficient synthesis of multiple compounds simultaneously without loss on yields. This method proved to be useful for repeating syntheses in small scales (5-10 mg) when using Schlenk apparatus was tedious task.

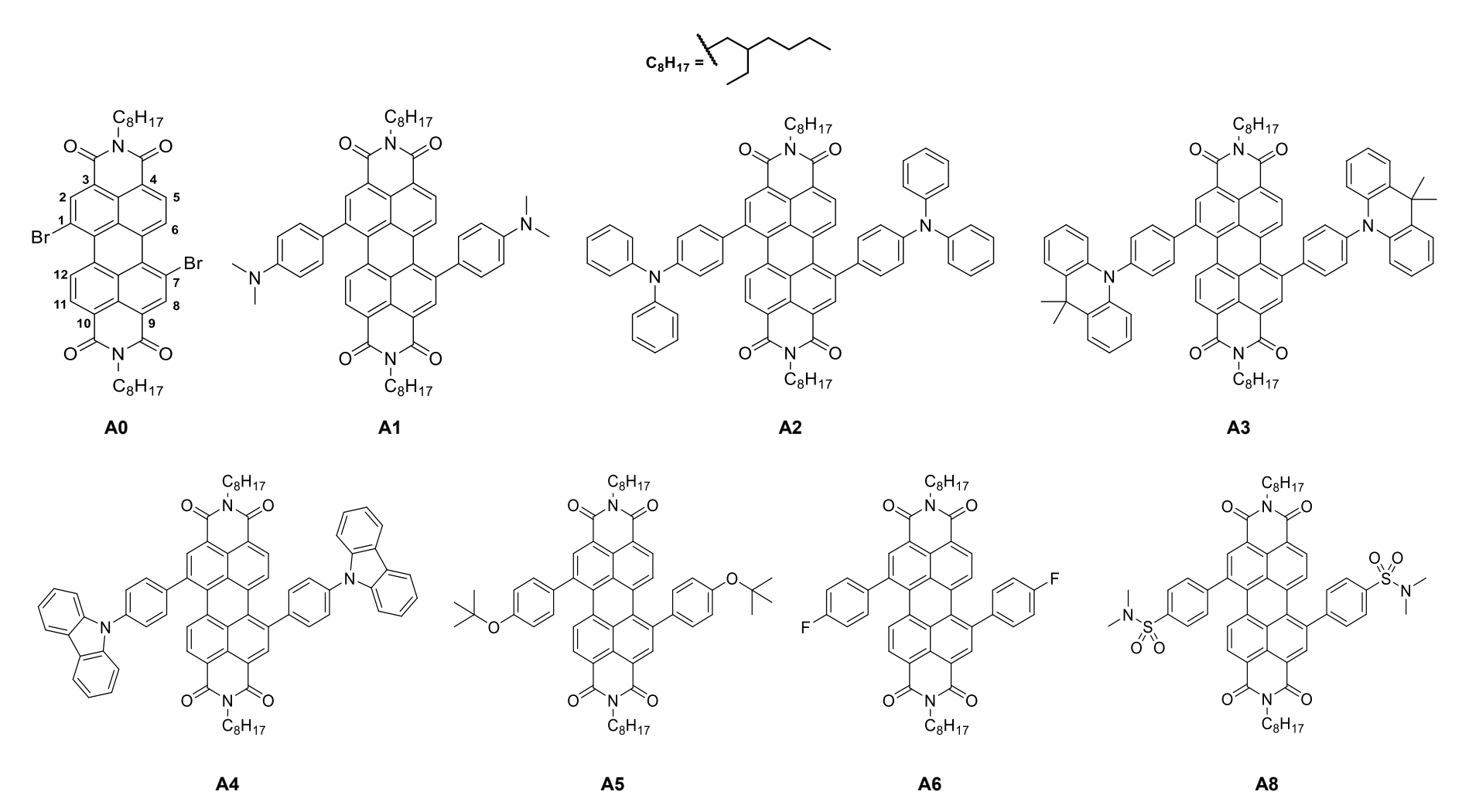


Figure 20 Obtained PDIs with Donor-Acceptor motiff (A1-A8).

I confirmed structures of obtained donor-acceptor perylene diimides (A1-A8) by analysing MALDITOF-MS (Table 2) and ¹HNMR (Table 3) spectra of these compounds.

Table 2 MALDITOF-MS analysis of A0-A8.

No.	Molecular formula	Monoisotopic mass	MALDITOF-MS peaks
A0	$C_{40}H_{40}Br_{2}N_{2}O_{4} \\$	770.1355	771.174 (M+H)+
A1	$C_{56}H_{60}N_{4}O_{4} \\$	852.461	853.471 (M+H)+
A2	$C_{76}H_{68}N_4O_4$	1100.524	1101.430 (M+H)+
A3	$C_{82}H_{76}N_{4}O_{4} \\$	1180.587	1165.619 (M-CH ₃)+ 1181.725 (M+H)+
A4	$C_{76}H_{64}N_4O_4$	1096.493	1098.551 (M+2H)+
A5	$C_{60}H_{66}N_{2}O_{6} \\$	910.492	911.532 (M+H)+
A6	$C_{52}H_{48}F_2N_2O_4\\$	802.358	801.043 (M-H)+
A7	$C_{64}H_{54}N_2O_4S_2\\$	978.352	980.400 (M+2H)+
A8	$C_{56}H_{60}N_4O_8S_2\\$	980.385	981.473 (M+H)+

In the mass spectra, signals corresponding to expected masses were found for every analysed compound. What is worth noticing is that for the compound A3, a signal of [M-CH₃]⁺ was more prominent than the usual (M+H)⁺ peak. It can be attributed to the fact that ionised 9,9-dimethyl-9,10-dihydroacridine (DMAC) moiety is able to form a more stable, aromatic cation, by losing one methyl group (Scheme 39). I observed this phenomenon in most, if not all, of DMAC derivatives I have worked with.

Scheme 39 Aromatization of the 9,9-dimethyl-9,10-dihydroacridine (DMAC) moiety might explain unusual abundance of $(M-CH3)^+$ ion on the MS of the A3.

Table 3 Chemical shifts (ppm) and coupling constants in the 1H NMR spectra of A0-A6 and A8. For the clarity, I have not included the protons of the 2-ethylhexyl chain in the table.

No.				Aroma	tic protons				Methyls
A0	9.47 (d) J = 8.24 Hz 2 H	8.91 (s) 2 H	S = 8.68 (d) J = 7.94 Hz 2 H						
A1	8.43 (s) 2 H	S_{02} (d) J = 7.93 Hz 2 H	7.80 (d) J = 8.24 Hz 2 H	7.30 (d) J = 8.54 Hz 4 H	6.68 (d) J = 8.55 Hz 4 H				2.99 (s) 4 x Me 12 H
A2	8.61 (s)		8.06 (d) $J = 8.23$ Hz	7.39 (d) J = 8.51 Hz	$7.35 ext{ (t)}$ $J = 7.42 ext{ Hz}$ $J = 8.23 ext{ Hz}$	7.22 (d) J = 7.69 Hz	J = 8.78 Hz	J = 7.41 Hz	
	2 H	2 H	2 H	4 H	8 H	8 H	4 H	4 H	
A 3	8.82 (s)	` '	8.08 (d) J = 8.23 Hz	$7.88 ext{ (d)}$ $J = 8.51 ext{ Hz}$	$7.55 ext{ (t)}$ $J = 7.69 ext{ Hz}$ $J = 8.24 ext{ Hz}$	7.19 (td) $J = 7.14 Hz$ $J = 1.37 Hz$	$J = 7.14 \; \mathrm{Hz}$	6.49 (dd) J = 8.24 Hz J = 0.82 Hz	1.76 (s) 4 x Me
	2 H	2 H	2 H	4 H	8 H	4 H	4 H	4 H	12 H
A 4	8.76 (s)	8.33 (d) J = 8.24 Hz	8.19 (d) J = 7.69 Hz	8.09 (d) J = 7.96 Hz	7.84 (t) $J = 8.24 Hz$	7.75 (d) $J = 8.51 Hz$		7.35 (m) J = 7.96 Hz	
A4	2 H	2 H	4 H	9 - 7.96 Hz 2 H	9 – 8.24 HZ 4 H	9 – 8.51 Hz 4 H	8 H	<i>3</i> = 7.96 Hz 4 H	
A5	8.57 (s)	` '	7.80 (d) J = 8.24 Hz	7.43 (d) J = 8.55 Hz	7.11 (d) J = 8.24 Hz				1.45 (s) 6 x Me
	2 H	2 H	2 H	4 H	4 H				18 H
A6	8.55 (s)	8.16 (d) $J = 8.24$ Hz	7.76 (d) $J = 8.24 Hz$	$J_{\rm H,H} = 8.24~{\rm Hz}$	7.21 (t) $J_{H,H} = 8.24$ Hz ${}^{3}J_{H,F} = 8.54$ Hz				
	$2~\mathrm{H}$	$2~\mathrm{H}$	$2~\mathrm{H}$	4 H	4 H				
A8	8.58 (s)	8.19 (d) J = 7.93 Hz	7.93 (d) J = 7.94 Hz	7.76 (d) J = 7.93 Hz	7.71 (d) J = 7.94 Hz				2.82 (s) 4 x Me
	2 H	2 H	4 H	4 H	2 H				12 H

¹H NMR spectra of **A0-A6** and **A8** are characterized by the signals coming from the perylene diimide core substituted on the C1 and C7. The most characteristic signal is a singlet coming from the H2/H8 protons around 8.43-8.82 ppm. Due to the symmetrical substitution pattern of these derivatives, it shows a single signal with double intensity.

Another important signals from PDI core are two doublets, of H5/H11 proton coupled with H6/H12 proton, which are most apparent in the substrate **A0**. These signals are more difficult to be assigned in the simple ¹HNMR spectra of **A1-A6** and **A8**, as additional signals from aromatic rings from the substituents overlap on each other.

Triplets visible in aromatic region (**A2-A4** and **A6**) are originating from aromatic substituents in C1 and C7 position in PDI. Compound **A6** displays triplet and doublet of doublets emerging from fluorobenzene ring. Fluorine atom in the ring is the source of additional couplings (spin $\frac{1}{2}$) with adjacent protons. These couplings occur via 3 bonds ($\frac{3}{2}$ _{H,F} = 8.54 Hz) and 4 bonds as well ($\frac{4}{2}$ _{H,F} = 5.18 Hz).

A1, A3, A5 and A8 demonstrate characteristic signals of methyl groups present in the C1 and C7 substituents (Table 3). ¹H NMR spectra of A0-A6 and A8 contain signals coming from alkyl substituent on imide nitrogen (*vide* subsection 3.1). In every case there are two doublets of doublets of relatively deshielded (~ 4 ppm) protons on carbon atoms adjacent to nitrogen atom (NCH and NCH'). Moreover, a septet originating from CH group can be found. This signal is accompanied by adequate number of multiplets of CH₂ groups and two triplets of CH₃ group.

4.2.4 Photoactivation of PDI – formation of the molecular catalyst

Photocatalytic tests were performed to screen synthesised compounds (A1-A8) for the photocatalytic activity. Synthesised compounds were screened for the activity in aqueous solution containing triethylamine, sodium dodecyl sulphate and potassium tetrachloroplatinate. Solutions were irradiated with sunlight and samples of gases above the solution were taken. Samples of gases were analysed on GC-MS for the presence of H₂ or other products suggestive of photocatalytic activity.

Most of the tested PDI derivatives were barely active as HER photosensitizers. The only exception was system sensitized with A4. This system was susceptible for photobleaching, changing colour from deep violet to yellow-orange (Figure 21). Surprisingly, this light-driven process was favourable for HER. Photobleached system was still efficient in generating hydrogen even more so than the non-degraded compound.

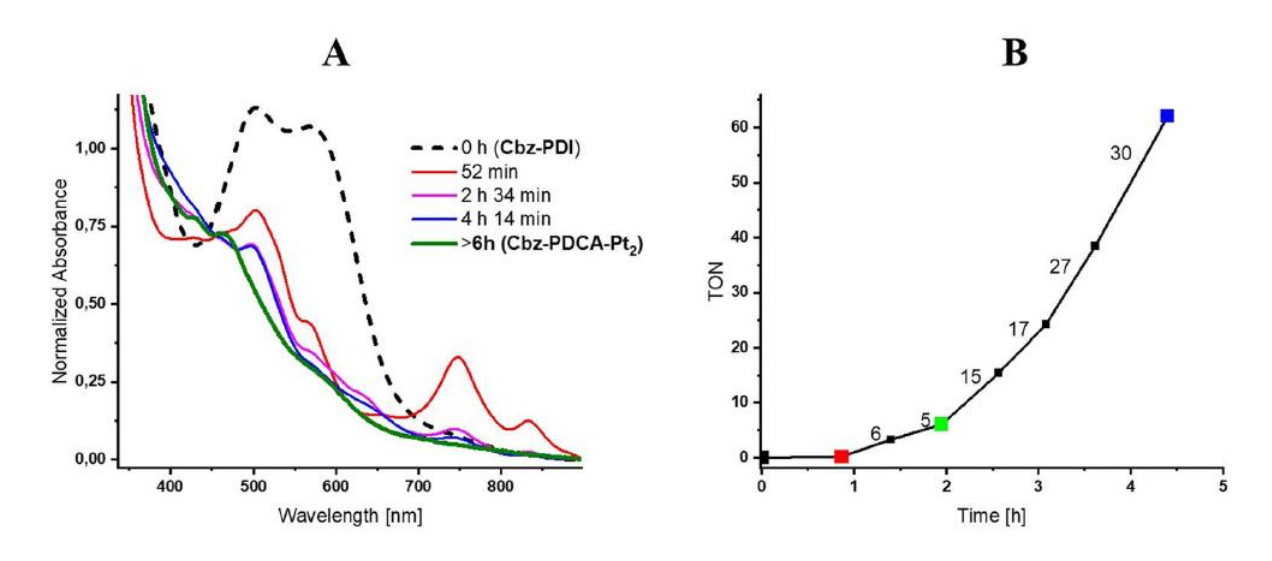


Figure 21 A - Absorption spectrum of A4 before and after irradiation with artificial sun Cbz-PDI – A4. B – evolution of hydrogen

I attempted to isolate product of photobleaching to identify it on LC-MS. First I evaporated TEA and water on rotary evaporator obtaining yellow-brown mass. Crude product contained SDS which could interfere with LC-MS, therefore it had to be removed. I tried to purify the concentrate on the column filled with silica gel. This approach turned out to be futile, as the crude isolate reverted its colour to violet quickly after contacting with silica gel. The only product I was able to isolate was A4. This suggested that photobleaching is reversible. Even though silica gel is considered neutral, its surface can be mildly acidic due to presence of Si-OH groups. Moreover, silica gel stored in the laboratory environment is able to adsorb many acidic contaminants from the air, like hydrochloric or acetic acid. Hence silica gel, in some circumstances, is able to catalyse acid catalysed reactions.[77] My suspicion is photobleaching process involved imide ring opening, and contact with SiO₂ reversed this process (Scheme 40).

Scheme 40 Proposed mechanism od photobleaching.

To verify this hypothesis I used different approach of purification. I removed SDS from the solution by molecular filtration thru Sephadex gel successfully obtaining fraction with photobleached product. Obtained sample was then analysed on LC-MS. Isolated sample turned out to contain species with higher molecular mass than expected. Detected peak of mass of 1518.41 corresponded to platinum complex of open ring form of A4 (Figure 22).

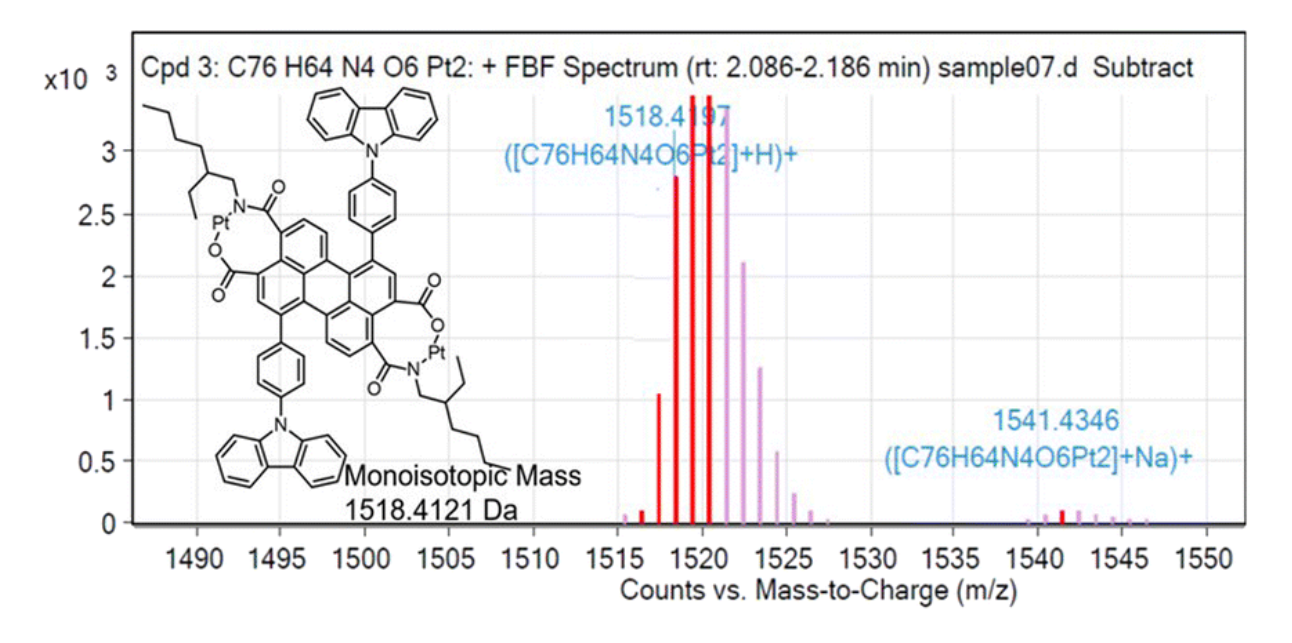


Figure 22 MS spectra of isolated photobleaching product

Presence of platinum in the molecule might be satisfactory explanation of its activity, though it does not explain high TON achieved by the species activated under low concentration of platinum. (Figure 23)

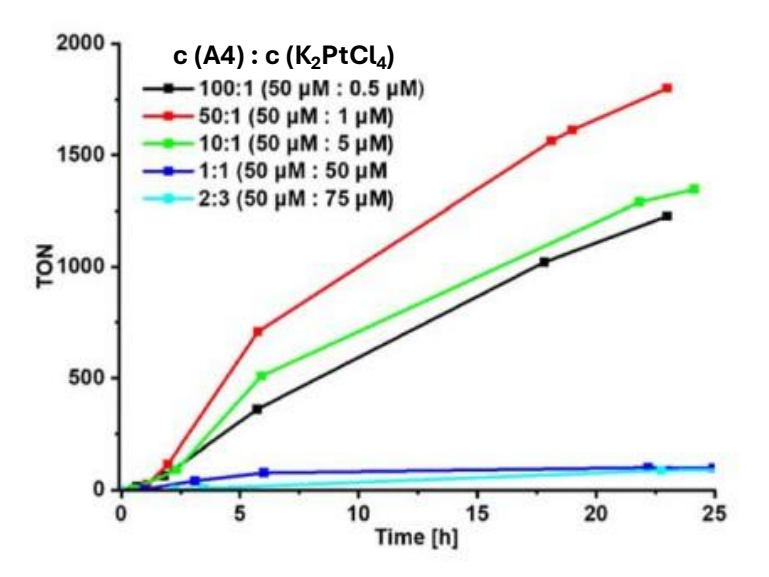


Figure 23 HER activity compared to the ratio of A4 to potassium tetrachloroplatinate.

Most probable explanation of this unusual activity is formation of core-shell nanoparticles. Core of the proposed species is made of un-activated **A4** and the surface is covered with activated **A4** species (Figure 24).

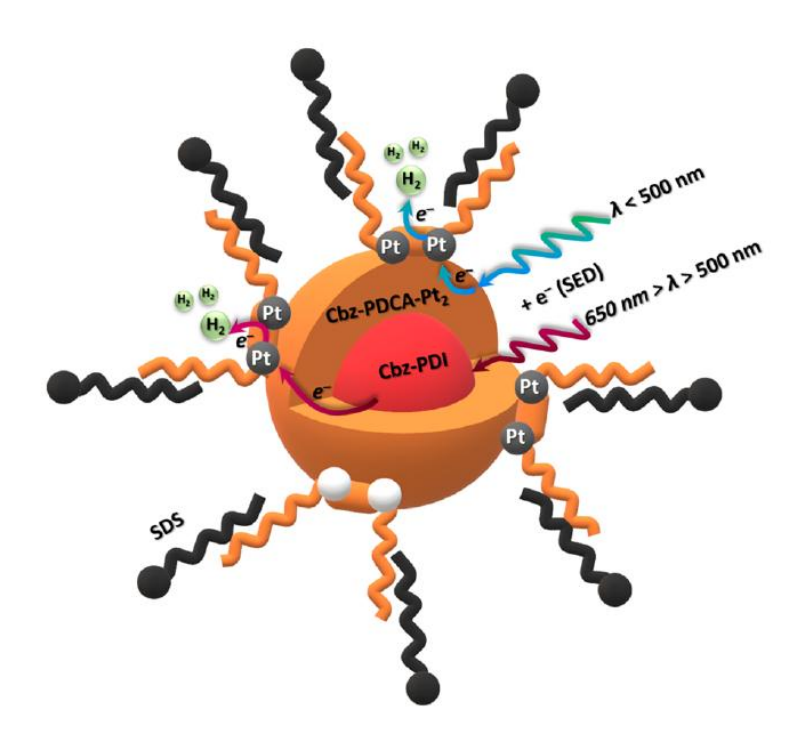


Figure 24 Core-shell structure of the formed photocatalytic system. Cbz-PDI-A4, $Cbz-PDCA-Pt_2$ – activated A4, SED – Sacrificial Electron Donor, SDS – Sodium Dodecyl Sulphate.

In proposed system, the core acts as light scavenging antenna and the shell is responsible for the photocatalytic activity. This model is a sufficient explanation of the activity of highly insoluble PDIs in micellar systems. [78]

4.3 CHLORINATED AND BROMINATED PDIS (A9-A12) — FURTHER RESEARCH ABOUT MOLECULAR CATALYST

Dyes substituted with heavy atoms, like bromine or iodine, in many instances perform better in photocatalytic reactions. It is attributed to heavy atom effect. Occurrence of this effect is proportional to the atomic number of the introduced atom. Heavier atoms increase chance of the intersystem crossing (ISC) therefore increase likelihood of excited molecules staying in T₁ state. Long-lived character of T₁ state reduces chances for early excited states decay via fluorescence. Consequently, there is greater probability of passing an electron from the excited molecule to another. [79] I wanted to investigate how increasing ISC by introduction of heavy atoms to selected compounds from the A series, would affect efficiency of HER and formation of molecular catalyst.

To halogenate selected perylene diimides I used *N*-chloro or *N*-bromosuccinimide (Scheme 41). These halogenating agents are known to be highly selective in halogenation reactions of electron rich aryl derivatives. Most probable mechanism of halogenation with NXS involves formation of highly electrophilic, solvated X⁺ (X= Cl, Br or I) ions.[80], [81]

Scheme 41 Synthesis of A9-A12.

During halogenation I stumbled on problems with reproductivity and unexplained degradation of products manifesting by immobile spots on TLC. I suspected undesirable effect of light on halogenation. Protecting of the reaction mixture from light partially solved the problem with reproductivity. Later on I noticed that reaction proceeds cleanly, when a brand new stir bar is used. There is a literature report about metals like palladium, platinum, gold etc. being trapped in the defects of PTFE coating of stir bars. What is worth mentioning, these contaminated stir bars are capable of catalysing Suzuki reaction without addition of catalyst. [82] Because these contaminants are almost impossible to remove by washing, I made sure to properly mark and store stir bars that were used in metal catalysed reactions. This mostly resolved my problems with occurrence of unpredictable side-reactions.

Ultimately I was able to obtain only products of tetrabromination (A9 and A10). My attempts to obtain pure dichlorinated (A11) and dibrominated (A12) derivatives failed. In the case of A11 I identified major, tetrachlorinated impurity impA11. In turn debromination attempts led to the mixture consisting of di- (A12), tri- (impA12) and tetrabrominated (imp'A12) derivatives. These results suggest that halogenation of these derivatives is difficult to be stopped at dihalogenated

products. It can be explained by negligible difference in reactivity of substrates and dihalogenated products with NXS.

 $Table\ 4\ \mathrm{MALDITOF\text{-}MS}$ analysis of $\mathbf{A9\text{-}A12}$ with major impurities highlighted.

No.	Molecular formula	Monoisotopic mass	MALDITOF-MS peaks
A9	C ₇₆ H ₆₄ Br ₄ N ₄ O ₄	1412.166	1412.206, 1414.214, 1416.222, 1418.236,
A)	O761164D141N4O4	1412.100	1410.222, 1410.230, 1420.244 (M)+
A10	$C_{82}H_{72}Br_{4}N_{4}O_{4} \\$	1492.229	1491.165 (M-H)+, 1494.195, 1496.193, 1498.208, 1500.194 (M)+
A11	$C_{76}H_{62}Cl_{2}N_{4}O_{4} \\$	1164.415	1165.411, 1166.383 (M)+
impA11	$C_{76}H_{60}Cl_4N_4O_4$	1232.337	1232.276, 1233.295, 1234.321, 1235.315, 1237.333, 1239.336 (M)+
A12	$C_{76}H_{62}Br_{2}N_{4}O_{4}$	1252.314	1252.155, 1254.167, 1256.178 (M)+
impA12	$C_{76}H_{61}Br_{3}N_{4}O_{4} \\$	1330.244	1330.063, 1332.071, 1336.097 (M)+
Imp'A12	$C_{76}H_{60}Br_{4}N_{4}O_{4}$	1408.135	1409.982, 1411.984, 1413.988, 1415.989 (M)+

Table 5 ¹HNMR of A9 and A10 with their non-halogenated parent compounds, A2 and A3, for comparison.

No.	Aromatic protons							Methyls	
A9	8.64	8.25	8.04	7.47	7.44	7.15	7.08		
	(s)	(d)	(d)	(d)	(d)	(d)	(d)		
		$7.96~\mathrm{Hz}$	$7.96~\mathrm{Hz}$	$8.79~\mathrm{Hz}$	$8.51~\mathrm{Hz}$	$8.51~\mathrm{Hz}$	$8.79~\mathrm{Hz}$		
	2 H	2 H	2 H	8 H	4 H	4 H	8 H		
A2	8.61 (s)	8.24 (d)	8.06 (d)	7.39 (d)	7.35 (t)	7.22 (d)	7.15 (d)	7.12 (t)	
		7.97 Hz	8.23 Hz	8.51 Hz	7.42 Hz	7.69 Hz	8.78 Hz	7.41 Hz	
					8.23 Hz				
	2 H	2 H	2 H	4 H	8 H	8 H	4 H	4 H	
A10	8.79 (s)	8.28 (d)	8.07 (d)	7.89 (d)	7.59 (d)	7.50 (d)	7.26 (dd)	6.35 (d)	1.71 (s)
		7.97 Hz	7.97 Hz	8.24 Hz	$2.20~\mathrm{Hz}$	$8.24~\mathrm{Hz}$	8.79 Hz,	8.79 Hz	
							$2.20~\mathrm{Hz}$		
	2 H	$2~\mathrm{H}$	2 H	4 H	4 H	4 H	4 H	4 H	12 H

A 3	8.82 (s)	8.32 (d)	8.08 (d)			7.19 (td)		6.49 (dd)	1.76 (s)
		7.97~Hz	8.23 Hz	8.51 Hz	7.69 Hz	7.14 Hz	7.14 Hz	8.24 Hz	4 x Me
					8.24 Hz	1.37 Hz	1.10 Hz	0.82 Hz	
	$2~\mathrm{H}$	2 H	2 H	4 H	8 H	4 H	4 H	4 H	12 H

I confirmed identity of halogenated derivatives (A9-A12) by analysing MALDITOF-MS (Table 4) and ¹HNMR (Table 5) spectra of A9 and A10.

On ¹HNMR, both **A9** and **A10** show 4 less protons than their corresponding parent compounds. This is consistent with the MALDI suggesting that **A9** and **A10** were tetrabrominated. It's worth mentioning that on MALDI isotopic peaks are also visible (M, M+2, M+4, M+6, M+8).

Unfortunately introduction of heavy atoms did not improve HER in any significant way. Unfavourable properties such as low solubility in the aqueous systems was most likely the cause.

4.4 Donor-acceptor perylene diimides for co-catalysis with TiO₂/Platinum nanoparticles

4.4.1 Why using TiO₂ nanoparticles

Although compounds from the series A have promising photophysical properties, adequate HOMO and LUMO energies only a few showed any substantial photocatalytic activity in HER. Orbital energies are a few among many parameters influencing properties of the compounds. The most obvious disadvantage of compounds from A series was low solubility. This property limited applications of these compounds as most of the activity relied on the unreliable formation of shell-core nanoparticles. One of the solution for this problem might be using PDIs for photosensitizing co-catalyst. To assure optimal coverage of the photosensitizer from the co-catalyst, anchoring groups can be used. [83], [84]

In one study[85] researchers were investigating effect of anchoring groups on efficiency of hydrogen production in TiO2|Pt photocatalytic systems sensitized with perylene monoimide (PMI) derivatives (Figure 25 and Figure 26).

Figure 25 Anchoring groups used in the cited research. [85]

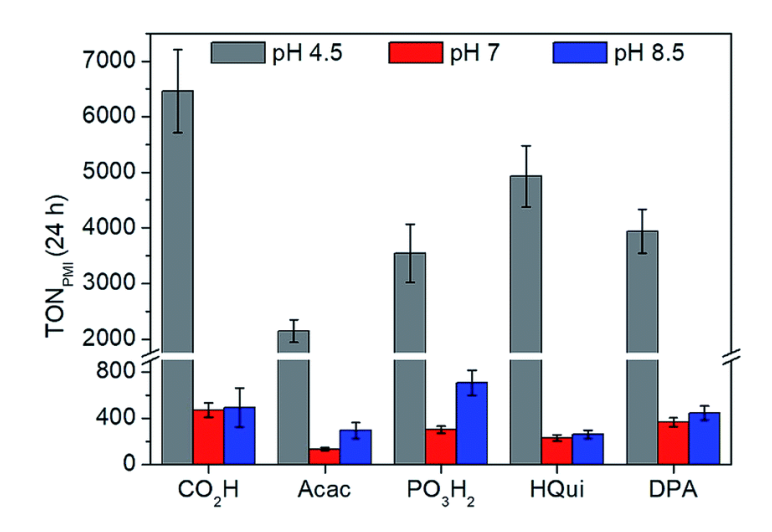


Figure 26 Results from the cited publication. [85] Carboxylic group seems to perform the best at pH 4.5.

Their results indicated that the best performing PMI derivative had carboxylic group and the optimal pH was 4.5.[86] I decided to use the same anchoring group for PDI derivatives for my research. My choice was dictated by the very close similarity of PDI to PMI.

4.4.2 Synthesis and analysis

4.4.2.1 Synthesis of model perylene monoamide (M5)

I replicated synthesis of the best performing compound (M5) from the publication about anchoring groups in PMI derivatives for water splitting. This

synthesis proceeded via $M1 \rightarrow M2 \rightarrow M3 \rightarrow M4 \rightarrow M5$ (presented on the Scheme 35 on the page 72). The last step required purification of the reaction mixture on Sephadex gel. Unfortunately I was unable to purify it on silica gel. Every approach, in various mixtures of solvents, resulted in smearing of the product and elution with impurities formed during synthesis.

Due to high price of the Sephadex, I decided to modify the synthetic route. Instead of performing Sonogashira coupling with 4-ethynylbenzoic acid, I used methyl 4-ethynylbenzoate. I was able to purify the coupling product, **M4**, on the cost-effective and commonly used silica gel column. After obtaining pure **M4** I performed basic hydrolysis of the methyl ester. After acidifying of the mixture I obtained **M5** in the carboxylic acid form (Scheme 42).

Scheme 42 Original (top) and my (bottom) synthetic path leading to the model PMI M5.

To confirm identity of **M1-M5**, these were analyzed on MALDI-TOF (Table 6) or/and ¹HNMR (Table 7). Mass and NMR spectra were consistent with the expected outcomes and published data.

Table 6 MALDITOF-MS analysis of M1-M5.

No.	Molecular formula	Monoisotopic mass	MALDITOF-MS peaks
M1	$\mathrm{C}_{36}\mathrm{H}_{31}\mathrm{NO}_2$	509.235	510.286 (M+H)+
M 2	$\mathrm{C}_{36}\mathrm{H}_{28}\mathrm{Br}_{3}\mathrm{NO}_{2}$	742.967	743.474, 745.486, 747.492 (M)+
М3	$\mathrm{C}_{56}\mathrm{H}_{54}\mathrm{BrNO}_{4}$	883.324	883.619, 884.629, 885.651 (M)+
M 4	$\mathrm{C}_{66}\mathrm{H}_{61}\mathrm{NO}_{6}$	963.449	964.474, 965.475 (M+H)+
M5	$\mathrm{C}_{65}\mathrm{H}_{59}\mathrm{NO}_{6}$	949.434	950.501 (M+H)+, 988.449 (M+K)+

Table 7 Chemical shifts (ppm) and coupling constants in the 1H NMR spectra of M2 and M4.

No.	Aroma	tic												Met	hyls		
M2	9.32 (dd) 7.63 Hz	9.1 (d) z 8.2		8.92 (s)	8.90 (s)	(d	44 d) 24 Hz	7.98 (d) 8.24 Hz	7.80 (t) 8.24		7.60 (d) 8.55 Hz	7.47 (dd) 8.54 Hz	6.98 (d) 2.12 Hz	1.33 (s)		1.30 (s)	
	0.92 Hz	${f z}$				0.	91 Hz,		7.93	$_{ m Hz}$		$2.44~\mathrm{Hz}$					
	1 H	1 H	[1 H	1 H	1	Н	1 H	1 H		1 H	1 H	1 H	9 H		9H	
M4	9.43 (d) 7.58 Hz	9.34 (d) 8.24 Hz	8.54 (d) 8.24 Hz	8.31 (s)	8.29 (s)	8.08 (d) 8.24 Hz	8.02 (d) 8.24 Hz	7.85 (d) 8.24 Hz	7.72 (m)	7.59 (d) 8.23 Hz	(d)	7.09 (dd) 8.85 Hz 2.75 Hz	6.93 (d) 2.75 Hz	3.95 (s)	1.34 (s)	1.29 (s)	1.25 (s)
	1 H	1 H	1 H	1 H	1 H	2 H	4 H	1 H	3 H	4 H	1 H	1 H	1 H	3 H	18 H	9 H	9 H

4.4.2.2 Inserting anchoring group to PDIs

After practicing synthetic steps on the perylene monoamide from the publication, I proceed to the synthesis of similar perylene diimide derivatives. My goal was to selectively insert single anchoring group to the PDI core. I aimed to do it via Sonogashira coupling of dibromo-PDI and methyl 4-ethynylbenzoate (Scheme 43). Methyl ester was meant to be removed by basic hydrolysis in the subsequent steps, as it was done with the model PMI derivative (Scheme 42 page 108).

Scheme 43 Synthesis of perylene diimide derivatives with anchoring group (B1-B10).

Knowing oxygen-free conditions are a necessary in Sonogashira coupling I wanted to test whether flushing reaction mixture in vials with argon is sufficient. I used a mixture of toluene and triethylamine as a solvent, as this solvent mixture was reported in the original literature about perylenemonoimide photosensitizer. Dibromo-PDI (A0) and 4-ethynylbenzoate were added in 1:1 molar ratio and the reaction was run in 50°C for 12 hours. I isolated a vibrant pink coloured product in a low yield. MALDI analysis of the isolated product revealed a peak of m/z 931.038. This suggests that a disubstituted product was formed ($C_{60}H_{54}N_2O_8$ - 930.388).

Furthermore I observed a formation of an unidentified, colourless, fluorescent side product. When reaction was run in strictly oxygen-free conditions under Schlenk apparatus, formation of the side-product was mostly eliminated. I suspect this side product was most likely a dimerized methyl 4-ethynylbenzoate. Traces of oxygen lead to palladium catalysed homocoupling of terminal alkynes via Glaser coupling (Scheme 44). This is common undesired reaction when performing Sonogashira coupling.[8], [87]

Scheme 44 Proposed explanation of the formation of fluorescent side product during coupling rection.

The problem of lack of selectivity of monosubstitution over disubstitution was still unresolved. Based on my trials, selectivity of substitution of bromine atoms in A0 is unaffected by stoichiometry, temperature of the reaction or traces of oxygen. This suggests that coupling reaction of methyl 4-ethynylbenzoate is kinetically more favourable with monosubstituted product than with substrate A0. Methyl 4-ethynylbenzoate reacts with the product of first substitution preferentially over A0. Hence no desired, monosubstituted, product can be isolated, as it reacts further as soon as it is formed (Scheme 45).

Scheme 45 Proposed explanation of the formation of undesired products.

I wanted to test whether free 4-ethynylbenzoic acid reacts in the same way as its methyl ester. When **A0** and 4-ethynylbenzoic acid were reacted in stoichiometric amounts, the coupling reaction progressed cleanly to **B0** (Scheme 46).

$$\begin{array}{c} C_{8}H_{17} \\ O \\ N \\ O \\ Pd(PPh_{3})_{4}/Cul \\ Pd(PPh_{3})_{4}/Cul \\ Toluene/NEt_{3} \\ 4 \\ 1 \\ O \\ R_{0} \\ \end{array}$$

Scheme 46 Successful synthesis of B0.

I suspect this difference between reactivity of methyl ester and free carboxylic acid can potentially be explained by following factors:

- 1) In the reaction conditions, product **B0** exists as anionic species (as triethylammonium salt), which most likely reduces its solubility in the non-polar toluene. As the consequence of lowered solubility of **B0**, it is less available for further substitution reactions.
- 2) 4-ethynylbenzoic acid is in anionic form as well. **B0** anion and 4-ethynylbenzoate anion are electrostatically repelling each other, making the reaction between these species less likely to occur.

Even though **B0** is a free acid, I was able to avoid purification on Sephadex gel. Most of the impurities formed during the synthesis could be easily separated from the desired product by using pure chloroform as an eluent. Due to high affinity of **B0** towards silica gel it was barely eluted in these conditions. It stayed on top, adsorbed on the silica gel while most of the non-polar impurities were eluted first. After eluting impurities and unreacted **A0**, I used chloroform with 1% acetic acid to elute pure **B0**

I used obtained **B0** to synthesize planned **B1-B10** (Figure 27).

Figure 27 Obtained PDIs with anchoring group (B0-B10).

I synthesized compounds B1-B10 via Suzuki coupling of B0 with corresponding boronic acid derivatives. Synthesized compounds were analyzed on MALDI-TOF (Table 8) and 1HNMR (Table 9).

Table 8 MALDITOF-MS analysis of B0-B10.

No.	Molecular formula	Monoisotopic mass	MALDITOF-MS peaks
B0	$\mathrm{C_{49}H_{45}BrN_{2}O_{6}}$	836.246	836.216 (M)+
B 1	$C_{57}H_{55}N_3O_6$	877.409	878.489 (M+H)+
B2	$C_{70}H_{63}N_3O_6\\$	1041.472	1026.916 [M-CH ₃] ⁺ 1043.842 [M+2H] ⁺
В3	$C_{67}H_{59}N_{3}O_{6}$	1001.440	1002.557 (M+H)+
B4	$C_{69}H_{61}N_{3}O_{8} \\$	1059.446	1059.444 (M)+
B5	$C_{67}H_{57}N_3O_6$	999.425	1000.662 (M+H)+
B6	$C_{59}H_{58}N_{2}O_{7} \\$	907.117	908.934 (M+H)+
B 7	$C_{56}H_{52}N_{2}O_{6}$	848.383	849.486 (M+H)+
B8	$C_{61}H_{52}N_{2}O_{6}S$	940.355	941.334 (M+H)+
В9	$C_{57}H_{55}N_3O_8S$	941.371	942.624 (M+H)+
B10	$C_{56}H_{49}N_3O_6$	860.020	861.430 (M+H)+

Table 9 Chemical shifts (ppm) and coupling constants in the 1H NMR spectra of (B0-B10).

No.													
$\mathbf{B0}$	9.87 (d)	9.56 (dd)	8.94 (s)	8.87 (s)	8.76 (dd)	8.69 (d)	8.18 (d)	7.72 (d)					
	$8.24~\mathrm{Hz}$	$8.23~\mathrm{Hz}$			$7.96~\mathrm{Hz}$	7.92	$8.24~\mathrm{Hz}$	$7.68~\mathrm{Hz}$					
		$3.02~\mathrm{Hz}$			$2.20~\mathrm{Hz}$								
	1 H	1H	1 H	1 H	1 H	1 H	$2~\mathrm{H}$	$2~\mathrm{H}$					
B1	9.83 (d)	8.73 (s)	8.70 (d)	8.59 (d)	8.15 (s)	8.15 (bd)	8.10 (d)	8.00 (d)	7.71 (d)	7.67 (d)	6.76 (d)	6.74 (d)	3.06 (s)
	$6.41~\mathrm{Hz}$	1 H	$8.24~\mathrm{Hz}$	$10.99~\mathrm{Hz}$			$7.02~\mathrm{Hz}$	$10.68 \mathrm{Hz}$	6.11 Hz	$7.02~\mathrm{Hz}$	$6.10~\mathrm{Hz}$	$7.02~\mathrm{Hz}$	
	1 H		1 H	1 H	1 H	1 H	1 H	1 H	2 H	1 H	1 H	1 H	6 H
B2	9.94 (d)	8.76 (d)	8.75 (s)	8.19 (s)	8.17 (d)	7.70 (m)	7.56(t)	7.49 (m)	7.16 (d)	7.14 (d)	$7.01(2\times t)$	6.44 (d)	1.72 (s)
	$9.16~\mathrm{Hz}$	7.94 Hz			$7.02~\mathrm{Hz}$		$7.63~\mathrm{Hz}$		$6.41~\mathrm{Hz}$	$7.32~\mathrm{Hz}$	$7.63~\mathrm{Hz}$	$8.24~\mathrm{Hz}$	
							$7.33~\mathrm{Hz}$				$7.33~\mathrm{Hz}$		
	1 H	1 H	1 H	1 H	2 H	4 H	$2~\mathrm{H}$	4 H	1 H	1 H	$2~\mathrm{H}$	2 H	6 H
B 3	9.73 (d)	8.56 (d)	8.53 (d)	8.49 (s)	8.46 (s)	8.42 (d)	8.18 (m)	7.96 (t)	7.72 (m)	7.51 (m)	7.18 (m)	7.10 (m)	$7.06(2\times t)$
	$8.24~\mathrm{Hz}$	$8.24~\mathrm{Hz}$	$7.33~\mathrm{Hz}$			$7.63~\mathrm{Hz}$		$8.54~\mathrm{Hz}$					$6.71~\mathrm{Hz}$
								$8.24~\mathrm{Hz}$					
	1 H	1 H	1 H	1 H	1 H	1 H	3 H	1 H	2 H	4 H	4 H	2 H	2 H
B 4	9.90 (d)	8.66 (d)	8.63 (s)	8.55 (s)	8.17 (d)	8.12 (d)	8.02 (d)	7.80 (d)	7.77-7.41	7.02 (d)	3.90 (s)		
	$7.94~\mathrm{Hz}$	$7.94~\mathrm{Hz}$			$7.63~\mathrm{Hz}$	$7.93~\mathrm{Hz}$	$9.16~\mathrm{Hz}$	$8.54~\mathrm{Hz}$	(m)	$7.02~\mathrm{Hz}$			
	1 H	1 H	1 H	1 H	1 H	2 H	2 H	2 H	6 H	2 H	6 H		

9.77 (d)	8.64 (s)	8.58 (d)	8.55 (s)	8.08 (d)	7.98 (d)	7.92 (d)	7.61 (d)	7.55 (d)	7.32 (t)	7.31 (d)	7.13 (t)	7.11 (d)
$8.24~\mathrm{Hz}$		$7.96~\mathrm{Hz}$		$8.24~\mathrm{Hz}$	$6.87~\mathrm{Hz}$	$7.96~\mathrm{Hz}$	$8.24~\mathrm{Hz}$	$7.68~\mathrm{Hz}$	$8.24~\mathrm{Hz}$	$8.24~\mathrm{Hz}$	$7.41~\mathrm{Hz}$	$6.86~\mathrm{Hz}$
1 H	1 H	1 H	1 H	1 H	4 H	1 H	$2~\mathrm{H}$	4 H	2 H	1 H	$2~\mathrm{H}$	1 H
9.69 (d)	8.53 (d)	8.43 (s)	8.36 (s)	8.10 (d)	7.90 (d)	7.74 (d)	7.71 (d)	7.68 (d)	7.66 (d)	7.50 (d)	7.66 (d)	2.41 (s)
$8.24~\mathrm{Hz}$	$8.24~\mathrm{Hz}$			$7.32~\mathrm{Hz}$	$6.71~\mathrm{Hz}$	$7.63~\mathrm{Hz}$	$8.85~\mathrm{Hz}$	$8.24~\mathrm{Hz}$	$8.24~\mathrm{Hz}$	$7.02~\mathrm{Hz}$	$8.24~\mathrm{Hz}$	
1 H	1 H	1 H	1 H	2 H	1 H	2 H	1 H	1 H	1 H	1 H	1 H	3 H
9.87 (d)	8.75 (s)	8.67 (d)	8.62 (bs)	8.58 (s)	8.13 (d)	8.02 (d)	7.98 (d)	7.93 (bt)	8.79 (d)	7.76 (d)		
$7.63~\mathrm{Hz}$		$9.16~\mathrm{Hz}$			$8.24~\mathrm{Hz}$	$8.54~\mathrm{Hz}$	$9.16~\mathrm{Hz}$		$6.41~\mathrm{Hz}$	$7.02~\mathrm{Hz}$		
1 H	1 H	1 H	1 H	1 H	2 H	1 H	1 H	2 H	4 H	2 H		
9.80 (d)	8.65 (d)	8.48 (s)	8.44 (s)	8.10 (d)	8.06 (d)	7.90 (d)	7.74 (d)	7.69 (d)	7.66 (d)	2.72 (s)	2.57 (s)	
$7.94~\mathrm{Hz}$	$8.24~\mathrm{Hz}$			$7.63~\mathrm{Hz}$	$8.24~\mathrm{Hz}$	$7.63~\mathrm{Hz}$	$7.32~\mathrm{Hz}$	$7.63~\mathrm{Hz}$	$7.94~\mathrm{Hz}$			
1 H	1 H	1 H	1 H	2 H	1 H	2 H	2 H	2 H	1 H	3 H	3 H	
9.80 (d)	8.64 (d)	8.50 (s)	8.43 (s)	8.10 (d)	8.05 (d)	7.87 (d)	7.74 (d)	7.70 (d)	7.66 (d)			
$7.94~\mathrm{Hz}$	$7.63~\mathrm{Hz}$			$7.33~\mathrm{Hz}$	$7.93~\mathrm{Hz}$	$7.33~\mathrm{Hz}$	$7.32~\mathrm{Hz}$	$7.32~\mathrm{Hz}$	$7.94~\mathrm{Hz}$			
1 H	1 H	1 H	1 H	2 H	1 H	2 H	2 H	2 H	1 H			
	8.24 Hz 1 H 9.69 (d) 8.24 Hz 1 H 9.87 (d) 7.63 Hz 1 H 9.80 (d) 7.94 Hz 1 H 9.80 (d) 7.94 Hz	8.24 Hz 1 H 1 H 9.69 (d) 8.53 (d) 8.24 Hz 8.24 Hz 1 H 1 H 9.87 (d) 8.75 (s) 7.63 Hz 1 H 1 H 9.80 (d) 8.65 (d) 7.94 Hz 1 H 1 H 9.80 (d) 8.64 (d) 7.94 Hz 7.63 Hz	8.24 Hz 7.96 Hz 1 H 1 H 1 H 9.69 (d) 8.53 (d) 8.43 (s) 8.24 Hz 8.24 Hz 1 H 1 H 1 H 9.87 (d) 8.75 (s) 8.67 (d) 7.63 Hz 9.16 Hz 1 H 1 H 1 H 9.80 (d) 8.65 (d) 8.48 (s) 7.94 Hz 8.24 Hz 1 H 1 H 1 H 9.80 (d) 8.64 (d) 8.50 (s) 7.94 Hz 7.63 Hz	8.24 Hz 7.96 Hz 1 H 1 H 1 H 9.69 (d) 8.53 (d) 8.43 (s) 8.36 (s) 8.24 Hz 8.24 Hz 1 H 1 H 1 H 1 H 1 H 1 H 9.87 (d) 8.75 (s) 8.67 (d) 8.62 (bs) 7.63 Hz 9.16 Hz 1 H 1 H 1 H 1 H 1 H 9.80 (d) 8.65 (d) 8.48 (s) 8.44 (s) 7.94 Hz 8.64 (d) 8.50 (s) 8.43 (s) 7.94 Hz 7.63 Hz 4.43 (s) 8.43 (s)	8.24 Hz 7.96 Hz 8.24 Hz 1 H 1 H 1 H 1 H 9.69 (d) 8.53 (d) 8.43 (s) 8.36 (s) 8.10 (d) 8.24 Hz 8.24 Hz 7.32 Hz 1 H 1 H 1 H 2 H 9.87 (d) 8.75 (s) 8.67 (d) 8.62 (bs) 8.58 (s) 7.63 Hz 9.16 Hz 1 H 1 H 1 H 9.80 (d) 8.65 (d) 8.48 (s) 8.44 (s) 8.10 (d) 7.94 Hz 8.24 Hz 7.63 Hz 7.63 Hz 1 H 1 H 1 H 2 H 9.80 (d) 8.64 (d) 8.50 (s) 8.43 (s) 8.10 (d) 7.94 Hz 7.63 Hz 7.33 Hz	8.24 Hz 7.96 Hz 8.24 Hz 6.87 Hz 1 H 1 H 1 H 1 H 4 H 9.69 (d) 8.53 (d) 8.43 (s) 8.36 (s) 8.10 (d) 7.90 (d) 8.24 Hz 8.24 Hz 7.32 Hz 6.71 Hz 1 H 1 H 1 H 2 H 1 H 9.87 (d) 8.75 (s) 8.67 (d) 8.62 (bs) 8.58 (s) 8.13 (d) 7.63 Hz 9.16 Hz T 8.24 Hz 1 H 1 H 1 H 1 H 2 H 9.80 (d) 8.65 (d) 8.48 (s) 8.44 (s) 8.10 (d) 8.06 (d) 7.94 Hz 8.64 (d) 8.50 (s) 8.43 (s) 8.10 (d) 8.05 (d) 9.80 (d) 8.64 (d) 8.50 (s) 8.43 (s) 8.10 (d) 8.05 (d)	8.24 Hz 7.96 Hz 8.24 Hz 6.87 Hz 7.96 Hz 1 H 1 H 1 H 1 H 4 H 1 H 9.69 (d) 8.53 (d) 8.43 (s) 8.36 (s) 8.10 (d) 7.90 (d) 7.74 (d) 8.24 Hz 8.24 Hz 7.32 Hz 6.71 Hz 7.63 Hz 1 H 1 H 1 H 2 H 1 H 2 H 9.87 (d) 8.75 (s) 8.67 (d) 8.62 (bs) 8.58 (s) 8.13 (d) 8.02 (d) 7.63 Hz 9.16 Hz	8.24 Hz 7.96 Hz 8.24 Hz 7.96 Hz 7.96 Hz 8.24 Hz 7.96 Hz 8.24 Hz 8.24 Hz 7.96 Hz 8.24 Hz 1 H 1 H 1 H 2 H 2 H 9.69 (d) 8.53 (d) 8.43 (s) 8.36 (s) 8.10 (d) 7.90 (d) 7.74 (d) 7.71 (d) 7.63 Hz 8.85 Hz 8.24 Hz 7.63 Hz 7.63 Hz 8.85 Hz 1 H 1 H 1 H 1 H 2 H 1 H 2 H 1 H 1 H 1 H 1 H 9.87 (d) 8.67 (d) 8.62 (bs) 8.58 (s) 8.13 (d) 8.02 (d) 7.98 (d) 7.99 (d) <td< th=""><th>8.24 Hz 7.96 Hz 8.24 Hz 6.87 Hz 7.96 Hz 7.68 Hz 1 H 1 H 1 H 1 H 4 H 1 H 2 H 4 H 9.69 (d) 8.53 (d) 8.43 (s) 8.36 (s) 8.10 (d) 7.90 (d) 7.74 (d) 7.71 (d) 7.68 (d) 8.24 Hz 8.24 Hz 7.32 Hz 6.71 Hz 7.63 Hz 8.85 Hz 8.24 Hz 1 H 1 H 1 H 2 H 1 H 2 H 1 H 1 H 1 H 9.87 (d) 8.75 (s) 8.67 (d) 8.62 (bs) 8.58 (s) 8.13 (d) 8.02 (d) 7.98 (d) 7.93 (bt) 7.63 Hz 9.16 Hz 1 H 1 H 2 H 1 H 1 H 2 H 9.80 (d) 8.65 (d) 8.44 (s) 8.10 (d) 8.06 (d) 7.90 (d) 7.74 (d) 7.69 (d) 7.94 Hz 1 H 1 H 1 H 2 H 1 H 2 H 2 H 9.80 (d) 8.64 (d) 8.50 (s) 8.43 (s) 8.10 (d) 8.05 (d) 7.87 (d) 7.74 (d) 7.70 (d) 9.80 (d) 8.64 (d) <</th><th>8.24 Hz 7.96 Hz 8.24 Hz 6.87 Hz 7.96 Hz 7.68 Hz 8.24 Hz 1 H 1 H 1 H 1 H 4 H 1 H 2 H 4 H 2 H 9.69 (d) 8.53 (d) 8.43 (s) 8.36 (s) 8.10 (d) 7.90 (d) 7.74 (d) 7.71 (d) 7.68 (d) 7.66 (d) 8.24 Hz 8.24 Hz 7.32 Hz 6.71 Hz 7.63 Hz 8.85 Hz 8.24 Hz 8.24 Hz 1 H 1 H 1 H 2 H 1 H 2 H 1 H 2 H 1 H 1 H 2 H 4 H 1 H 1 H 2 H 1 H 1 H 2 H 4 H 1 H 1 H 2 H 1 H 1 H 2 H 2 H 2 H 2 H<!--</th--><th>8.24 Hz 7.96 Hz 8.24 Hz 6.87 Hz 7.96 Hz 7.96 Hz 8.24 Hz 1 H 1 H 1 H 2 H 4 H 2 H 2 H 1 H 9.69 (d) 8.53 (d) 8.43 (s) 8.36 (s) 8.10 (d) 7.90 (d) 7.74 (d) 7.71 (d) 7.68 (d) 7.66 (d) 7.50 (d) 8.24 Hz 8.24 Hz 7.32 Hz 6.71 Hz 7.63 Hz 8.25 Hz 8.24 Hz 8.24 Hz 7.02 Hz 1 H 1 H 1 H 1 H 2 H 1 H 2 H 1 H 1 H 2 H 2 H 2 H 2 H 2 H 2 H 2 H 2 H 2 H 2 H 2 H 2 H 2 H 2 H 2 H 2 H 2 H 3 H 3 H 3 H<!--</th--><th>8.24 Hz 7.96 Hz 8.24 Hz 6.87 Hz 7.96 Hz 7.96 Hz 8.24 Hz 7.68 Hz 8.24 Hz 8.24 Hz 7.41 Hz 1 H 1 H 1 H 1 H 4 H 1 H 2 H 4 H 2 H 1 H 2 H 9.69 (d) 8.53 (d) 8.43 (s) 8.36 (s) 8.10 (d) 7.90 (d) 7.74 (d) 7.71 (d) 7.68 (d) 7.66 (d) 7.50 (d) 7.66 (d) 8.24 Hz 8.24 Hz 8.24 Hz 8.24 Hz 8.24 Hz 8.24 Hz 7.02 Hz 8.24 Hz 9.69 (d) 8.53 (d) 8.43 (s) 8.10 (d) 7.90 (d) 7.74 (d) 7.68 (d) 7.66 (d) 7.50 (d) 7.66 (d) 9.87 (d) 8.75 (s) 8.67 (d) 8.62 (bs) 8.58 (s) 8.13 (d) 8.02 (d) 7.98 (d) 7.93 (bt) 8.79 (d) 7.76 (d) 7.76 (d) 9.80 (d) 8.65 (d) 8.44 (s) 8.10 (d) 8.06 (d) 7.90 (d) 7.74 (d) 7.66 (d) 7.94 Hz 9.60 (d) 7.66 (d) 7.76 (d) 7.74 (d) 7.66 (d) 7.66 (d) 7.76 (d) 7.77 (d) 7.77 (d) 7.77 (</th></th></th></td<>	8.24 Hz 7.96 Hz 8.24 Hz 6.87 Hz 7.96 Hz 7.68 Hz 1 H 1 H 1 H 1 H 4 H 1 H 2 H 4 H 9.69 (d) 8.53 (d) 8.43 (s) 8.36 (s) 8.10 (d) 7.90 (d) 7.74 (d) 7.71 (d) 7.68 (d) 8.24 Hz 8.24 Hz 7.32 Hz 6.71 Hz 7.63 Hz 8.85 Hz 8.24 Hz 1 H 1 H 1 H 2 H 1 H 2 H 1 H 1 H 1 H 9.87 (d) 8.75 (s) 8.67 (d) 8.62 (bs) 8.58 (s) 8.13 (d) 8.02 (d) 7.98 (d) 7.93 (bt) 7.63 Hz 9.16 Hz 1 H 1 H 2 H 1 H 1 H 2 H 9.80 (d) 8.65 (d) 8.44 (s) 8.10 (d) 8.06 (d) 7.90 (d) 7.74 (d) 7.69 (d) 7.94 Hz 1 H 1 H 1 H 2 H 1 H 2 H 2 H 9.80 (d) 8.64 (d) 8.50 (s) 8.43 (s) 8.10 (d) 8.05 (d) 7.87 (d) 7.74 (d) 7.70 (d) 9.80 (d) 8.64 (d) <	8.24 Hz 7.96 Hz 8.24 Hz 6.87 Hz 7.96 Hz 7.68 Hz 8.24 Hz 1 H 1 H 1 H 1 H 4 H 1 H 2 H 4 H 2 H 9.69 (d) 8.53 (d) 8.43 (s) 8.36 (s) 8.10 (d) 7.90 (d) 7.74 (d) 7.71 (d) 7.68 (d) 7.66 (d) 8.24 Hz 8.24 Hz 7.32 Hz 6.71 Hz 7.63 Hz 8.85 Hz 8.24 Hz 8.24 Hz 1 H 1 H 1 H 2 H 1 H 2 H 1 H 2 H 1 H 1 H 2 H 4 H 1 H 1 H 2 H 1 H 1 H 2 H 4 H 1 H 1 H 2 H 1 H 1 H 2 H 2 H 2 H 2 H </th <th>8.24 Hz 7.96 Hz 8.24 Hz 6.87 Hz 7.96 Hz 7.96 Hz 8.24 Hz 1 H 1 H 1 H 2 H 4 H 2 H 2 H 1 H 9.69 (d) 8.53 (d) 8.43 (s) 8.36 (s) 8.10 (d) 7.90 (d) 7.74 (d) 7.71 (d) 7.68 (d) 7.66 (d) 7.50 (d) 8.24 Hz 8.24 Hz 7.32 Hz 6.71 Hz 7.63 Hz 8.25 Hz 8.24 Hz 8.24 Hz 7.02 Hz 1 H 1 H 1 H 1 H 2 H 1 H 2 H 1 H 1 H 2 H 2 H 2 H 2 H 2 H 2 H 2 H 2 H 2 H 2 H 2 H 2 H 2 H 2 H 2 H 2 H 2 H 3 H 3 H 3 H<!--</th--><th>8.24 Hz 7.96 Hz 8.24 Hz 6.87 Hz 7.96 Hz 7.96 Hz 8.24 Hz 7.68 Hz 8.24 Hz 8.24 Hz 7.41 Hz 1 H 1 H 1 H 1 H 4 H 1 H 2 H 4 H 2 H 1 H 2 H 9.69 (d) 8.53 (d) 8.43 (s) 8.36 (s) 8.10 (d) 7.90 (d) 7.74 (d) 7.71 (d) 7.68 (d) 7.66 (d) 7.50 (d) 7.66 (d) 8.24 Hz 8.24 Hz 8.24 Hz 8.24 Hz 8.24 Hz 8.24 Hz 7.02 Hz 8.24 Hz 9.69 (d) 8.53 (d) 8.43 (s) 8.10 (d) 7.90 (d) 7.74 (d) 7.68 (d) 7.66 (d) 7.50 (d) 7.66 (d) 9.87 (d) 8.75 (s) 8.67 (d) 8.62 (bs) 8.58 (s) 8.13 (d) 8.02 (d) 7.98 (d) 7.93 (bt) 8.79 (d) 7.76 (d) 7.76 (d) 9.80 (d) 8.65 (d) 8.44 (s) 8.10 (d) 8.06 (d) 7.90 (d) 7.74 (d) 7.66 (d) 7.94 Hz 9.60 (d) 7.66 (d) 7.76 (d) 7.74 (d) 7.66 (d) 7.66 (d) 7.76 (d) 7.77 (d) 7.77 (d) 7.77 (</th></th>	8.24 Hz 7.96 Hz 8.24 Hz 6.87 Hz 7.96 Hz 7.96 Hz 8.24 Hz 1 H 1 H 1 H 2 H 4 H 2 H 2 H 1 H 9.69 (d) 8.53 (d) 8.43 (s) 8.36 (s) 8.10 (d) 7.90 (d) 7.74 (d) 7.71 (d) 7.68 (d) 7.66 (d) 7.50 (d) 8.24 Hz 8.24 Hz 7.32 Hz 6.71 Hz 7.63 Hz 8.25 Hz 8.24 Hz 8.24 Hz 7.02 Hz 1 H 1 H 1 H 1 H 2 H 1 H 2 H 1 H 1 H 2 H 2 H 2 H 2 H 2 H 2 H 2 H 2 H 2 H 2 H 2 H 2 H 2 H 2 H 2 H 2 H 2 H 3 H 3 H 3 H </th <th>8.24 Hz 7.96 Hz 8.24 Hz 6.87 Hz 7.96 Hz 7.96 Hz 8.24 Hz 7.68 Hz 8.24 Hz 8.24 Hz 7.41 Hz 1 H 1 H 1 H 1 H 4 H 1 H 2 H 4 H 2 H 1 H 2 H 9.69 (d) 8.53 (d) 8.43 (s) 8.36 (s) 8.10 (d) 7.90 (d) 7.74 (d) 7.71 (d) 7.68 (d) 7.66 (d) 7.50 (d) 7.66 (d) 8.24 Hz 8.24 Hz 8.24 Hz 8.24 Hz 8.24 Hz 8.24 Hz 7.02 Hz 8.24 Hz 9.69 (d) 8.53 (d) 8.43 (s) 8.10 (d) 7.90 (d) 7.74 (d) 7.68 (d) 7.66 (d) 7.50 (d) 7.66 (d) 9.87 (d) 8.75 (s) 8.67 (d) 8.62 (bs) 8.58 (s) 8.13 (d) 8.02 (d) 7.98 (d) 7.93 (bt) 8.79 (d) 7.76 (d) 7.76 (d) 9.80 (d) 8.65 (d) 8.44 (s) 8.10 (d) 8.06 (d) 7.90 (d) 7.74 (d) 7.66 (d) 7.94 Hz 9.60 (d) 7.66 (d) 7.76 (d) 7.74 (d) 7.66 (d) 7.66 (d) 7.76 (d) 7.77 (d) 7.77 (d) 7.77 (</th>	8.24 Hz 7.96 Hz 8.24 Hz 6.87 Hz 7.96 Hz 7.96 Hz 8.24 Hz 7.68 Hz 8.24 Hz 8.24 Hz 7.41 Hz 1 H 1 H 1 H 1 H 4 H 1 H 2 H 4 H 2 H 1 H 2 H 9.69 (d) 8.53 (d) 8.43 (s) 8.36 (s) 8.10 (d) 7.90 (d) 7.74 (d) 7.71 (d) 7.68 (d) 7.66 (d) 7.50 (d) 7.66 (d) 8.24 Hz 8.24 Hz 8.24 Hz 8.24 Hz 8.24 Hz 8.24 Hz 7.02 Hz 8.24 Hz 9.69 (d) 8.53 (d) 8.43 (s) 8.10 (d) 7.90 (d) 7.74 (d) 7.68 (d) 7.66 (d) 7.50 (d) 7.66 (d) 9.87 (d) 8.75 (s) 8.67 (d) 8.62 (bs) 8.58 (s) 8.13 (d) 8.02 (d) 7.98 (d) 7.93 (bt) 8.79 (d) 7.76 (d) 7.76 (d) 9.80 (d) 8.65 (d) 8.44 (s) 8.10 (d) 8.06 (d) 7.90 (d) 7.74 (d) 7.66 (d) 7.94 Hz 9.60 (d) 7.66 (d) 7.76 (d) 7.74 (d) 7.66 (d) 7.66 (d) 7.76 (d) 7.77 (d) 7.77 (d) 7.77 (

The ¹H NMR spectra of **B0-A5** and **B7-B10** are characterized by the signals coming from the perylene diimide core substituted on the C1 and C7 and. Due to the asymmetric substitution, the signals from PDI core are present as multiple, distinct signals rather than fewer signals with double intensity. This is unlike pattern of A-series derivatives, for which signals were often of double intensity due to symmetry.

The most characteristic signals of PDI core are two separate singlets recorded in the range 8.19-8.94 ppm coming from the H2 and H8 protons respectively.

Another characteristic signals, are pair of doublets coming from two pairs of protons. This pattern is characteristic for para-substituted phenyl ring and can be assigned to protons from anchoring group. Unfortunately C1 substituents often contain similar patter of substitution. Moreover these substituents are aromatic rings which makes assignment of signals more challenging. This is most apparent when comparing ¹HNMR of substrate **B0** and other **B** series compounds. Signals which are relatively easy to find in **B0**, i.e. 8.18 ppm (d, 2H) and 7.72 ppm (d, 2H), are obscured in other derivatives by signals of protons from the aromatic substituents.

Signals from C1 substituents are important for differentiation of compounds from B series. Most characteristic signals are coming from methyl groups:

B1 singlet at 3.06 ppm with integration corresponding for 6 protons. Multiplicity, chemical shift and integration suggest this signal is coming from methyls from N,N-dimethylaniline substituent.

B2 singlet at 1.72 ppm with integration of 6 is consistent with expected characteristics of the signal coming from the two methyl groups found on the 9,9-dimethyl-9,10-dihydroacridine substituent.

B4 singlet at 3.90 ppm with integration of 6. Chemical shift is characteristic for methoxy groups attached to aromatic ring.

B7 singlet at 2.41 ppm corresponding to 3 protons, consistent with signals expected from a single methyl group connected to phenyl ring.

B9 two singlets at 2.72 ppm and 2.57 ppm each corresponding to 3 protons. These signals are coming from methyls connected to nitrogen atom on the sulphonamide group. Due to partial inhibition of rotation of S-N bond in sulphonamide group these appear as two separate signals instead of one.

Although not coming from a methyl, it is worth mentioning characteristic signal in **B8** compound. It is a broad singlet at 8.62 ppm corresponding to one proton. I assume it is a signal coming from 3-dibenzothiophenyl group. Neighbouring electronegative sulphur atom causes proton indicated with the arrow, to be more acidic, hence it appears as broad singlet instead of sharp one.

4.4.3 Verification of photocatalytic properties in HER

Compounds from **B** series were able to photosensitize titanium dioxide/platinum nanoparticles. From all tested compounds, **B5** – with the carbazole donor, was the most active (Figure 28). Interestingly, dimethoxycarbazole derivative **B4**, was second best compound from this series TON.

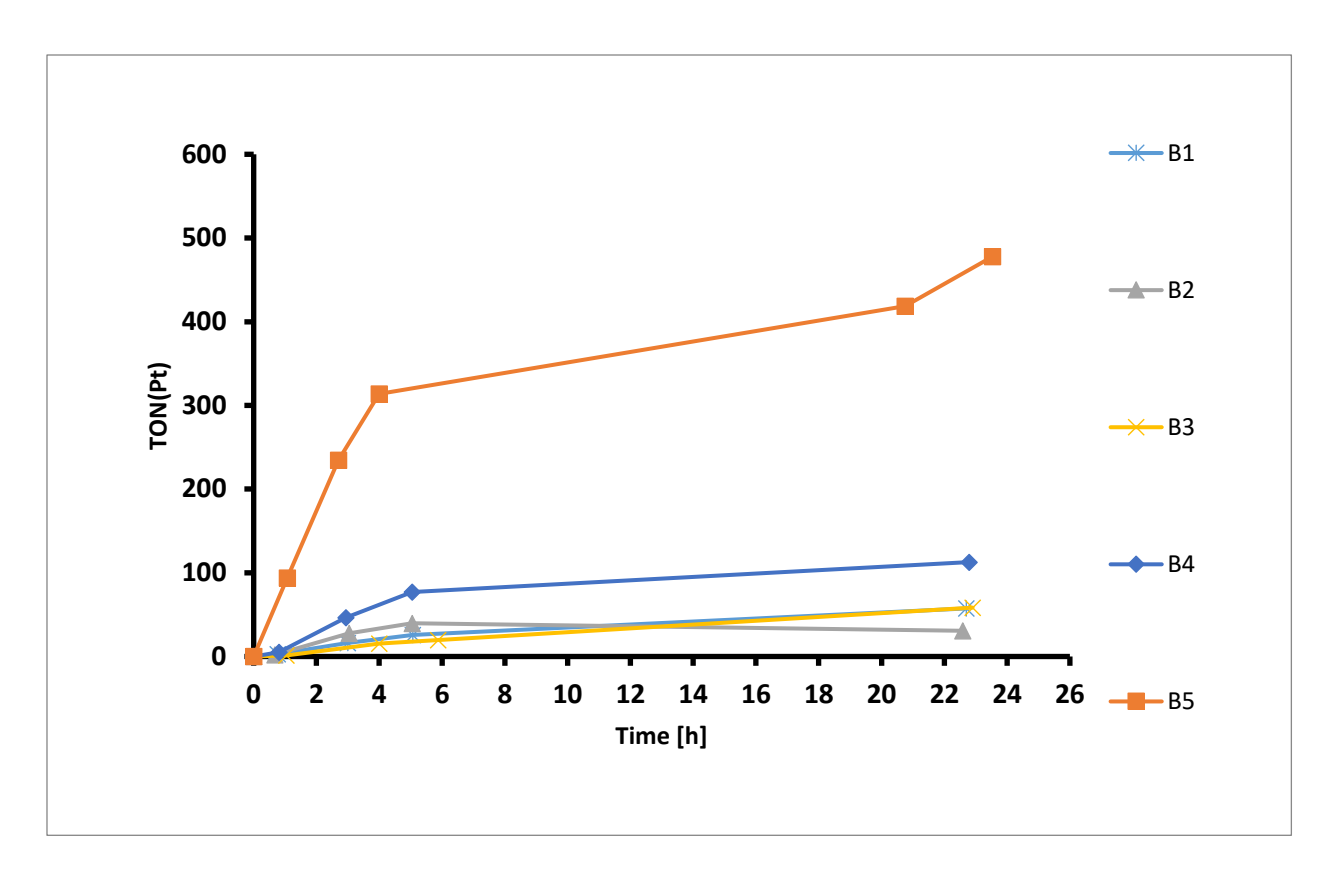


Figure 28 Sensibilization of TiO2/Pt nanoparticles in the presence of BuNphSO3Na $\,$ C= 0,0062 M and AA = 0,1 M $\,$

4.5 CHLORINATED AND BROMINATED PERYLENE DIIMIDES WITH DONOR-ACCEPTOR MOTIF WITH ANCHOR (B11-B15)

4.5.1 Screening of compounds - DFT calculations

Promising preliminary results of activity of **B5** made me wonder whether efficiency can be improved by using heavy atom effect.

Using DFT methods I optimized geometries of the seven PDI-anchor derivatives which structurally resemble **B0**, and later synthesized monochloro (**B11**), monobromo (**B12**), monoiodo (**B13**), dibromo (**B14**) and diiodo (**B15**) derivatives of **B5**. Subsequently I estimated their HOMO and LUMO energy levels (Figure 29).

In all compounds used for calculations, LUMO level lies the level close to water reduction level (-4.03 eV). It is not affected by halogenation of the "donor" fragment of the molecule, suggesting that the LUMO is located mostly on the PDI core. Closeness of the energy levels of the LUMOs and theoretical water reduction value suggests that these compounds might be good candidates for water splitting.

HOMO energy decreases by around 0,1-0,25 eV after introducing halogen atom to the carbazole donor. The type and number of halogen atoms introduced to the donor, does not corelate with any significant changes in the values of energy levels between halogenated derivatives. Hence I suspect that these derivatives might be a good tool to investigate whether heavy atom effect affects in photosensitizing for HER and OER in water splitting reaction.

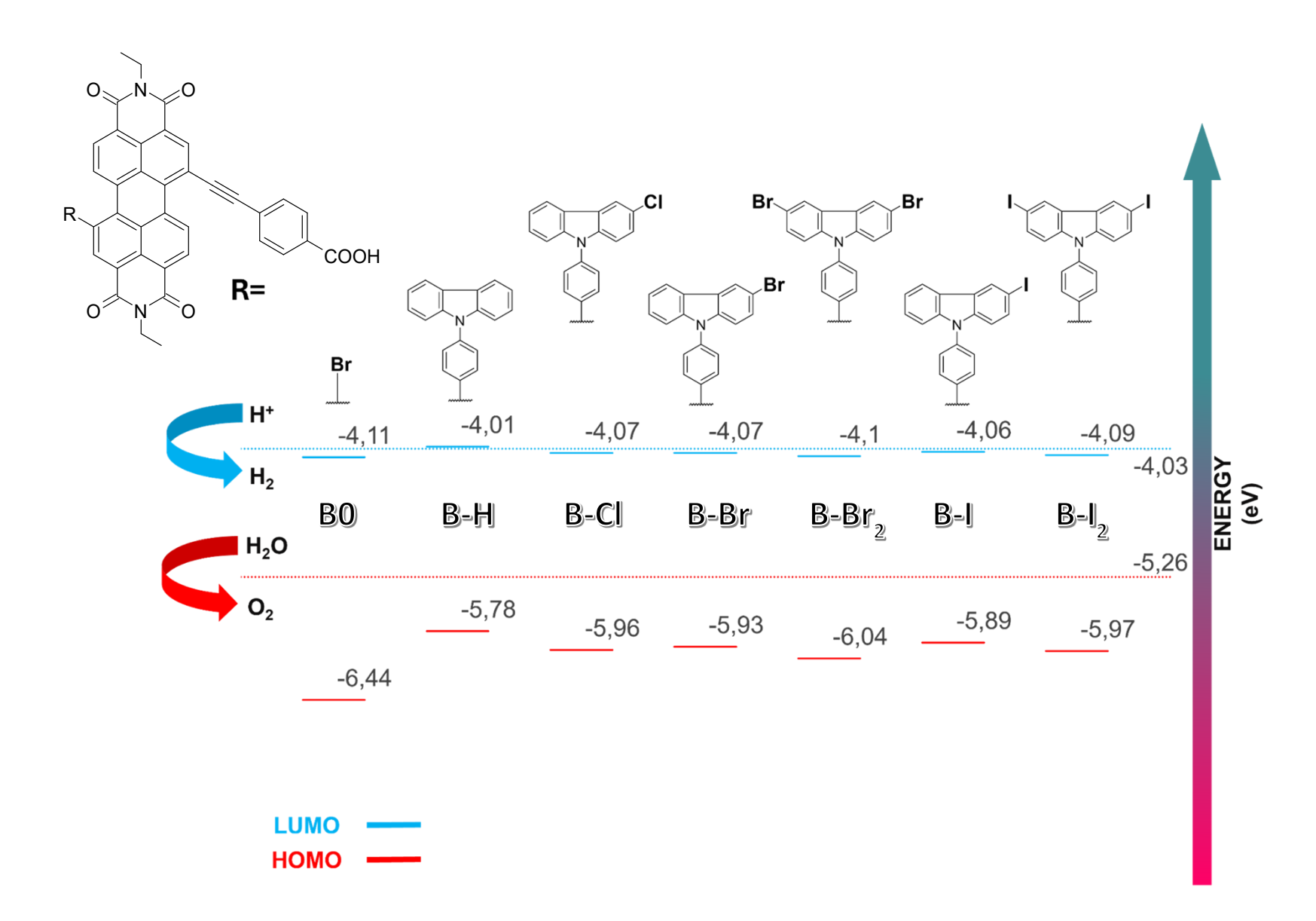


Figure 29 calculated HOMO and LUMO energy levels of halogenated derivative from B-series compared to water redox potentials.

4.5.2 Synthesis and HPLC analysis of selected PDIs with anchors

I approached synthesis of halogenated derivatives of **B5** in a similar fashion as in obtaining halogenated derivatives from **A** series. I used N-halosuccinimides as halogenating reagents (Scheme 47).

Scheme 47 Synthesis of B11-B15.

Figure 30 Structures of B11-B15.

Although TLC is an easy and convenient way of tracing progress of reactions, it may be useless in some circumstances. PDIs containing carboxylic anchor moiety are illustrative example of the problem. Carboxylic group has strong hydrogen bond donor-acceptor property. Due to this fact, these derivatives bond

tightly on silica gel. Consequently these compounds appear to have indistinguishable retardation factors (Rf) on regular TLC plates. For this reason I needed to use a different analytical technique for this group of compounds. I successfully optimized method for HPLC analysis of these perylene diimides.

The only available column at the time of my research was Luna 5 μ m C18, TMS-endcapped 100 Å 250 x 4.6 mm. C18 columns are usually used for polar compounds, like sugar, and amine acid derivatives. This is the column for reverse phase HPLC (RP-HPLC) and commonly used mobile phases are water, acetonitrile (ACN) and methanol (MeOH) based. In RP-HPLC elution strength is reversely proportional to polarity of the eluent used. As a result, more polar solvents, for instance water, promote retention on the stationary state, and less polar, namely MeOH or ACN, promote elution.

Adjusting analytical conditions with this set of equipment was challenging, but possible. I tested various mixtures of water, ACN and MeOH in isocratic conditions without a success. Even pure ACN was unable to properly elute analysed compounds. I attributed it to strong interactions of long C₁₈ chains from stationary phase with highly non-polar PDIs. Moreover, very low solubility of analysed compounds in eluent mixture might also be part of the issues. The case illustrates there are other, than eluent strength, factors affecting elution of highly non-polar compounds on columns for RT-HPLC.

After trials I found out that PDIs with carboxylic group were soluble in acetone and very slightly soluble in isopropanol (iPrOH). Since acetone was incompatible with linings of tubes of available HPLC apparatus, it could not be used as a part of mobile phase. Thus I decided to use iPrOH.

iPrOH has high viscosity and a problem with high back-pressure emerged. I solved this by raising temperature of the column oven to 50°C and maintaining eluent flow at relatively low, for this size column, rate of 2 ml/min. This effectively reduced pressures in the system.

Nevertheless due to low concentrations of the saturated solutions of PDIs in iPrOH, I was unable to acquire high quality chromatograms. Hence I decided to

use 2:1 mixture of acetonitrile and acetone to prepare 1 mg/ml solutions of my samples. Keeping in mind the volume of injection was small, 10-15 μ l, I assumed apparatus will remain unaffected by acetone.

Increasing concentration greatly improved signal detection, yet peaks were broad. To overcome this issue I decided to run analyses in gradient of solvents. As a result of trials and errors I found out optimal conditions (Figure 31).

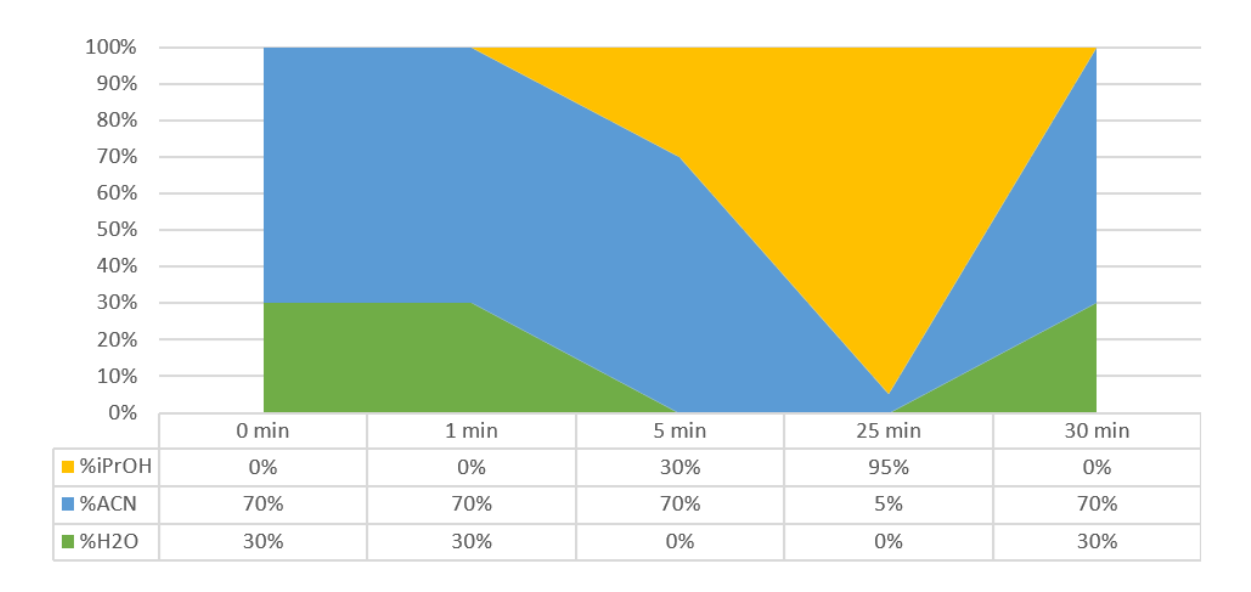


Figure 31 Optimal solvent gradient for analysis of PDIs

Initially I used a 7:3 mixture of ACN and water. This mixture allowed for adsorption of analytes at the beginning of the column and elution of traces of acetone.

After one minute I started to increase amount of iPrOH up to 30% while simultaneously decreasing amount of water in the mobile phase. This resulted in enough partition between the stationary and mobile phases to differentiate retention times (RT) (Figure 32).

When water content dropped to 0% I started further increase amount of iPrOH in the mixture until it reached 95%. I observed that increasing elution strength in two phases resulted in reduction of tailing of peaks compared to linear increase of the elution strength in one step.

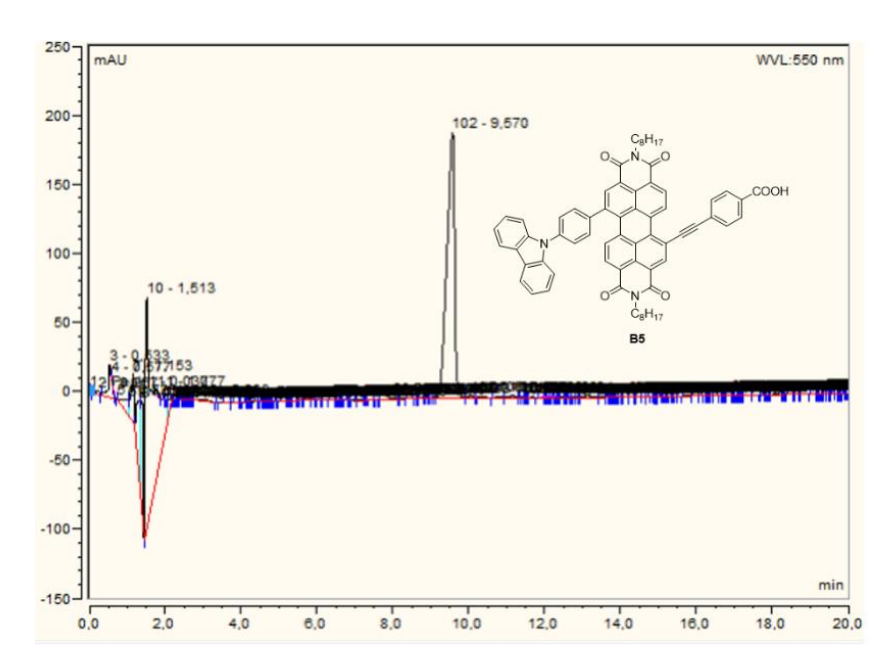


Figure 32 Analysis of B5. Detection wavelength: 550 nm.

of Optimization analysis conditions allowed for control of halogenation reactions of B5. Control halogenation progress was difficult particularly in case of iodination, as I could not rely on MALDI. Long and weak iodine-carbon bond was prone for dissociation during acquiring MALDI (Figure 33). Thus I was unable to discriminate between mono-iodinated (B13) and di-iodinated **B5** (**B15**), as due to iodine dissociation, similar spectra were tooand uninformative.

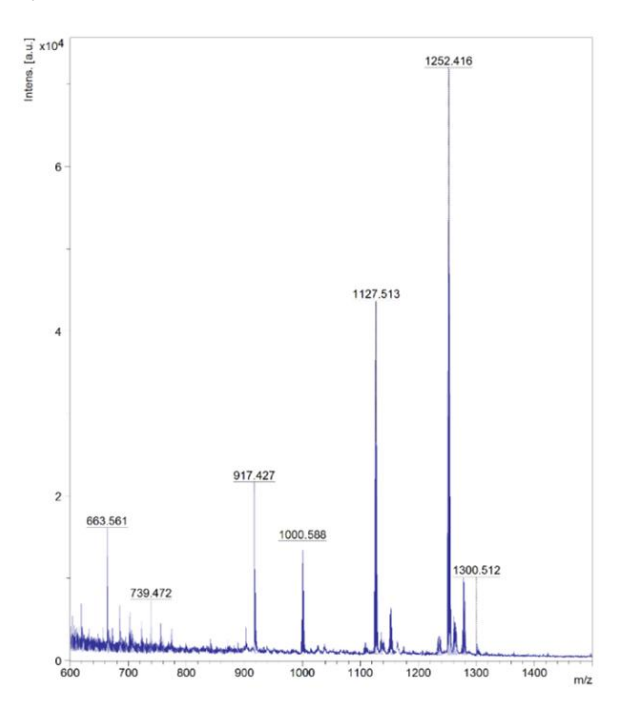
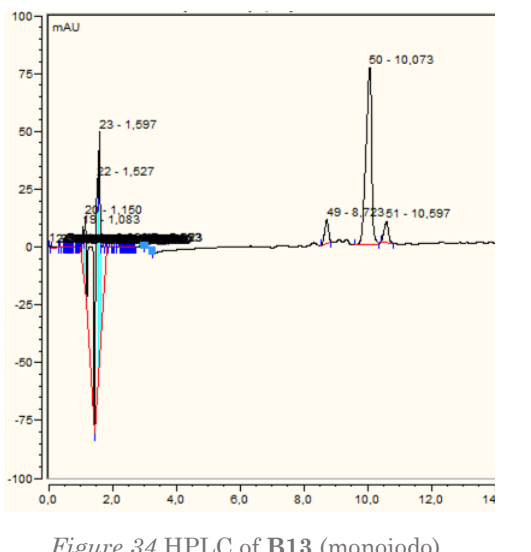


Figure 33 MALDI of $\bf B15$. Peaks from dissociation of iodine atoms (1127.513 and 1000.588) are visible.



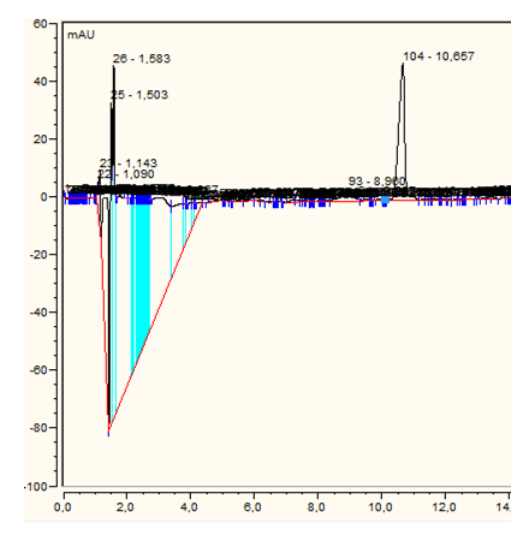


Figure 34 HPLC of B13 (monoiodo)

Figure 35 HPLC of B15 (diiiodo)

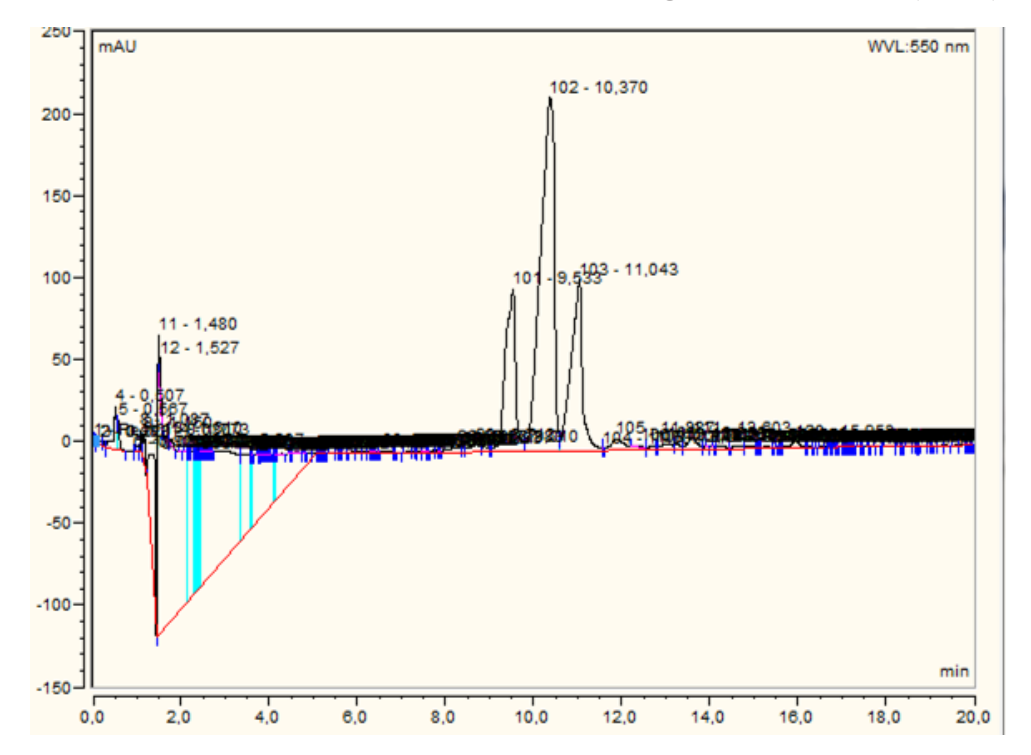


Figure 36 HPLC chromatogram of co-injection of B5, B13 and B15.

Injection of sole B13 or B15 was not helpful. Retention times were too similar (Figure 34 and Figure 35) and the only way of telling them apart was coinjection of these compounds. Results of co-injection of B5, B13 and B15 indicate positive correlation between number of inserted halogen atoms and retention times. Unsubstituted (B5) elutes first, monoiodo derivative (B13) elutes next, and diiodo (B15) derivative elutes least. This is consistent with the character of compounds. Insertion of halogen atoms increases lipophilicity, therefore increasing interactions with stationary phase. I need to emphasize that for the same compound there was a slight variability in RTs between each injection. Therefore

this method is useful only in comparative analysis. Co-injection of a reference, pure PDI standard (substrate or a product), is necessary for a proper assessment of the reaction progress. Identification of the **B11-B15** is backed up by the MALDI-TOF (Table 10) and ¹HNMR (Table 11**Błąd! Nie można odnaleźć źródła odwołania.**) data. For every compound I found signals corresponding to the expected masses.

Table 10 MALDITOF-MS analysis of B11-B15.

No.	Molecular formula	Monoisotopic mass	MALDITOF-MS peaks
B11	$\mathrm{C}_{67}\mathrm{H}_{56}\mathrm{ClN}_{3}\mathrm{O}_{6}$	1034.650	1035.4 (M+H)+
B12	$C_{67}H_{56}BrN_{3}O_{6}$	1077.335	1077.4, 1079.5 (M)+
B13	$C_{67}H_{56}IN_{3}O_{6} \\$	1125.321	1125.5 (M)+, 1126.5
B14	$C_{67}H_{55}Br_2N_3O_6\\$	1155.246	(M+H)+ 1154.3, 1156.3, 1158.3, 1160.3 (M+H)+
B 15	$C_{67}H_{55}I_{2}N_{3}O_{6}$	1251.218	1252.4 (M+H)+

¹H NMR spectra of the **B11-B15** are similar to the spectrum of the parent **B5**. Most characteristic signals are two singlets, which are coming from the unsymmetrically substituted PDI core. However, halogenation of the carbazole-9-yl substituents causes appearance of additional singlet in the spectra of **B11-B15**. Presence of this singlet is a confirmation of the identity of obtained compounds. Due to quite complicated splitting patterns, it is easier to find distinction between mono- and di-substituted derivatives by comparing total number of protons in aromatic area. In case of monohalogenated derivatives (**B11-B13**), total number of protons sums up to 21, in case of diiodo (**B15**) the sum is 20. It is consistent with the expected amount of protons, as parent compound, **B5**, has 22 aromatic protons.

Table 11 Chemical shifts (ppm) and coupling constants in the 1H NMR spectra of B11-B13 and B15.

No								A	Aromati	c prote	ons							
B11	10.03	8.82	8.80	8.72	8.29	8.28	8.23	8.21	8.16	7.90	7.86	7.80	7.57	7.55	7.50	7.49	7.45	7.31
	(d)	(d)	(s)	(s)	(d)	(d)	(s)	(d)	(d)	(d)	(d)	(d)	(d)	(d)	(t)	(d)	(d)	(t)
	7.81	10.25			8.30	7.32		7.81	7.81	7.80	7.81	8.30	8.78	8.79	6.83	8.30	8.78	6.83
	${ m Hz}$	Hz			Hz	Hz		Hz	Hz	Hz	${ m Hz}$	${ m Hz}$	${ m Hz}$	${ m Hz}$	Hz	$_{ m Hz}$	${ m Hz}$	${ m Hz}$
															8.30			8.30
															Hz			Hz
	1 H	1 H	1 H	1 H	1 H	1 H	1 H	1 H	2 H	1 H	2 H	2 H	1 H	1 H	1 H	1 H	1 H	1 H
B12	9.93	8.73	8.66	8.65	0.20	0 0 1	0.10	0.19	08.09	7 90	7 90	7 70	7 55	7 10	7.47	7.31		
D12					8.36	8.24	8.19	8.13		7.86	7.80	7.78	7.55	7.48				
	(d)	(d)	(s)	(s)	(s)	(d)	(d)	(d)	(d)	(d)	(d)	(d)	(d)	(t)	(d)	(t)		
	7.93	7.94				7.93	7.94	7.63	7.93	7.93	7.93	7.33	7.32	7.32	7.32	7.32		
	Hz	Hz				Hz	Hz	Hz	Hz	Hz	Hz	Hz	Hz	Hz	Hz	Hz		
	1 H	1 H	1 H	1 H	1 H	1 H	1 H	2 H	1 H	2 H	2 H	2 H	2 H	1 H	1 H	1 H		
B13	9.94	8.74	8.68	8.66	8.55	8.24	8.18	8.13	08.09	7.86	7.81	7.77	7.72	7.50	7.48	7.37	7.30	
210	(d)	(d)	(s)	(s)	(s)	(d)	(d)	(d)	(d)	(d)	(d)	(d)	(d)	(d)	(t)	(d)	(t)	
	8.24	8.24	(6)	(6)	(6)	7.94	7.01	7.94	8.24	7.94	7.01	7.93	9.16	7.32	7.94	8.54	7.94	
	Hz	Hz				Hz	Hz	Hz	Hz	Hz	$^{7.01}$	Hz	Hz	Hz	Hz	Hz	Hz	
	11Z 1 H	11Z 1 H	1 H	1 H	1 H	11Z 1 H	11Z 1 H	2 H	11Z 1 H	2 H	2 H	2 H	11Z 1 H	11Z 1 H	11Z 1 H	11Z 1 H	11Z 1 H	
	1 11	1 11	1 11	1 11	1 11	1 11	1 11	4 11	1 11	2 11	2 11	2 11	1 11	1 11	1 11	1 11	1 11	
B15	10.01	8.78	8.77	8.69	8.59	8.26	8.14	8.12	7.88	7.84	7.76	7.37						
	(d)	(d)	(s)	(s)	(s)	(d)	(d)	(d)	(d)	(d)	(d)	(d)						
	8.55	8.24	()	· /	()	7.63	8.24	7.94	7.93	8.24	7.94	8.54						
	$_{ m Hz}$	Hz				Hz	Hz	Hz	Hz	Hz	Hz	Hz						
	1 H	1 H	1 H	1 H	$2~\mathrm{H}$	1 H	2 H	1 H	2 H	2 H	4 H	2 H						
	1 11	1 11	1 11	1 11	_ 11	1 11	- 11	1 11	- 11	- 11	1 11	_ 11						

4.5.3 Verification of photocatalytic properties in HER

Selected halogenated compounds from **B** series were tested for the activity as photosensitizers for TiO₂ | Pt_{1%} system for HER in the presence of ascorbic acid as sacrificial reagent. Every tested compound exhibited activity in optimized conditions. **B5** (H), **B11** (Cl) and **B13** (I) had similar TON of around 2000. Compound **B12** (Br) showed TON of around 3500.(Figure 37)

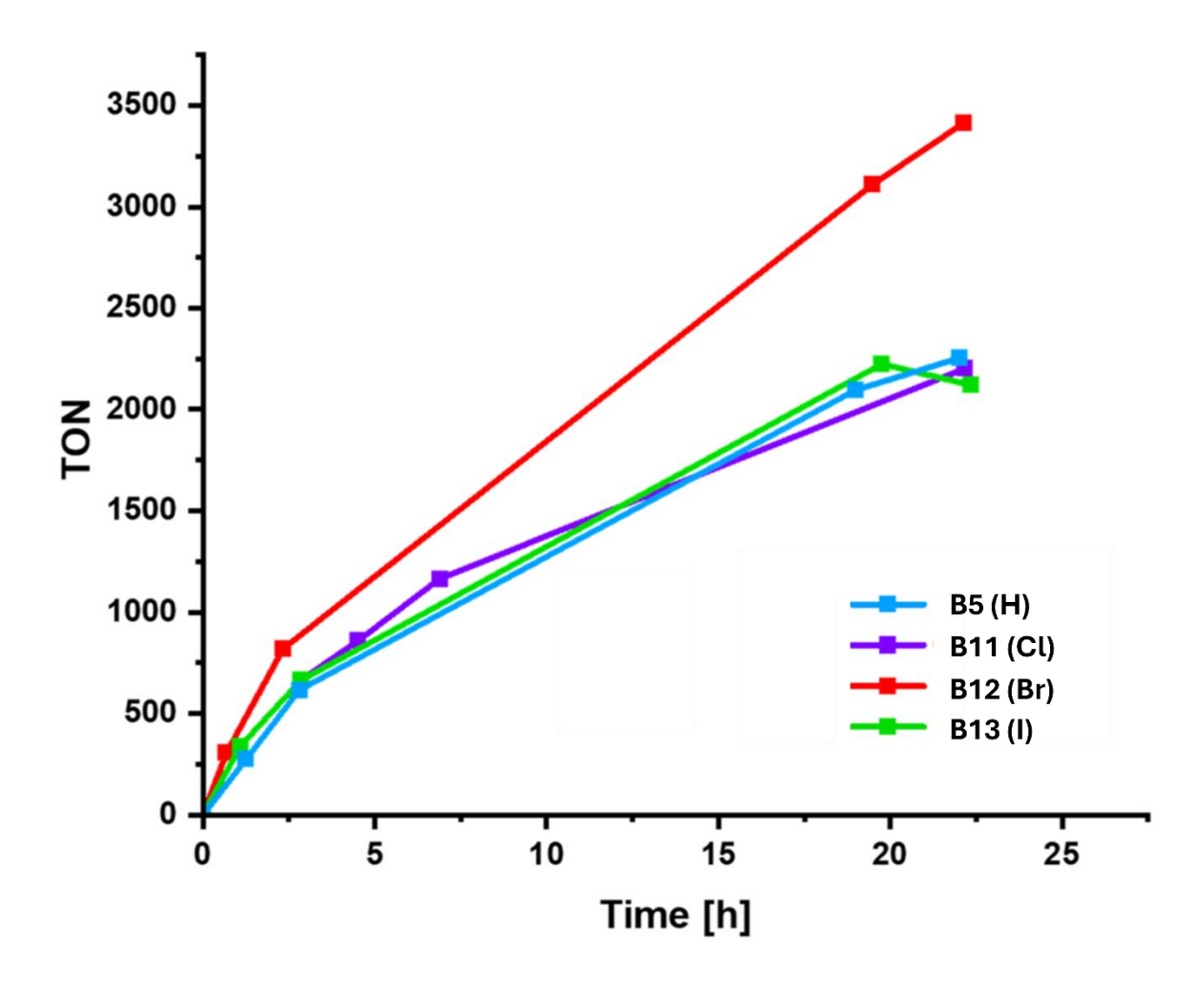


Figure 37 PhotoHER tests performed for 1 mg of Donor-PDI-Anchor | TiO_2 | $Pt_{1\%}$ in 3 mL of H_2O with ascorbic acid (AA) as Sacrificial Reagent, c(AA) = 0.1 M at 30° C with c(SDS) = 6.2 mM.

The same compounds were tested without AA and SDS and compared to PMI model compound from the publication about anchoring groups. **M5** (**PMI**) and **B11** (**Cl**) were almost inactive in these conditions. Iodo- derivative was the most active with TON around 1800, bromo- derivative was the second best performing compound with TON slightly below 1800. Non-halogenated derivative achieved around 200 TON after 24 hours. (Figure 38)

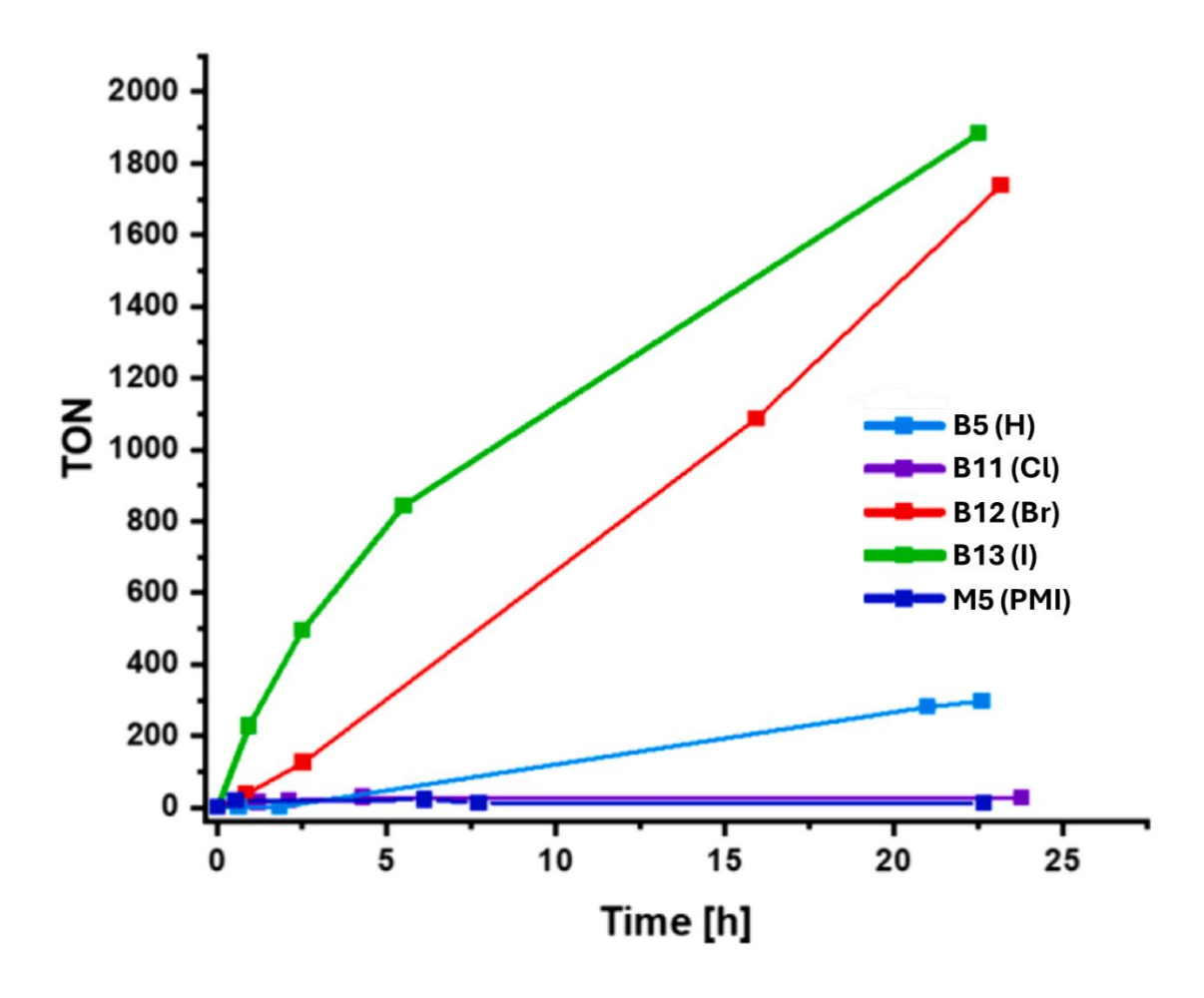
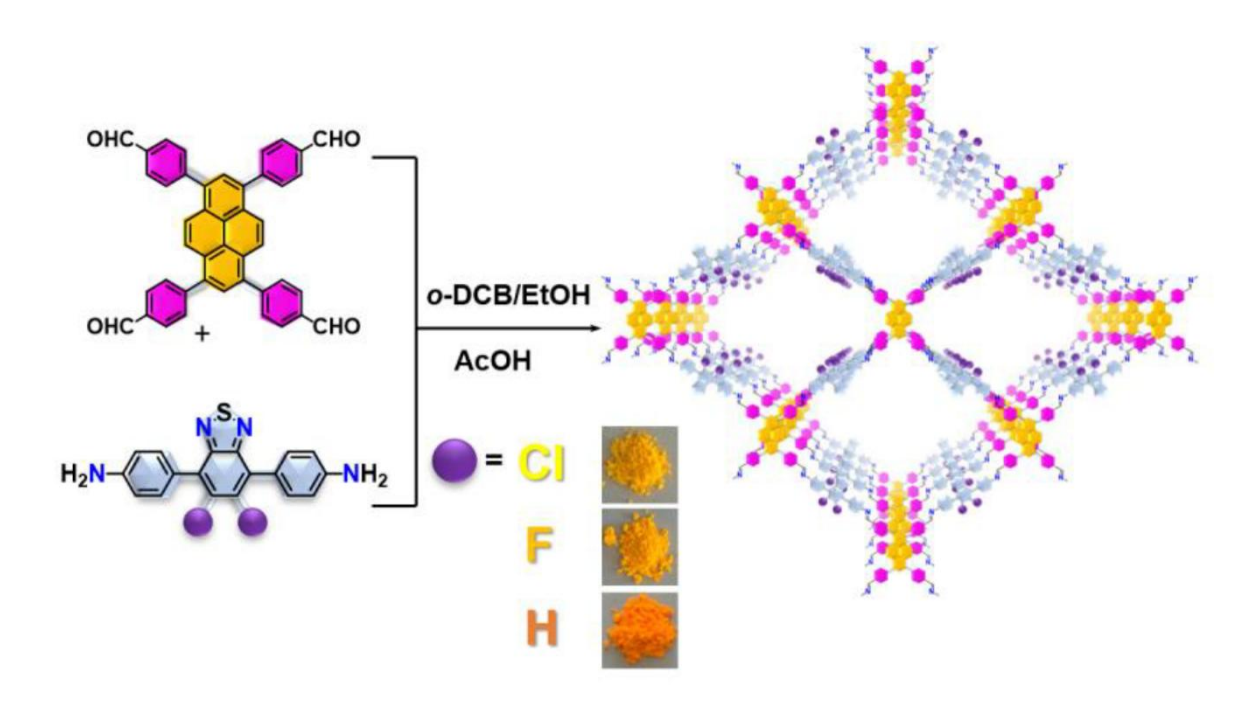


Figure 38 Test of activity in photoHER with Donor-PDI-Anchor $|\operatorname{TiO}_2|$ $|\operatorname{Pt}_{1\%}|$ in 3 mL of pure $|\operatorname{H}_2O|$ without Sacrificial Reagent (Ascorbic Acid)

4.6 Benzothiadiazoles co-catalysis with carbon-based quantum dots

Compounds from series **A** and **B** were proven to work in photo-HER. Unfortunately systems based on these compounds relied on the expensive platinum. Ideally the goal was to avoid platinum or other metals. It was shown that benzothiadiazole based covalent organic frameworks (COFs) can work as metal free photocatalysts for water splitting (Figure 39 and Figure 40).[88] The main drawback of the COFs is their low solubility. My research was focusing on synthesis of simplified photosensitizers based on mentioned benzothiadiazole COFs.



 ${\it Figure~39~Benzothiadiazole~based~COFs~for~metal-free~water~splitting.} \textbf{[88]}$

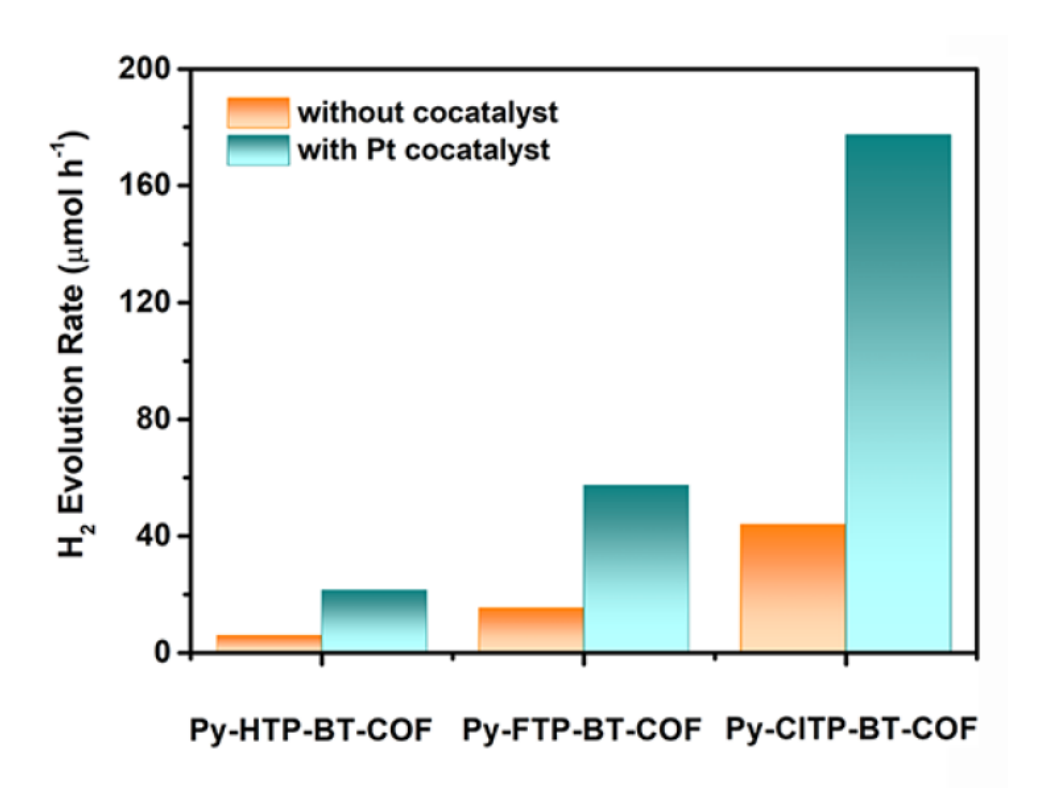


Figure 40 Activity of benzothiadiazole COFs in photo-HER.[88]

4.6.1 Screening of compounds - DFT calculations

Using DFT methods I optimized geometries of the six benzothiadiazole derivatives which were based on the COFs. Subsequently I estimated their HOMO and LUMO energy levels.

Compounds with donor and carboxylic anchoring group (C1 and C4) have lower HOMO and LUMO energy levels (Figure 41) compared to their corresponding derivatives with amino anchoring group (C2 and C5). Band gaps of the amino and carboxylic derivatives are comparable.

Compounds with two amino groups (C3 and C6) tend to have bigger band gaps than derivatives with one or none amine group.

Derivatives with two chlorine atoms in the benzothiadiazole core have lowered both HOMO and LUMO energies compared to their non-halogenated analogues.

Every of the calculated compounds has LUMO energies suitable for HER. Only carboxylic derivatives might have HOMO energies suitable for OER.

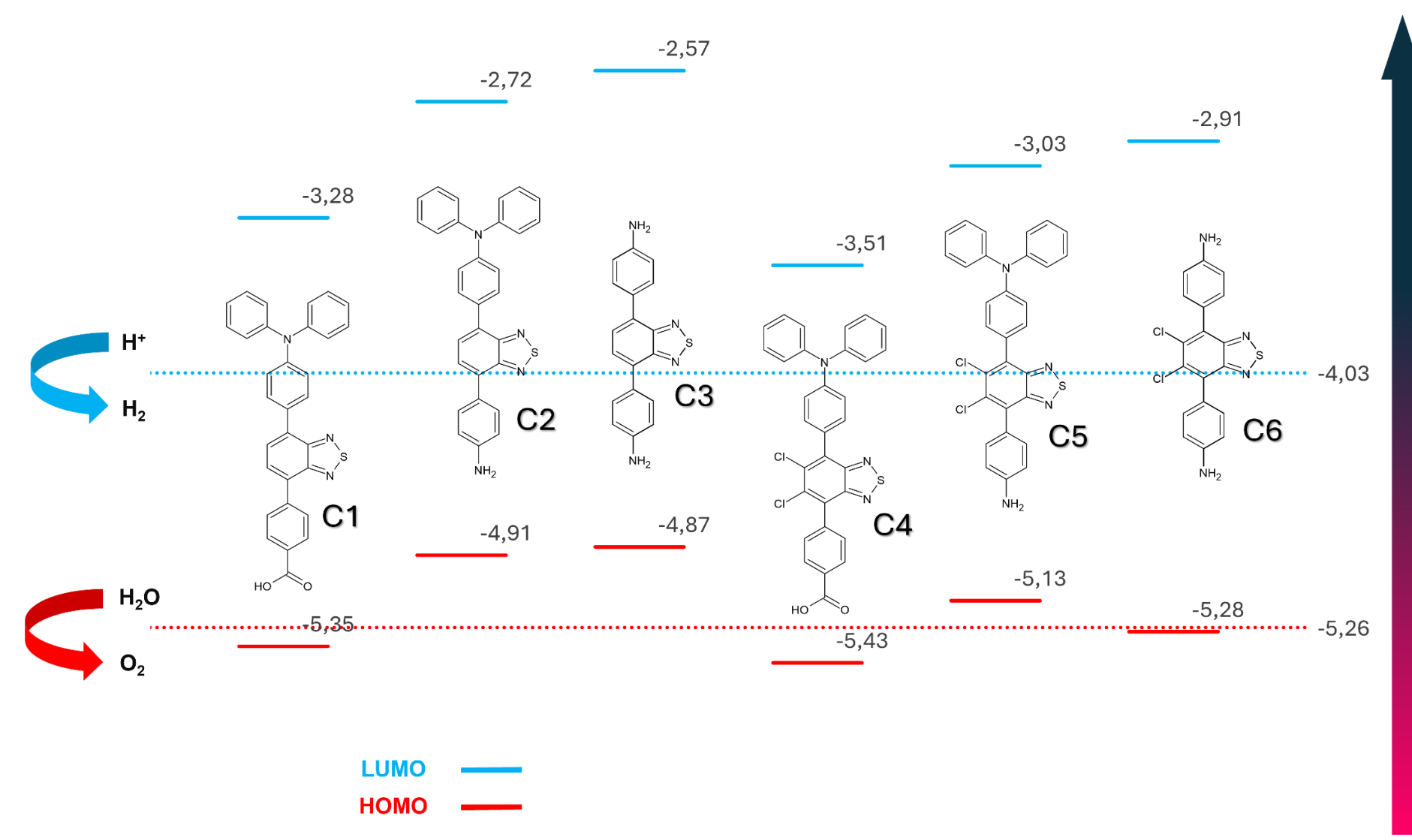


Figure 41 Calculated HOMO and LUMO energy levels of C1-C6 compared to water redox potentials.

4.6.2 Synthesis and analysis

Scheme 48 Synthesis of C1 and C4.

I synthesized benzothiadiazole (BTDZ) derivatives with carboxylic anchor in two steps starting with dibromo derivative (Scheme 48). I selectively substituted just one bromine in dibromo derivatives of BTDZ with triphenylamine group. I improved selectivity by slightly modifying my usual Suzuki coupling conditions (Pd(PPh₃)₄/K₂CO₃/dioxane/H₂O). I used 1.1:1 ratio of boronic acid to di-bromo BTDZ to minimize over-substitution. Additionally I used 18-crown-6 as a catalyst which allowed reaction to progress at 30°C. 18-crown-6 selectively binds and sequester potassium cation, leaving out "naked" counter anions. Such isolated anions are more nucleophilic and reactive which in some cases allows for using milder conditions.[89] In subsequent step I run reaction without crown ether, as there was only one bromine left for substitution. Substitution of the only bromine atom in C01 and C04 led to C1 and C4 respectively.

When I was synthesizing derivatives with amino anchoring group (C2, C3, C5. C6) using same conditions as for C1/C4, I noticed formation of unusually high amount of side products. This manifested as multiple bands on TLC plates. These bands had very similar properties and Rf values. These bands were indistinguishable from the desired compound. This complicated isolation of the desired product, and made it highly uneconomical.

My attempt of optimization of the conditions by exchanging dioxane to another solvent (THF, NMP, toluene, DMF, DCM) resulted in similar mixture of side products. This led me to the conclusion that catalyst Pd(PPh₃)₄, even tough versatile, might be unsuitable for coupling with boronic derivative containing amino group. Multiple attempts leading to mixture of various side products suggests this catalyst has low selectivity for this particular coupling.

There is no reliable rule for prediction of selectivity of Suzuki reaction. Site-selectivity is influenced by steric factors of ligands, electronic effects in aryl halides, and substituents in both coupling partners.[90] Moreover there is possibility of Buchwald-Hartwig-like amination reaction. Although it is rare, this type of reactions were reported to occur even in the aqueous solutions.[91], [92] Possibility of multiple reaction pathways in connection with multiple reaction sites is satisfactory explanation of the formation of side products.

Scheme 49 Synthesis of C2, C3, C5 and C6.

While looking for the solution I found a paper about complexes of tris-(o-tolyl)phosphine and palladium. The authors claim that these complexes undergo unusually rapid oxidative addition to the aryl halides. Moreover tris-(o-tolyl)phosphine ligand favours dimerization of the resulting complexes. This is contrasting to the nature of complexes with PPh₃, as these are predominantly monomeric.[93]

I substituted P(o-tol)₃ for PPh₃ which resolved problem with side-reactions (Scheme 49). I suspect dimeric nature of the formed complexes might had key role in reducing amount of on-site-specific coupling reactions during incorporating amino anchoring group.

For every compound MALDI spectra (Table 12) showed peaks corresponding to ions with expected mass.

Table 12 MALDITOF-MS results for synthesized benzothiadiazoles. * - compounds with numbering starting with 0, for example C01, are substrates used for the synthesis of the target compounds.

No.	Molecular formula	Monoisotopic mass	MALDITOF-MS peaks
C01*	$\mathrm{C}_{24}\mathrm{H}_{16}\mathrm{BrN}_{3}\mathrm{S}$	458.382	459.025, 460.037 (M)+
C02*	$C_6H_4Br_2Cl_2N_2$	331.812	331.782, 332.775, 333.782, 334.775. 335.781 (M)+
C03*	$\mathrm{C_6N_2Br_2Cl_2S}$	359.753	360.791, 361.767, 362.787, 364.786 (M)+
C04*	$C_{24}H_{14}BrCl_2N_3S$	524.947	524.949, 527.005, 528.030, 530.028 (M)+
C1	$C_{31}H_{21}N_3O_2S\\$	499.135	500.200 (M+H)+
C2	$C_{30}H_{22}N_{4}S \\$	470.135	471.144 (M+H)+
C3	$C_{18}H_{14}N_{4}S \\$	318.403	318.102 (M)+
C4	$C_{31}H_{19}Cl_2N_3O_2S$	567.058	567.069 (M)+ 568.083 (M+H)+
C 5	$C_{30}H_{20}Cl_2N_4S$	538.078	538.100, 540.108 (M)+
C6	$C_{18}H_{12}Cl_2N_4S$	386.016	386.074 (M)+ 387.080 (M+H)+

Table 13 Chemical shifts (ppm) and coupling constants in the 1H NMR spectra of C01, C1-C4 and C6.

No.						Signals					
C01	7.89 (d)	7.80 (d)	7.54 (d)	7.29 (t)	7.18 (d)	7.07 (t)					_
	J = 7.32 Hz	J = 7.32 Hz	J = 7.63	J = 7.32 Hz	J = 7.32	J = 7.32					
	1 H	2 H	$_{ m Hz}$	4 H	${ m Hz}$	$_{ m Hz}$					
			1 H		6 H	2 H					
C1	8.29 (d)	8.11 (d)	7.90 (d)	7.85 (d)	7.79 (d)	7.31(t)	7.30 (d)	7.21(t)	7.20 (d)	7.08(t)	
	J = 7.94 Hz	J = 7.94 Hz	J = 8.24	J = 7.32 Hz	J = 7.32	J = 7.63	J = 7.93	$J = 9.31 \; Hz$	J = 8.24 Hz	J = 7.32 Hz	
	2 H	2 H	${ m Hz}$	1 H	${ m Hz}$	$_{ m Hz}$	Hz	$2~\mathrm{H}$	4 H	2 H	
			$2~\mathrm{H}$		1 H	$2~\mathrm{H}$	$2~\mathrm{H}$				
C2	7.87 (d)	7.83 (d)	7.72 (d)	7.69 (d)	7.29(t)	7.28 (d)	7.20(t)	7.19 (d)	7.06 (t)	6.85 (d)	3.90 (bs)
	J = 8.24 Hz	J = 8.24 Hz	J = 7.32	J = 7.32 Hz	J = 7.63	J = 7.63	J = 9.15	J = 8.24 Hz	J = 7.02 Hz	J = 8.24 Hz	
	$2~\mathrm{H}$	2 H	Hz	1 H	Hz	$_{ m Hz}$	Hz	4 H	$2~\mathrm{H}$	$2~\mathrm{H}$	$2~\mathrm{H}$
			1 H		$2~\mathrm{H}$	$2~\mathrm{H}$	2 H				
C3	7.81 (d)	7.66 (s)	6.83 (d)	3.82 (bs)							
	J = 7.94 Hz		J = 7.63								
	4 H	$2~\mathrm{H}$	Hz	4 H							
			4 H								
C4	8.31 (d)	7.69 (d)	7.46 (d)	7.33 (t)	7.32(t)	7.24 (dd)	7.20 (d)	7.10 (tt)			
	J = 8.54 Hz	J = 8.54 Hz	J = 8.85	J = 7.32 Hz	J = 7.33	J = 8.55	J = 8.85	J = 7.33 Hz			
			Hz		${ m Hz}$	$_{ m Hz}$	Hz	J = 1.22 Hz			
	2 H	$2~\mathrm{H}$		2 H		J = 1.22		$2~\mathrm{H}$			
			$2~\mathrm{H}$		$2~\mathrm{H}$	$_{ m Hz}$	2 H				
						4 H					
$\mathbf{C6}$	7.40 (d)	6.85 (d)	3.88 (bs)								
	J = 8.55 Hz	J = 8.54 Hz	, ,								
	4 H	4 H									

The ¹H NMR spectra (Table 13) of **C01** and **C1-C3** are characterized by signals coming from protons from benzothiadiaziole core. In asymmetric substituted BTDZs (**C01**, **C1** and **C2**) these signals appear as two doublets corresponding to one proton each. In case of highly symmetric **C3**, this signal is reduced to one singlet corresponding to two protons. BTDZs with halogenated core lack of these signals as they lack protons.

C01, C1, C2, C4 are characterised by signals coming from the donor part of the molecule. In C4 spectrum triplet of triplets with fairly low secondary coupling constant (J = 1.22 Hz) can be found. This low value is characteristic of coupling with protons in the meta position via 4 bonds. It would suggest that this signal comes from the proton located in monosubstituted phenyl ring, in the para position related to the substituent. The same long-distance coupling pattern can be found in signal coming from 4 protons from donor rings. The splitting pattern, doublet of doublets, suggests that these are protons in the ortho position relative to the substituent. Visibility of these couplings via 4 bonds is highly dependent on the quality of the spectra and these couplings are not visible in some cases.

BTDZs with amino anchoring group show characteristic broad singlet around 3.90 ppm coming from the protons from the -NH₂ group. Analogical signal from the carboxylic anchoring group is not visible due to the quick exchange of proton to deuterium on the carboxylic group.

C3 and C6 are highly symmetrical compounds. C6 has the least complex spectrum of all compounds, besides broad singlet from amino group, it has two doublets in the aromatic area, coming from the para substituted benzene ring. C3 has similar spectrum but with additional singlet coming from protons on the benzothiadiazole.

Verification of photocatalytic properties in HER

4.6.2.1 C1 and C4 – photosensitization of TiO₂|Pt nanoparticles

Compounds C1 and C4 were tested as photosensitizers for TiO2|Pt nanoparticles with two different anionic surfactants – sodium dodecylsulfonate (SDS) and sodium butylnapthalene sulfonate (Figure 42). Both compounds were active and showed higher activity in the presence of sodium butylnaphthalene sulfonate. C1 was more active than C4 in both surfactants.

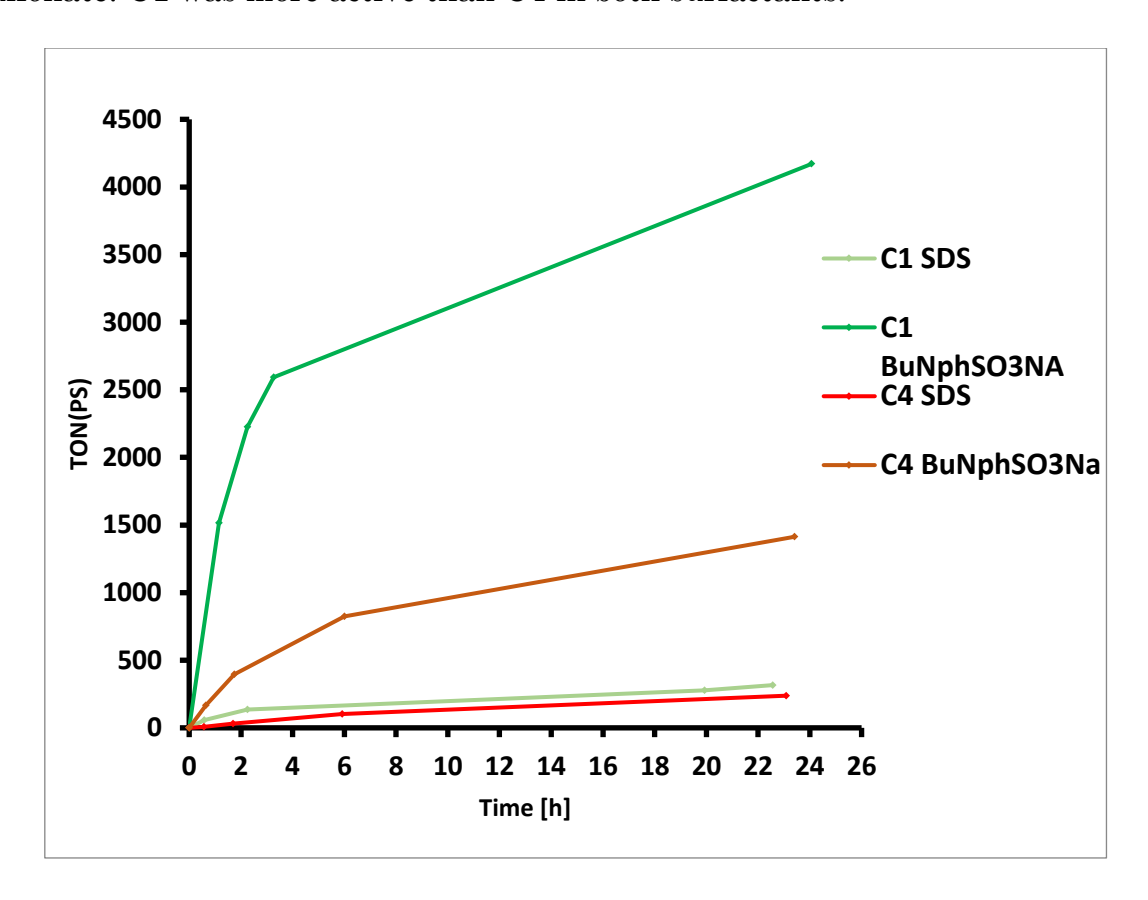


Figure 42 PhotoHER tests of C1 and C4 for 1 mg of BDTZ | TiO_2 | $Pt_{1\%}$ in 3 mL of H_2O with ascorbic acid (AA) as Sacrificial Reagent, c(AA) = 0.1 M at 30° C with c(Surfactant) = 6.2 mM.

4.6.2.2 C2 and C5 – photosensitization of GQD

Compounds **C2** and **C5** were tested as photosensitizers for Graphene Quantum Dots (GQD) (Figure 43). TON can not be calculated due to unknown molar mass of the GQD. Number of moles of hydrogen produced per one gram of GQD was calculated instead, **C2** showed activity of around 250 µmol/g after 24 hours, **C5** showed activity of 500 µmol/g after 27 hours.

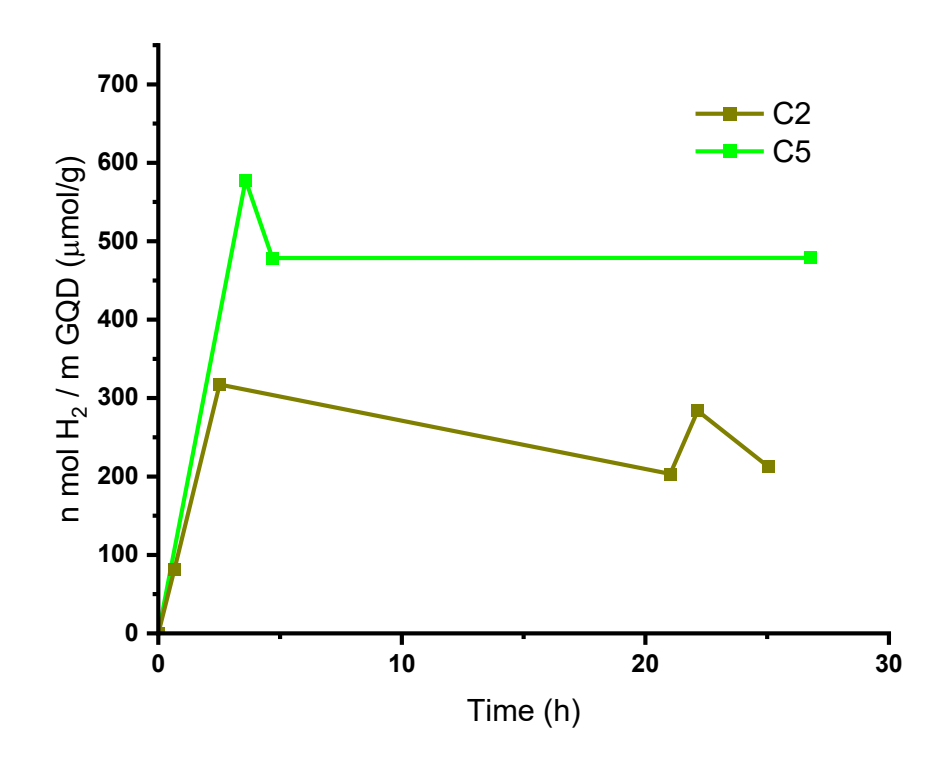


Figure 43 Photosensitization of GQD with C2 and C5 0.1 M TEA

4.6.2.3 C3 and C6 - photosensitization of GQD

C3 and C6 were tested as photosensitizers for GQD (Figure 44). In the presence of TEA and AA both were active. C6 reached maximum of around 1000 μ mol/g after 3 hours and later on it dropped to 500 μ mol/g. C3 reached activity of over 12000 μ mol/g after 30 hours and started losing its activity after about 50 hours (Figure 45).

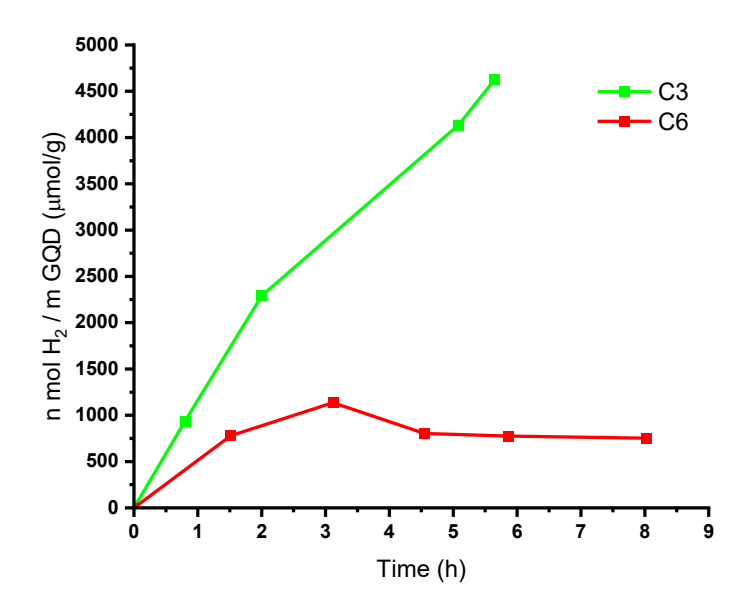
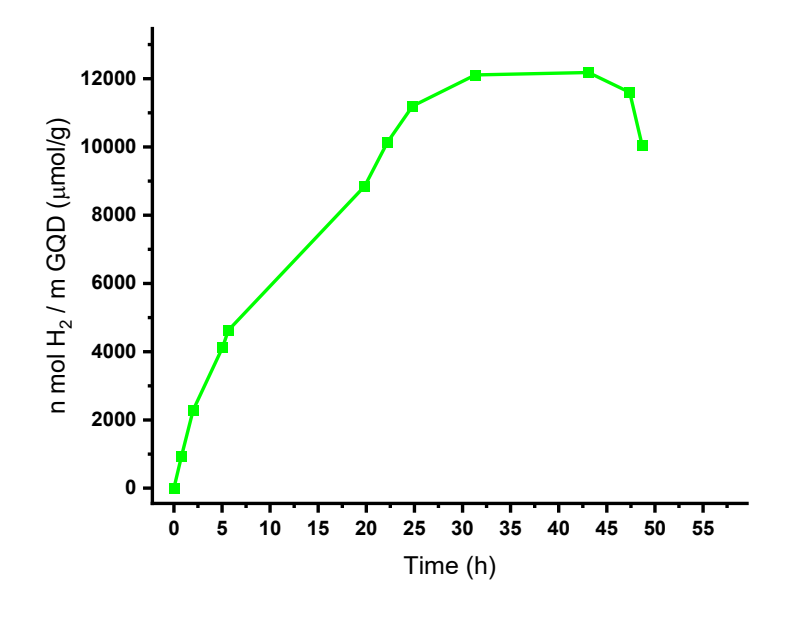


Figure 44 Photosensitization of GQD with C3 and C6 0.1 M TEA + 0.2 M AA



 $Figure~45~P{\rm hotosensitization}$ of GQD with C3 0.1 M TEA + 0.2 M AA

5. SUMMARY AND CONCLUSIONS

- 1. I used DFT calculations to predict crucial properties of the compounds planned to be synthesized.
- 2. I successfully designed and synthesized multiple series of novel organic compounds based on perylenediimide (PDI) and benzothiadiazole (BTDZ) cores, intended for use as photocatalysts in hydrogen production. I confirmed their structures by analysing their MALDI and ¹HNMR spectra.
- 3. I developed a simplified and efficient vial-based method for performing Suzuki coupling reactions, suitable for small-scale synthesis.
- 4. I isolated and identified the elusive, active species formed during photoirradiation of PDI with carbazole donor (A4). I proved that was a platinum complex with ring-open form of A4. This was crucial for explaining the formation of catalytically active core-shell nanoparticles.
- 5. I Developed a selective, high-yield synthetic method to attach a single carboxylic acid anchoring group to the PDI core (compounds **B1-B10**). This modification enabled the compounds to effectively attach to and photosensitize a TiO₂/Platinum co-catalyst system, significantly improving performance.
- 6. I optimized synthesis of series of halogenated (chloro, bromo, iodo) PDI-anchor derivatives (**B11-B15**) with carbazole donor to investigate the heavy-atom effect.
- 7. Created and optimized a novel gradient HPLC method for the analysis and purification of PDI derivatives containing carboxylic acid groups, overcoming the limitations of traditional techniques like TLC.
- 8. Brominated (**B12**) and iodinated (**B13**) derivatives showed significantly enhanced photocatalytic activity for HER compared to the non-halogenated parent compound. This proved beneficial effect of incorporating heavy atom.

- 9. Obtained halogenated compounds from **B** series worked without sacrificial electron donors proving beneficial impact of the heavy-atom effect for charge separation.
- 10.I Successfully optimized challenging Suzuki coupling conditions for the synthesis of benzothiadiazole derivatives, particularly for substrates containing amino groups. I achieved that by employing specific ligand (tris-(o-tolyl)phosphine) and 18-crown-6 ether. This approach improve selectivity and yield.
- 11. Synthesized BZTDs were successfully working in photosensitizing graphene quantum dots, making these systems totally metal-free. Therefore I obtained compounds capable of fully organic photocatalytic activity in HER reaction.

6. References

- [1] A. Galushchinskiy, R. González-Gómez, K. McCarthy, P. Farràs, and A. Savateev, "Progress in Development of Photocatalytic Processes for Synthesis of Fuels and Organic Compounds under Outdoor Solar Light," *Energy & Fuels*, vol. 36, no. 9, pp. 4625–4639, May 2022, doi: 10.1021/acs.energyfuels.2c00178.
- [2] D. Cambié et al., "Energy-Efficient Solar Photochemistry with Luminescent Solar Concentrator Based Photomicroreactors," Angewandte Chemie International Edition, vol. 58, no. 40, pp. 14374–14378, Oct. 2019, doi: 10.1002/anie.201908553.
- [3] M. Akita and T. Koike, "Sunlight-driven trifluoromethylation of olefinic substrates by photoredox catalysis: A green organic process," *Comptes Rendus Chimie*, vol. 18, no. 7, pp. 742–751, Jul. 2015, doi: 10.1016/j.crci.2015.01.013.
- [4] D. Ravelli, S. Protti, P. Neri, M. Fagnoni, and A. Albini, "Photochemical technologies assessed: the case of rose oxide," *Green Chemistry*, vol. 13, no. 7, p. 1876, 2011, doi: 10.1039/c0gc00507j.
- [5] J. Schneider and D. W. Bahnemann, "Undesired Role of Sacrificial Reagents in Photocatalysis," *J Phys Chem Lett*, vol. 4, no. 20, pp. 3479–3483, Oct. 2013, doi: 10.1021/jz4018199.
- [6] Y. Bai, K. Hippalgaonkar, and R. S. Sprick, "Organic materials as photocatalysts for water splitting," J Mater Chem A Mater, vol. 9, no. 30, pp. 16222–16232, 2021, doi: 10.1039/d1ta03710b.
- [7] H. Nagakawa and M. Nagata, "Photoreforming of Organic Waste into Hydrogen Using a Thermally Radiative CdO x /CdS/SiC Photocatalyst," *ACS Appl Mater Interfaces*, vol. 13, no. 40, pp. 47511–47519, Oct. 2021, doi: 10.1021/acsami.1c11888.
- [8] C. C. C. Johansson Seechurn, M. O. Kitching, T. J. Colacot, and V. Snieckus, "Palladium-catalyzed cross-coupling: A historical contextual perspective to

- the 2010 nobel prize," *Angewandte Chemie International Edition*, vol. 51, no. 21, pp. 5062–5085, 2012, doi: 10.1002/anie.201107017.
- [9] M. Farhang, A. R. Akbarzadeh, M. Rabbani, and A. M. Ghadiri, "A retrospective-prospective review of Suzuki–Miyaura reaction: From cross-coupling reaction to pharmaceutical industry applications," *Polyhedron*, vol. 227, p. 116124, Nov. 2022, doi: 10.1016/j.poly.2022.116124.
- [10] D. Cartagenove, S. Bachmann, J. A. Van Bokhoven, K. Püntener, and M. Ranocchiari, "Heterogeneous Metal-Organic Framework Catalysts for Suzuki-Miyaura Cross Coupling in the Pharma Industry," *Chimia (Aarau)*, vol. 75, no. 11, p. 972, Nov. 2021, doi: 10.2533/chimia.2021.972.
- [11] M. J. Buskes and M.-J. Blanco, "Impact of Cross-Coupling Reactions in Drug Discovery and Development," *Molecules*, vol. 25, no. 15, p. 3493, Jul. 2020, doi: 10.3390/molecules25153493.
- [12] A. F. P. Biajoli, C. S. Schwalm, J. Limberger, T. S. Claudino, and A. L. Monteiro, "Recent Progress in the Use of Pd-Catalyzed C-C Cross-Coupling Reactions in the Synthesis of Pharmaceutical Compounds," *J Braz Chem Soc*, vol. 25, no. 12, pp. 2186–2214, Dec. 2014, doi: 10.5935/0103-5053.20140255.
- [13] Y. Zhu, W. Dong, and W. Tang, "Palladium-catalyzed cross-couplings in the synthesis of agrochemicals," *Advanced Agrochem*, vol. 1, no. 2, pp. 125–138, Dec. 2022, doi: 10.1016/j.aac.2022.11.004.
- [14] Z. Feng *et al.*, "Regioselective and Stepwise Syntheses of Functionalized BODIPY Dyes through Palladium-Catalyzed Cross-Coupling Reactions and Direct C–H Arylations," *J Org Chem*, vol. 81, no. 15, pp. 6281–6291, Aug. 2016, doi: 10.1021/acs.joc.6b00858.
- [15] G. Reginato, M. Calamante, A. Dessì, A. Mordini, M. Peruzzini, and L. Zani, "Cross-coupling reactions: Some applications to the synthesis of thiazolothiazole- and benzobisthiazole-based dyes for new generation solar cells (DSSC)," *J Organomet Chem*, vol. 771, pp. 117–123, Nov. 2014, doi: 10.1016/j.jorganchem.2014.01.024.

- [16] P. Ruiz-Castillo and S. L. Buchwald, "Applications of Palladium-Catalyzed C-N Cross-Coupling Reactions," *Chem Rev*, vol. 116, no. 19, pp. 12564–12649, Oct. 2016, doi: 10.1021/acs.chemrev.6b00512.
- [17] C. C. C. Johansson Seechurn, M. O. Kitching, T. J. Colacot, and V. Snieckus, "Palladium-catalyzed cross-coupling: A historical contextual perspective to the 2010 nobel prize," *Angewandte Chemie International Edition*, vol. 51, no. 21, pp. 5062–5085, 2012, doi: 10.1002/anie.201107017.
- [18] M. C. D'Alterio, É. Casals-Cruañas, N. V. Tzouras, G. Talarico, S. P. Nolan, and A. Poater, "Mechanistic Aspects of the Palladium-Catalyzed Suzuki-Miyaura Cross-Coupling Reaction," *Chemistry A European Journal*, vol. 27, no. 54, pp. 13481–13493, Sep. 2021, doi: 10.1002/chem.202101880.
- [19] K. Tamao, K. Sumitani, and M. Kumada, "Selective Carbon-Carbon Bond Formation by Cross-Coupling of Grignard Reagents with Organic Halides. Catalysis by Nickel-Phosphine Complexes," *J Am Chem Soc*, vol. 94, no. 12, pp. 4374–4376, 1972, doi: 10.1021/ja00767a075.
- [20] R. J. P. Corriu and J. P. Masse, "Activation of Grignard reagents by transition-metal complexes. A new and simple synthesis of trans-stilbenes and polyphenyls," *J Chem Soc Chem Commun*, vol. 0, no. 3, p. 144a, 1972, doi: 10.1039/c3972000144a.
- [21] C. E. I. Knappke and A. Jacobi von Wangelin, "35 years of palladium-catalyzed cross-coupling with Grignard reagents: how far have we come?," *Chem Soc Rev*, vol. 40, no. 10, p. 4948, Sep. 2011, doi: 10.1039/c1cs15137a.
- [22] A. Dieck and R. F. Heck, "Organophosphinepalladium Complexes as Catalysts for Vinylic Hydrogen Substitution Reactions," *J Am Chem Soc*, vol. 96, no. 4, pp. 1133–1136, 1974, doi: 10.1021/ja00811a029.
- [23] M. Bagherzadeh, M. Amini, A. Ellern, and L. Keith Woo, "Palladium and copper complexes with oxygen-nitrogen mixed donors as efficient catalysts for the Heck reaction," *Inorganica Chim Acta*, vol. 383, pp. 46–51, Mar. 2012, doi: 10.1016/j.ica.2011.10.040.

- [24] T. Ghosh, "Reductive Heck Reaction: An Emerging Alternative in Natural Product Synthesis," *ChemistrySelect*, vol. 4, no. 16, pp. 4747–4755, Apr. 2019, doi: 10.1002/slct.201804029.
- [25] S. Jagtap, "Heck Reaction—State of the Art," Catalysts, vol. 7, no. 9, p. 267, Sep. 2017, doi: 10.3390/catal7090267.
- [26] J. Le Bras and J. Muzart, "Intermolecular Dehydrogenative Heck Reactions," *Chem Rev*, vol. 111, no. 3, pp. 1170–1214, Mar. 2011, doi: 10.1021/cr100209d.
- [27] J. Xie, R. Liang, and Y. Jia, "Recent Advances of Catalytic Enantioselective Heck Reactions and <scp>Reductive-Heck</scp> Reactions," *Chin J Chem*, vol. 39, no. 3, pp. 710–728, Mar. 2021, doi: 10.1002/cjoc.202000464.
- [28] I. P. Beletskaya and A. V. Cheprakov, "The Heck Reaction as a Sharpening Stone of Palladium Catalysis," *Chem Rev*, vol. 100, no. 8, pp. 3009–3066, Aug. 2000, doi: 10.1021/cr9903048.
- [29] K. Sonogashira, Y. Tohda, and N. Hagihara, "A convenient synthesis of acetylenes: catalytic substitutions of acetylenic hydrogen with bromoalkenes, iodoarenes and bromopyridines," *Tetrahedron Lett*, vol. 16, no. 50, pp. 4467–4470, 1975, doi: 10.1016/S0040-4039(00)91094-3.
- [30] S. Handa, J. D. Smith, Y. Zhang, B. S. Takale, F. Gallou, and B. H. Lipshutz, "Sustainable HandaPhos- *ppm* Palladium Technology for Copper-Free Sonogashira Couplings in Water under Mild Conditions," *Org Lett*, vol. 20, no. 3, pp. 542–545, Feb. 2018, doi: 10.1021/acs.orglett.7b03621.
- [31] A. R. Gholap, K. Venkatesan, R. Pasricha, T. Daniel, R. J. Lahoti, and K. V. Srinivasan, "Copper- and Ligand-Free Sonogashira Reaction Catalyzed by Pd(0) Nanoparticles at Ambient Conditions under Ultrasound Irradiation," *J. Org. Chem.*, vol. 70, no. 12, pp. 4869–4872, Jun. 2005, doi: 10.1021/jo0503815.
- [32] E. ichi Negishi, A. O. King, and N. Okukado, "Selective Carbon-Carbon Bond Formation via Transition Metal Catalysis. 3. A Highly Selective Synthesis of Unsymmetrical Biaryls and Diarylmethanes by the Nickel- or Palladium-

- Catalyzed Reaction of Aryl- and Benzylzinc Derivatives with Aryl Halides," *Journal of Organic Chemistry*, vol. 42, no. 10, pp. 1821–1823, 1977, doi: 10.1021/jo00430a041.
- [33] C. Dai and G. C. Fu, "The First General Method for Palladium-Catalyzed Negishi Cross-Coupling of Aryl and Vinyl Chlorides: Use of Commercially Available Pd(P(t -Bu) 3) 2 as a Catalyst," *J Am Chem Soc*, vol. 123, no. 12, pp. 2719–2724, Mar. 2001, doi: 10.1021/ja003954y.
- [34] S. Thapa, A. Vangala, and R. Giri, "Copper-Catalyzed Negishi Coupling of Diarylzinc Reagents with Aryl Iodides," *Synthesis (Stuttg)*, vol. 48, no. 04, pp. 504–511, Jan. 2016, doi: 10.1055/s-0035-1560397.
- [35] J. K. Stille, "The Palladium-Catalyzed Cross-Coupling Reactions of Organotin Reagents with Organic Electrophiles," *Angewandte Chemie International Edition in English*, vol. 25, no. 6, pp. 508–524, Jun. 1986, doi: 10.1002/anie.198605081.
- [36] G. A. Grasa and S. P. Nolan, "Palladium/imidazolium salt catalyzed coupling of aryl halides with hypervalent organostannates," *Org Lett*, vol. 3, no. 1, pp. 119–120, Jan. 2001, doi: 10.1021/ol006827f.
- [37] C.-W. Huang, M. Shanmugasundaram, H.-M. Chang, and C.-H. Cheng, "Highly chemoselective coupling of allenylstannanes with organic iodides promoted by Pd(PPh3)4/LiCl: an efficient method for the synthesis of substituted allenes," *Tetrahedron*, vol. 59, no. 20, pp. 3635–3641, May 2003, doi: 10.1016/S0040-4020(03)00516-7.
- [38] Y. Hatanaka and T. Hiyama, "Cross-coupling of organosilanes with organic halides mediated by a palladium catalyst and tris(diethylamino)sulfonium difluorotrimethylsilicate," *J Org Chem*, vol. 53, no. 4, pp. 918–920, Feb. 1988, doi: 10.1021/jo00239a056.
- [39] J.-Y. Lee and G. C. Fu, "Room-Temperature Hiyama Cross-Couplings of Arylsilanes with Alkyl Bromides and Iodides," J Am Chem Soc, vol. 125, no. 19, pp. 5616–5617, May 2003, doi: 10.1021/ja0349352.

- [40] K. Itami, T. Nokami, and J. Yoshida, "Palladium-Catalyzed Cross-Coupling Reaction of Alkenyldimethyl(2-pyridyl)silanes with Organic Halides: Complete Switch from the Carbometalation Pathway to the Transmetalation Pathway," *J Am Chem Soc*, vol. 123, no. 23, pp. 5600–5601, Jun. 2001, doi: 10.1021/ja015655u.
- [41] N. Miyaura and A. Suzuki, "Palladium-Catalyzed Cross-Coupling Reactions of Organoboron Compounds," *Chem Rev*, vol. 95, no. 7, pp. 2457–2483, 1995, doi: 10.1021/cr00039a007.
- [42] M. A. Selepe and F. R. Van Heerden, "Application of the Suzuki-Miyaura reaction in the synthesis of flavonoids," Apr. 2013. doi: 10.3390/molecules18044739.
- [43] C. Liu, C. Liu, X. M. Li, Z. M. Gao, and Z. L. Jin, "Oxygen-promoted Pd/C-catalyzed Suzuki-Miyaura reaction of potassium aryltrifluoroborates," *Chinese Chemical Letters*, vol. 27, no. 5, pp. 631–634, May 2016, doi: 10.1016/j.cclet.2015.12.022.
- [44] S. Kotha, K. Lahiri, and D. Kashinath, "Recent applications of the Suzuki-Miyaura cross-coupling reaction in organic synthesis."
- [45] S. Singh Gujral, S. Khatri, P. Riyal, and V. Gahlot, "Suzuki Cross Coupling Reaction- A Review," *Indo Global Journal of Pharmaceutical Sciences*, vol. 02, no. 04, pp. 351–367, 2012, doi: 10.35652/igjps.2012.41.
- [46] J. Louie and J. F. Hartwig, "Palladium-catalyzed synthesis of arylamines from aryl halides. Mechanistic studies lead to coupling in the absence of tin reagents," *Tetrahedron Lett*, vol. 36, no. 21, pp. 3609–3612, 1995, doi: 10.1016/0040-4039(95)00605-C.
- [47] M. S. Oderinde *et al.*, "Highly Chemoselective Iridium Photoredox and Nickel Catalysis for the Cross-Coupling of Primary Aryl Amines with Aryl Halides," *Angewandte Chemie International Edition*, vol. 55, no. 42, pp. 13219–13223, Oct. 2016, doi: 10.1002/anie.201604429.

- [48] B. S. Takale, F. Y. Kong, and R. R. Thakore, "Recent Applications of Pd-Catalyzed Suzuki-Miyaura and Buchwald-Hartwig Couplings in Pharmaceutical Process Chemistry," Mar. 01, 2022, *Multidisciplinary Digital Publishing Institute (MDPI)*. doi: 10.3390/org3010001.
- [49] R. Dorel, C. P. Grugel, and A. M. Haydl, "The Buchwald–Hartwig Amination After 25 Years," *Angewandte Chemie*, vol. 131, no. 48, pp. 17276–17287, Nov. 2019, doi: 10.1002/ange.201904795.
- [50] X. Huang and S. L. Buchwald, "New Ammonia Equivalents for the Pd-Catalyzed Amination of Aryl Halides," Org Lett, vol. 3, no. 21, pp. 3417–3419, Oct. 2001, doi: 10.1021/ol0166808.
- [51] J. P. Wolfe, J. Åhman, J. P. Sadighi, R. A. Singer, and S. L. Buchwald, "An Ammonia Equivalent for the Palladium-Catalyzed Amination of Aryl Halides and Triflates," *Tetrahedron Lett*, vol. 38, no. 36, pp. 6367–6370, Sep. 1997, doi: 10.1016/S0040-4039(97)01465-2.
- [52] K. E. Torraca, X. Huang, C. A. Parrish, and S. L. Buchwald, "An Efficient Intermolecular Palladium-Catalyzed Synthesis of Aryl Ethers," *J Am Chem Soc*, vol. 123, no. 43, pp. 10770–10771, Oct. 2001, doi: 10.1021/ja016863p.
- [53] T. H. Jepsen *et al.*, "Synthesis of functionalized dibenzothiophenes- An efficient three-step approach based on Pd-catalyzed C-C and C-S bond formations," *European J Org Chem*, no. 1, pp. 53–57, 2011, doi: 10.1002/ejoc.201001393.
- [54] H. Tokuyama, S. Yokoshima, T. Yamashita, and T. Fukuyama, "A novel ketone synthesis by a palladium-catalyzed reaction of thiol esters and organozinc reagents," *Tetrahedron Lett*, vol. 39, no. 20, pp. 3189–3192, 1998, doi: 10.1016/S0040-4039(98)00456-0.
- [55] S.-Q. Tang, J. Bricard, M. Schmitt, and F. Bihel, "Fukuyama Cross-Coupling Approach to Isoprekinamycin: Discovery of the Highly Active and Bench-Stable Palladium Precatalyst POxAP," *Org Lett*, vol. 21, no. 3, pp. 844–848, Feb. 2019, doi: 10.1021/acs.orglett.9b00031.

- [56] M. Perez-Lorenzo, "ChemInform Abstract: Palladium Nanoparticles as Efficient Catalysts for Suzuki Cross-Coupling Reactions," *ChemInform*, vol. 43, no. 14, p. no-no, Apr. 2012, doi: 10.1002/chin.201214255.
- [57] M. C. D'Alterio, È. Casals-Cruañas, N. V. Tzouras, G. Talarico, S. P. Nolan, and A. Poater, "Mechanistic Aspects of the Palladium-Catalyzed Suzuki-Miyaura Cross-Coupling Reaction," Sep. 24, 2021, John Wiley and Sons Inc. doi: 10.1002/chem.202101880.
- [58] M. S. Wong and X. L. Zhang, "Ligand promoted palladium-catalyzed homocoupling of arylboronic acids," *Tetrahedron Lett*, vol. 42, no. 24, pp. 4087–4089, Jun. 2001, doi: 10.1016/S0040-4039(01)00637-2.
- [59] J. Q. Xie, R. X. Liang, and Y. X. Jia, "Recent Advances of Catalytic Enantioselective Heck Reactions and Reductive-Heck Reactions," Mar. 01, 2021, Shanghai Institute of Organic Chemistry. doi: 10.1002/cjoc.202000464.
- [60] R. X. Liang and Y. X. Jia, "Aromatic π-Components for Enantioselective Heck Reactions and Heck/Anion-Capture Domino Sequences," *Acc Chem Res*, vol. 55, no. 5, pp. 734–745, Mar. 2022, doi: 10.1021/acs.accounts.1c00781.
- [61] M. N. Hopkinson, C. Richter, M. Schedler, and F. Glorius, "An overview of N-heterocyclic carbenes," *Nature*, vol. 510, no. 7506, pp. 485–496, 2014, doi: 10.1038/nature13384.
- [62] T. E. Barder, S. D. Walker, J. R. Martinelli, and S. L. Buchwald, "Catalysts for Suzuki-Miyaura coupling processes: Scope and studies of the effect of ligand structure," *J Am Chem Soc*, vol. 127, no. 13, pp. 4685–4696, Apr. 2005, doi: 10.1021/ja042491j.
- [63] P. Ruiz-Castillo and S. L. Buchwald, "Applications of Palladium-Catalyzed C-N Cross-Coupling Reactions," *Chem Rev*, vol. 116, no. 19, pp. 12564–12649, 2016, doi: 10.1021/acs.chemrev.6b00512.
- [64] J. H. Tidwell, S. L. Buchwald, M. Kosugi, M. Kameyama, and T. Migita, "Palladium-Catalyzed Aromatic Aminations with in Situ Generated

- Aminostannanes," 1994. [Online]. Available: https://pubs.acs.org/sharingguidelines
- [65] A. F. P. Biajoli, C. S. Schwalm, J. Limberger, T. S. Claudino, and A. L. Monteiro, "Recent progress in the use of Pd-catalyzed C-C cross-coupling reactions in the synthesis of pharmaceutical compounds," *J Braz Chem Soc*, vol. 25, no. 12, pp. 2186–2214, 2014, doi: 10.5935/0103-5053.20140255.
- [66] J. Rayadurgam, S. Sana, M. Sasikumar, and Q. Gu, "Palladium catalyzed C-C and C-N bond forming reactions: An update on the synthesis of pharmaceuticals from 2015-2020," Organic Chemistry Frontiers, vol. 8, no. 2, pp. 384–414, 2021, doi: 10.1039/d0qo01146k.
- [67] S. Tabassum, A. F. Zahoor, S. Ahmad, R. Noreen, S. G. Khan, and H. Ahmad, Cross-coupling reactions towards the synthesis of natural products, vol. 26, no. 1. Springer International Publishing, 2022. doi: 10.1007/s11030-021-10195-6.
- [68] Q. Zhang, B. Li, S. Huang, H. Nomura, H. Tanaka, and C. Adachi, "Efficient blue organic light-emitting diodes employing thermally activated delayed fluorescence," *Nat Photonics*, vol. 8, no. 4, pp. 326–332, 2014, doi: 10.1038/nphoton.2014.12.
- [69] J. Y. Hu *et al.*, "Bisanthracene-based donor-acceptor-type light-emitting dopants: Highly efficient deep-blue emission in organic light-emitting devices," *Adv Funct Mater*, vol. 24, no. 14, pp. 2064–2071, 2014, doi: 10.1002/adfm.201302907.
- [70] D. Zhang *et al.*, "A molecular photosensitizer achieves a V oc of 1.24 V enabling highly efficient and stable dye-sensitized solar cells with copper(II/I)-based electrolyte," *Nat Commun*, vol. 12, no. 1, pp. 2–11, 2021, doi: 10.1038/s41467-021-21945-3.
- [71] European Environmental Agency, Renewable energy in Europe recent growth and knock-on effects, no. 1. 2016. [Online]. Available: http://www.eea.europa.eu/publications/renewable-energy-in-europe-2016/download

- [72] H. Ahmad, S. K. Kamarudin, L. J. Minggu, and M. Kassim, "Hydrogen from photo-catalytic water splitting process: A review," *Renewable and Sustainable Energy Reviews*, vol. 43, pp. 599–610, 2015, doi: 10.1016/j.rser.2014.10.101.
- [73] A. Keerthi and S. Valiyaveettil, "Regioisomers of Perylenediimide: Synthesis, Photophysical, and Electrochemical Properties," *J Phys Chem B*, vol. 116, no. 15, pp. 4603–4614, Apr. 2012, doi: 10.1021/jp210736x.
- [74] I. E. Serdiuk, C. H. Ryoo, K. Kozakiewicz, M. Mońka, B. Liberek, and S. Y. Park, "Twisted acceptors in the design of deep-blue TADF emitters: crucial role of excited-state relaxation in the photophysics of methyl-substituted s-triphenyltriazine derivatives," *J Mater Chem C Mater*, vol. 8, no. 18, pp. 6052–6062, May 2020, doi: 10.1039/C9TC07102D.
- [75] C. Liu, C. Liu, X. M. Li, Z. M. Gao, and Z. L. Jin, "Oxygen-promoted Pd/C-catalyzed Suzuki-Miyaura reaction of potassium aryltrifluoroborates," *Chinese Chemical Letters*, vol. 27, no. 5, pp. 631–634, May 2016, doi: 10.1016/j.cclet.2015.12.022.
- [76] C. Liu, Q. Ni, P. Hu, and J. Qiu, "Oxygen-promoted PdCl2-catalyzed ligand-free Suzuki reaction in aqueous media," Org Biomol Chem, vol. 9, no. 4, pp. 1054–1060, Feb. 2011, doi: 10.1039/c0ob00524j.
- [77] P. J. Kropp et al., "Surface-Mediated Reactions. 6. Effects of Silica Gel and Alumina on Acid-Catalyzed Reactions," J Org Chem, vol. 60, no. 13, pp. 4146–4152, Jun. 1995, doi: 10.1021/jo00118a035.
- [78] E. Hoffman *et al.*, "Photochemical transformation of a perylene diimide derivative beneficial for the *in situ* formation of a molecular photocatalyst of the hydrogen evolution reaction," *J Mater Chem A Mater*, vol. 12, no. 9, pp. 5233–5243, Jan. 2024, doi: 10.1039/D3TA05930H.
- [79] J. Yoon et al., "The heavy-atom effect on xanthene dyes for photopolymerization by visible light," Polym Chem, vol. 10, no. 42, pp. 5737– 5742, Nov. 2019, doi: 10.1039/c9py01252d.

- [80] S. Sivakamasundari and R. Ganesan, "Kinetics and mechanism of the bromination of aromatic compounds by N-bromosuccinimide in solution," Int J Chem Kinet, vol. 12, no. 11, pp. 837–850, Nov. 1980, doi: 10.1002/kin.550121103.
- [81] W. Gołebiewski and M. Gucma, "Applications of N-Chlorosuccinimide in Organic Synthesis," *Synthesis (Stuttg)*, vol. 2007, no. 23, pp. 3599–3619, Dec. 2007, doi: 10.1055/s-2007-990871.
- [82] E. O. Pentsak, D. B. Eremin, E. G. Gordeev, and V. P. Ananikov, "Phantom Reactivity in Organic and Catalytic Reactions as a Consequence of Microscale Destruction and Contamination-Trapping Effects of Magnetic Stir Bars," ACS Catal, vol. 9, no. 4, pp. 3070–3081, Apr. 2019, doi: 10.1021/acscatal.9b00294.
- [83] X. Yao et al., "Impact of Anchoring Groups on the Photocatalytic Performance of Iridium(III) Complexes and Their Toxicological Analysis," Molecules, vol. 29, no. 11, p. 2564, May 2024, doi: 10.3390/molecules29112564.
- [84] K. L. Materna, R. H. Crabtree, and G. W. Brudvig, "Anchoring groups for photocatalytic water oxidation on metal oxide surfaces," *Chem Soc Rev*, vol. 46, no. 20, pp. 6099–6110, Oct. 2017, doi: 10.1039/C7CS00314E.
- [85] J. Warnan *et al.*, "Solar electricity and fuel production with perylene monoimide dye-sensitised TiO2 in water," *Chem Sci*, vol. 10, no. 9, pp. 2758–2766, 2019, doi: 10.1039/C8SC05693E.
- [86] J. Warnan *et al.*, "Solar electricity and fuel production with perylene monoimide dye-sensitised TiO2 in water," *Chem Sci*, vol. 10, no. 9, pp. 2758–2766, 2019, doi: 10.1039/C8SC05693E.
- [87] A. Toledo, I. Funes-Ardoiz, F. Maseras, and A. C. Albéniz, "Palladium-Catalyzed Aerobic Homocoupling of Alkynes: Full Mechanistic Characterization of a More Complex Oxidase-Type Behavior," *ACS Catal*, vol. 8, no. 8, pp. 7495–7506, Aug. 2018, doi: 10.1021/acscatal.8b01540.

- [88] W. Chen *et al.*, "Modulating Benzothiadiazole-Based Covalent Organic Frameworks via Halogenation for Enhanced Photocatalytic Water Splitting," *Angewandte Chemie International Edition*, vol. 59, no. 39, pp. 16902–16909, Sep. 2020, doi: 10.1002/anie.202006925.
- [89] F. L. Cook, C. W. Bowers, and C. L. Liotta, "Chemistry of naked anions. III. Reactions of the 18-crown-6 complex of potassium cyanide with organic substrates in aprotic organic solvents," *J Org Chem*, vol. 39, no. 23, pp. 3416– 3418, Nov. 1974, doi: 10.1021/jo00937a026.
- [90] J. Almond-Thynne, D. C. Blakemore, D. C. Pryde, and A. C. Spivey, "Site-selective Suzuki–Miyaura coupling of heteroaryl halides understanding the trends for pharmaceutically important classes," *Chem Sci*, vol. 8, no. 1, pp. 40–62, 2017, doi: 10.1039/C6SC02118B.
- [91] G. Wüllner, H. Jänsch, F. Schubert, and G. Boche, "Palladium-catalyzed amination of aromatic halides in water-containing solvent systems: a two-phase protocol," *Chemical Communications*, vol. 107, no. 15, pp. 1509–1510, 1998, doi: 10.1039/a803819h.
- [92] P. Wagner *et al.*, "T-BuXPhos: A highly efficient ligand for Buchwald-Hartwig coupling in water," *Green Chemistry*, vol. 16, no. 9, pp. 4170–4178, 2014, doi: 10.1039/c4gc00853g.
- [93] J. F. Hartwig and F. Paul, "Oxidative Addition of Aryl Bromide after Dissociation of Phosphine from a Two-Coordinate Palladium(0) Complex, Bis(tri-o-tolylphosphine)Palladium(0)," *J Am Chem Soc*, vol. 117, no. 19, pp. 5373–5374, May 1995, doi: 10.1021/ja00124a026.

7. ACADEMIC ACHIEVEMENTS

Entries with asterisk [*] are publications, presentations and posters connected do my thesis.

Lp.	Opis bibliograficzny	Punkty
1*	Hoffman Estera, Kozakiewicz Karol , Rybczyńska Małgorzata, Mońka Michał, Grzywacz Daria, Liberek Beata, Bojarski Piotr, Serdiuk Illia: Photochemical transformation of a perylene diimide derivative beneficial for the in situ formation of a molecular photocatalyst of the hydrogen evolution reaction, Journal of Materials Chemistry A: materials for energy and sustainability, Royal Society of Chemistry, vol. 12, nr 9, 2024, s. 5233-5243, DOI:10.1039/D3TA05930H	140
2	Mońka Michał, Gogoc Szymon, Kozakiewicz Karol , Ievtukhov Vladyslav, Grzywacz Daria, Ciupak Olga, Kubicki Aleksander, Bojarski Piotr, Data Przemysław, Serdiuk Illia: Application of the heavy-atom effect for (sub)microsecond thermally activated delayed fluorescence and an all-organic light-emitting device with low-efficiency roll-off, ACS Applied Materials & Interfaces, American Chemical Society, vol. 16, nr 12, 2024, s. 15107-15120, DOI:10.1021/acsami.3c19627	200
3*	Rybczyńska Małgorzata, Hoffman Estera, Kozakiewicz Karol , Mońka Michał, Grzywacz Daria, Ciupak Olga, Liberek Beata, Bojarski Piotr, Serdiuk Illia: Charge separation control in organic photosensitizers for photocatalytic water splitting without sacrificial electron donors, Journal of Catalysis, Academic Press, vol. 435, 2024, Numer artykułu: 115539, s. 1-11, DOI:10.1016/j.jcat.2024.115539	140
4*	Rybczyńska Małgorzata, Hoffman-Rusin Estera, Kozakiewicz Karol , Mońka Michał, Grzywacz Daria, Ciupak Olga, Liberek Beata, Bojarski Piotr, Serdiuk Illia: Charge separation control in organic photosensitizers for photocatalytic water splitting without sacrificial electron donors [preprint], Journal of Catalysis, Academic Press, 2024, s. 1-23, DOI:10.71853/wgwq-m888	
5*	Kozakiewicz Karol , Hoffman Estera, Mońka Michał, Grzywacz Daria, Rybczyńska Małgorzata, Bojarski Piotr, Serdiuk Illia, Liberek Beata: Synthesis of perylenediimide derivatives with wide photophysical properties for photosensitizing in water splitting reaction, 2024, Summer School on Organic Synthesis under Non-Classical Conditions, Warsaw	Poster
6*	Rybczyńska Małgorzata, Kozakiewicz Karol , Hoffman-Rusin Estera, Bojarski Piotr, Serdiuk Illia: Could the Pt TiO2 nanoparticles sensitized with perylene diimide derivatives be a solution for green hydrogen production from water?, 2023, 16th International conference on materials chemistry 2023, poster	Poster
7	Mońka Michał, Grzywacz Daria, Hoffman Estera, Ievtukhov Vladyslav, Kozakiewicz Karol , Rogowski Radosław, Kubicki Aleksander, Liberek Beata, Bojarski Piotr, Serdiuk Illia: Decisive role of heavy-atom orientation for efficient enhancement of spin—orbit coupling in organic thermally activated delayed fluorescence emitters, Journal of Materials Chemistry C, Royal Society of Chemistr, vol. 10, nr 32, 2022, s. 11719-11729, DOI:10.1039/D2TC01729F	140
8	Mońka Michał, Serdiuk Illia, Kozakiewicz Karol , Hoffman-Rusin Estera, Szumilas Jan, Kubicki Aleksander, Park Soo Young, Bojarski Piotr: Understanding the internal heavy-atom effect on thermally activated delayed fluorescence: application of Arrhenius and Marcus theories for spin—orbit coupling analysis, Journal of Materials Chemistry C, Royal Society of Chemistr, vol. 10, nr 20, 2022, s. 7925-7934, DOI:10.1039/D2TC00476C	140
9*	Kozakiewicz Karol , Hoffman-Rusin Estera, Mońka Michał, Grzywacz Daria, Rybczyńska Małgorzata, Liberek Beata, Bojarski Piotr, Serdiuk Illia: Tuning of photophysical properties of perylenediimide derivatives for photosensitizing purposes; Proceedings Volume PC12208,	– Poster

	Organic and Hybrid Light Emitting Materials and Devices XXVI; PC122081G (2022) https://doi.org/10.1117/12.2646607 Event: SPIE Organic Photonics + Electronics, 2022, San Diego, California, United States	
10	Skoroszewska Dominika, Myszka Henryk, Grzywacz Daria, Kozakiewicz Karol , Serdiuk Illia: Porównanie metod syntezy dibenzoselenofenu, 2022, XIX Wrocławskie Studenckie Sympozjum Chemiczne 2022, referat wygłoszony	
11	Hoffman Estera, Mońka Michał, Grzywacz Daria, Kozakiewicz Karol , Serdiuk Illia, Bojarski Piotr: Photophysical properties and heavy atom effect donor-acceptor structures based on phenazines, 2022, 7th International Workshop on Advanced Spectroscopy and Optical Materials 2022, poster	
12	Serdiuk Illia, Mońka Michał, Kozakiewicz Karol , Liberek Beata, Bojarski Piotr, Park Soo Young: Vibrationally assisted direct intersystem crossing between the same charge-transfer states for thermally activated delayed fluorescence: analysis by Marcus–Hush theory including reorganization energy, Journal of Physical Chemistry B, American Chemical Society, vol. 125, nr 10, 2021, 2696–2706, DOI:10.1021/acs.jpcb.0c10605	140
13	Reszka Milena, Serdiuk Illia, Kozakiewicz Karol , Nowacki Andrzej, Myszka Henryk, Bojarski Piotr, Liberek Beata: Influence of a 4'-substituent on the efficiency of flavonol-based fluorescent indicators of β-glycosidase activity, Organic & Biomolecular Chemistry, vol. 18, nr 38, 2020, s. 7635-7648, DOI:10.1039/D0OB01505A	100
14	Serdiuk Illia, Ryoo Chi Hyun, Kozakiewicz Karol , Mońka Michał, Liberek Beata, Park Soo Young: Twisted acceptors in the design of deep-blue TADF emitters: crucial role of excited-state relaxation in the photophysics of methyl-substituted s-triphenyltriazine derivatives, Journal of Materials Chemistry C, Royal Society of Chemistr, vol. 8, nr 18, 2020, s. 6052-6062, DOI:10.1039/c9tc07102d	140
15	Bednarko Justyna, Stachurski Oktawian, Wielińska Justyna, Kozakiewicz Karol , Liberek Beata, Nowacki Andrzej: Threocytidines: insight into the conformational preferences of artificial threose nucleic acid (TNA) building blocks in B3LYP studies, Journal of Molecular Graphics & Modelling, vol. 80, 2018, s. 157-172, DOI:10.1016/j.jmgm.2018.01.007	25
16	Kozakiewicz Karol , Reszka Milena, Serdiuk Illia, Liberek Beata: Synteza i potencjalne zastosowania nowych pochodnych flawonoli, 2018, I Konferencja Naukowa "Chemia - Biznes - Środowisko" 2018, poster	
17	Reszka Milena, Kozakiewicz Karol , Serdiuk Illia, Liberek Beata: Wpływ podstawnika na czułość glukozydów flawonoli jako fluorescencyjnych indykatorów β-glukozydaz, 2017, Konferencja Młodych Naukowców "Nowe wyzwania dla polskiej nauki", II Edycja 2017, referat wygłoszony	_
18	Kozakiewicz Karol , Reszka Milena, Serdiuk Illia, Liberek Beata: Nowe aspekty syntezy 4'-podstawionych pochodnych flawonoli, 2017, Konferencja Młodych Naukowców "Nowe wyzwania dla polskiej nauki", II Edycja 2017, poster	_

"I've studied, alas, philosophy,

Law and medicine, recto and verso

And how I regret it, theology also

Oh, God, how hard I've slaved away,

With what result? Poor fool that I am,

I'm no whit wiser than when I began!"

- Johan Wolfgang von Goethe, "Faust" 1898, translation by Bayard Taylor